



**N OVA**  
NOVA SCHOOL OF  
SCIENCE & TECHNOLOGY

DEPARTMENT OF  
CHEMISTRY

SARA BEATRIZ RODRIGUES GASPAR

Biochemistry degree

**NO2PROBE: APPLICATION OF A NEW NITRITE  
POINT-OF-CARE TEST IN BIOMEDICINE**

SUBMITTED TO OBTAINING OF THE BIOCHEMISTRY  
MASTER'S DEGREE

NOVA University of Lisbon

October, 2022





# NO<sub>2</sub>PROBE: APPLICATION OF A NEW NITRITE POINT-OF-CARE TEST IN BIOMEDICINE

**SARA BEATRIZ RODRIGUES GASPAR**

BSc in Biochemistry

**Adviser:** Maria Gabriela Almeida,  
Associate Professor, CiiEM

**Co-adviser:** Ricardo Alves  
Assistent Professor, CiiEM

## **Examination Committee:**

**Chair:** Pedro António de Brito Tavares  
Assistant Professor, NOVA FCT

**Rapporteurs:** Bárbara Silva Rocha  
Assistant Professor, Faculty of Pharmacy, University of  
Coimbra

**Adviser:** Maria Gabriela Almeida  
Associate Professor, CiiEM

SUBMITTED TO OBTAIN THE BIOCHEMISTRY MASTER'S DEGREE

NOVA University of Lisbon

October, 2022



NO2Probe: Application of a new nitrite point-of-care test in biomedicine

Copyright © Sara Gaspar Rodrigues Gaspar, NOVA School of Science and Technology and the NOVA University of Lisbon have the right, perpetual and without geographical boundaries, to file and publish this dissertation through printed copies reproduced on paper or on digital form, or by any other means known or that may be invented, and to disseminate through scientific repositories and admit its copying and distribution for non-commercial, educational or research purposes, as long as credit is given to the author and editor.

## Dedictory

*Às minhas Estrelas.*

# AGRADECIMENTOS

Esta fase não teria sido fácil se não tivesse a ajuda de cada um de vocês, pais, irmãos, amigos e professores.

Quero agradecer à professora Gabriela Almeida que me proporcionou continuar com o seu projeto. Obrigada por toda a ajuda e dicas que me deu, foram essenciais para conseguir terminar a tese com sucesso. Gostei bastante de me aventurar pelo mundo dos biossensores, gostei ainda mais de ter o contacto com as análises clínicas, saí da minha zona de conforto, mas fez-me crescer e por tudo isto, muito obrigada.

Deixo um agradecimento especial ao professor Ricardo Alves pelo apoio que me deu na Clínica Dentária Egas Moniz. Tornou a minha interação com os pacientes da clínica, muito mais fácil e leve. Muito obrigada pela ajuda. Agradeço também ao professor Luís Proença pelo auxílio que me deu na análise estatística deste estudo. As suas dicas e explicações ajudaram-me bastante, por isso, muito obrigada.

Agradeço ao Miguel e à Joana por toda a ajuda prestada durante a minha tese. Não só me ajudaram com o “sabes onde estão os frascos?” mas também partilharam comigo o conhecimento deles, o que tornou tudo muito mais fácil.

Quero deixar um agradecimento muito especial, dedicado aos meus pais, uma vez que sem o apoio deles, não me refiro só a monetário que é uma das partes importantes do conseguir estudar fora, não teria a coragem de enfrentar a distância de casa na licenciatura, agora menos distante no mestrado. Obrigada por todos os conselhos, saibam que os ouvi a todos. Espero que tenham orgulho nesta tese que acaba por ser um bocadinho vossa.

Aos meus irmãos, que espero que leiam esta tese, se faz favor. A toda a minha família, madrinha, tias, tios e muitos primos que me ajudaram a ultrapassar a partida da minha avó no início desta tese. Também é para ti, Glorita. Obrigada.

Às minhas meninas Catarina, Carolina e Margarida, obrigada por tudo. Desde Évora até hoje e de hoje em diante. Como eu gosto de vocês. Agradeço por me ajudarem a passar esta etapa de uma forma leve, sempre a rir. Já sabem, quando for apresentar a tese, mantenham-se sérias. Quero também deixar na minha tese um beijinho e um obrigada às minhas Marias, ao André e ao Henrique. Se estão aqui é porque são especiais. Adoro-vos.

Pelo amor, carinho e amizade, quero agradecer ao meu Luís. Espero que te orgulhes desta tese. Ainda falta a apresentação, vou olhar para ti para me acalmar.

Obrigada a todos!





# ABSTRACT

Periodontal disease (PD) results from the inflammatory response to the presence of bacterial biofilms. The disease progression goes through two phases: gingivitis, characterized by bleeding and gingiva gums swelling, and periodontitis, an aggravated condition that can lead to bone, gingival, and teeth loss. For diagnosis, time-consuming periodontal charts and X-rays are evaluated. Thus, it is convenient to recognize clinical biomarkers measuring each individual's PD occurrence and extent. The nitrite ( $\text{NO}_2^-$ ) level in saliva has been pointed out in this regard, but it is not yet clinically used as a PD biomarker. Thus, the study objectives were to evaluate the relationship between PD and nitrite concentration in non-stimulated saliva samples, and the implementation of a new specific and sensitive biosensor, the NO2Probe, for nitrite quantification during the medical appointment.

The approach involved the screen-printed carbon electrodes (SPE) modification and optimization with the multihemic nitrite reductase enzyme (ccNiR), which catalyzes the direct reduction reaction of nitrite into ammonia. As an oxygen scavenging system, an ascorbate oxidase (AOx) layer was added and, finally, a polymer layer (PVA), to “delay” the ccNiR saturation. The amperometric biosensor (SPE/ccNiR/AOx/PVA) covers a linearity range between 5-300  $\mu\text{M}$ , with a sensitivity of 0.015  $\mu\text{M}^{-1}$ . The obtained values were compared with the conventional Griess method. The biosensor was statistically validated.

Initially, the centrifugation and freezing steps of the samples were evaluated, evaluating the two methods, and verifying that, with the biosensor, centrifugation is not necessary. In the Griess method, centrifugation is essential, as the nitrite concentration in non-centrifuged samples ( $199 \pm 3 \mu\text{M}$ ) decreases after centrifugation ( $68.8 \pm 0.5 \mu\text{M}$ ). When frozen, the  $\text{NO}_2^-$  concentration decreases, probably due to the  $\text{NO}_2^-$  instability. It was concluded that samples should be analyzed fresh as soon as possible.

In the pilot study, carried out at the CiiEM Dental Clinic, it was not possible to establish a concrete relationship between the  $\text{NO}_2^-$  concentration and the disease stages and grades. Contrary to the expectations, the periodontally healthy group ( $n=11$ ) had higher  $\text{NO}_2^-$  concentration ( $257 \pm 30 \mu\text{M}$ ) higher than those observed in the PD patients group ( $n=24$ ).

**Keywords:** Periodontal disease, Nitrite, Point-of-care test, Biosensors



## RESUMO

A Doença Periodontal (PD) decorre da resposta inflamatória à presença de biofilmes bacterianos. A progressão desta, passa por duas fases: a gengivite, caracterizada pelo sangramento e inchaço da gengiva, e a periodontite, condição agravada que pode conduzir à perda de tecidos ósseo, gengival e de dentes. Para diagnóstico, são avaliados morosos periodontogramas e os raios-X. Assim, é conveniente o reconhecimento de biomarcadores clínicos aferindo a ocorrência e extensão da PD em cada indivíduo. O nível de nitrito ( $\text{NO}_2^-$ ) na saliva, tem sido apontado nesse sentido, mas ainda não é utilizado clinicamente como biomarcador da PD. Assim, os objetivos foram: avaliar a relação entre a PD e a concentração de nitrito, em amostras de saliva não estimulada, e a implementação de um novo biossensor, o NO2Probe, específico e sensível para quantificação de nitrito durante a consulta.

A abordagem passou pela modificação e otimização de elétrodos impressos de carbono (SPE) com a enzima multihémica redutase do nitrito (ccNiR), que catalisa a reação de redução direta do nitrito a amónia. Como sistema de remoção de oxigénio, adicionou-se uma camada de Ascorbato oxidase (AOx) e, finalmente, uma camada de polímero (PVA), para “atrasar” a saturação da ccNiR. O biossensor amperométrico (SPE/ccNiR/AOx/PVA) mostrou abranger uma gama de linearidade entre 5-300  $\mu\text{M}$ , com sensibilidade de 0.015  $\mu\text{M}^{-1}$ . Os valores obtidos foram comparados com o método convencional de Griess. Estatisticamente, o biossensor foi validado.

Inicialmente, foram avaliados os passos centrifugação e congelamento das amostras avaliando os dois métodos, verificando-se que, com o biossensor, não é necessário centrifugar amostras. Já pelo método de Griess, a centrifugação é fundamental, pois a concentração de nitrito em amostras não centrifugadas ( $199 \pm 3 \mu\text{M}$ ) decresce após centrifugação ( $68.8 \pm 0.5 \mu\text{M}$ ). Quando congeladas, há diminuição da concentração de nitrito, provavelmente devido à instabilidade deste. Concluiu-se que as amostras devem ser analisadas de fresco, o mais rápido possível.

No estudo piloto, conduzido na Clínica Dentária do CiiEM, não foi possível estabelecer uma relação concreta entre a concentração de nitrito e os estadios e graus da doença. Contrariamente ao esperado, o grupo composto por indivíduos periodontalmente saudáveis ( $n=11$ ), apresentaram concentrações de nitrito ( $257 \pm 30 \mu\text{M}$ ) superiores às verificadas no grupo de doentes ( $n=24$ ).

**Palavras-chave:** Doença periodontal, Nitrito, Detecção *point-of-care*, Biossensores



# Table of Contents

<b>AGRADECIMENTOS</b> .....	<b>vii</b>
<b>ABSTRACT</b> .....	<b>ix</b>
<b>RESUMO</b> .....	<b>xi</b>
<b>Figures Index</b> .....	<b>xvii</b>
<b>Table Index</b> .....	<b>xxii</b>
<b>List of Abbreviations and Symbols</b> .....	<b>xxv</b>
<b>1. INTRODUCTION</b> .....	<b>1</b>
1.1. Periodontal Disease .....	1
1.1.1. Definition and Classification .....	1
1.1.2. Causes .....	4
1.1.3. Periodontitis prevalence and incidence .....	5
1.1.4. Symptoms and Clinical Diagnosis .....	7
1.1.5. Risk Factors.....	7
1.2. Nitrites in human physiology .....	8
1.2.1. NO physiological paper .....	8
1.2.2. L-arginine pathway .....	9
1.2.3. NO <sub>3</sub> <sup>-</sup> -NO <sub>2</sub> <sup>-</sup> -NO pathway .....	13
1.2.3.1. Nitrite and the enterosalivary circulation .....	13
1.2.4. External sources .....	15
1.3. Health risks .....	16
1.3.1. Cancer .....	17
1.3.2. Methemoglobinemia .....	17
1.4. Physiological role.....	18
1.4.1. Periodontal disease biomarkers .....	18
1.4.2. Hypoxia and vasodilatation .....	21
1.4.3. Signaling molecule .....	22
1.5. Nitrite determination Methods .....	22
1.5.1. Traditional methods .....	22
1.5.2. Biosensors .....	24

1.6.	Hypothesis.....	28
1.7.	Objectives.....	28
<b>2.</b>	<b>MATERIALS AND METHODS.....</b>	<b>33</b>
	Experimental section.....	33
2.1.	Reagents and Solutions .....	33
2.2.	Equipment .....	34
2.3.	Clinical Study.....	34
2.3.1.	Ethical Considerations.....	34
2.3.2.	Inclusion and Exclusion criteria .....	34
2.3.3.	Patient Data collection.....	35
2.3.3.1.	Clinical Data .....	35
2.3.3.2.	Questionnaire .....	35
2.3.4.	Salivary fluid sampling and preparation .....	36
2.4.	Nitrite quantification .....	36
2.4.1.	Electrochemical Biosensor .....	36
2.4.2.	Griess Method .....	38
2.5.	Statistical analysis .....	39
<b>3.</b>	<b>RESULTS AND DISCUSSION .....</b>	<b>43</b>
3.1.	Nitrite Quantification .....	43
3.1.1.	Griess Method .....	43
3.1.2.	Electrochemical Method – Biosensor Optimization.....	44
3.2.	Sample pretreatment – a preliminary study.....	49
3.2.1.	Turbidity Influence .....	49
3.2.2.	Effect of freezing.....	50
3.3.	Pilot Clinical Study.....	51
3.3.1.	Biosensor Validation.....	51
3.3.1.1.	Centrifugation effect .....	51
3.3.1.2.	Effect of sample freezing .....	54
3.3.1.3.	Method Validation.....	56
3.3.2.	Nitrite and Periodontal disease .....	57
<b>4.</b>	<b>CONCLUSIONS .....</b>	<b>69</b>

4.1. FUTURE WORK.....	70
<b>REFERENCES .....</b>	<b>74</b>
<b>Appendices.....</b>	<b>84</b>





## Figures Index

- Figure 1.1** - Scheme of periodontal disease evolution. Healthy gingiva is characterized by the pink/coral color and absence of bacterial plaque. The first phase of PD is gingivitis which is characterized by red gums, bleeding, and the presence (or not) of bacterial plaque. Periodontitis is distinguished from gingivitis because of the presence of gums pull away, bacterial plaque presence, bleeding, and sometimes accompanied by bone and teeth loss. (**Adapted from Highfield, 2009**). ..... 2
- Figure 1.2** - Periodontitis population prevalence (both genders), in developed (Portugal, Germany, and the United States of America) and less developed countries (India, Republic of Korea, and Sub-Saharan Africa). (**From GDB compare**) ..... 6
- Figure 1.3** - Periodontitis prevalence (left), and incidence (right), in the population of both genders, in Portugal (**adapted from GDB compare**). Data were collected for different age groups: 10-24 (green), 25-49 (blue), 50-69 (purple), and >70 (coral) years old. Prevalence refers to the number of active cases in the population. The Incidence determines the number of cases in a risk population in a determined time window (**Fajardo-Gutiérrez, 2017**). ..... 6
- Figure 1.4** - The two physiological pathways to obtain NO. a) The L-arginine pathway uses this amino acid as the substrate of NOS enzymes in Normoxia conditions, to obtain NO. b) Nitrate-nitrite-NO pathway occurs without the presence of oxygen (hypoxia conditions) in this case,  $\text{NO}_3^-$  is reduced to  $\text{NO}_2^-$  which in turn is reduced to NO. The two pathways have a connection point since NO provided from the L-arginine route can be oxidized to  $\text{NO}_3^-$ . (**Adapted from Lundberg, 2008**). ..... 9
- Figure 1.5** - Human endothelial NOS enzyme (PDB 4D1O). The figure represents the principal chain of the heme domain of the protein with 440 amino acid residues (dark blue). L-arginine (yellow) has a specific binding site, near protoporphyrin IX containing Fe (red). The image shows other ligands: two tetrahydrobiopterin (pink), and three gadolinium ions (orange). The structure was prepared with the *PyMOL* program..... 11
- Figure 1.6** - L-arginine pathway and the three NOS enzyme isoforms. a) nNOS is located in the neuronal tissue and converts L-arginine into L-citrulline. b) eNOS is localized in endothelial cells. c) iNOS is inducible, in macrophages, by an inflammatory reaction mediated by cytokine release. (**Adapted from Kleinbongard, 2006; Kevil et al., 2011**). ..... 11
- Figure 1.7** - Endothelium distribution of nitrite. In endothelial cells, the eNOS enzyme is present and promotes the enzymatic conversion of L-arginine into L-citrulline resulting in NO production. The NO can cross through the plasmatic cell membrane, which will be converted into nitrate, mediated by  $\text{NO}^\cdot$  dioxygenase present in red blood cells (RBC), and oxidized into nitrite – by  $\text{NO}^\cdot$  oxidase action accompanied by ceruloplasmin. (**Adapted from Shiva, 2010**)..... 12
- Figure 1.8** - The  $\text{NO}_3^-$ - $\text{NO}_2^-$ -NO pathway starts with  $\text{NO}_3^-$  loading from exogenous (diet) and endogenous oxidation of  $\text{NO}^\cdot$ . In the oral cavity,  $\text{NO}_3^-$  is reduced into  $\text{NO}_2^-$  by facultative anaerobic bacteria. In acidic conditions, the salivary fluid goes to the stomach and  $\text{NO}_2^-$  is protonated into  $\text{HNO}_2$ . Several reactions later,  $\text{NO}_3^-$  and  $\text{NO}_2^-$  are formed. In the intestine,  $\text{NO}_2^-$  is absorbed and

transported through the blood flow for two different routes: to be stored in salivary glands or be excreted by kidneys. The cycle starts again with the presence of nitrite in salivary glands returning to the oral cavity. (**Adapted from Rocha, 2011**). ..... 13

**Figure 1.9** - Enterosalivary pathway. This pathway starts with  $\text{NO}_3^-$  from the diet. Commensal bacteria are nitrate-reducing and intervene to produce  $\text{NO}_2^-$  which is reduced into  $\text{NO}\cdot$  and, part of the  $\text{NO}\cdot$  is reconverted into  $\text{NO}_2^-$  in the intestines, enhancing the latter concentration in blood. Finally,  $\text{NO}_2^-$  goes to the kidneys to be expelled from the organism or turns to the salivary glands to be stored. (**Adapted from Kevil et al., 2011**). ..... 14

**Figure 1.10** – Periodontitis disease mechanism starts with the presence of bacterial biofilm that has recognition patterns – PAMPs – that induce an inflammatory response. In this process are involved immune cells – neutrophils, macrophages, monocytes, and others – that release important biomolecules, such as MMP-8 (a protease), IL-1 $\beta$ , and TNF- $\alpha$  (interleukins) known as bacterial killers. The PGE2 is a prostaglandin, associated with bone tissue resorption. Soft tissue destruction is caused by collagen and fibronectin degradation. In addition, iNOS expression increases in macrophages, and the  $\text{NO}_2^-$  concentration is higher, inhibiting leukocyte recruitment. Consequently, the inflammation resolution failed without the macrophages' apoptosis. (**Adapted from He, 2018; Jain, 2021**). ..... 20

**Figure 1.11** - Nitrite as a signaling molecule. Acting as an sGC stimulator, inhibitor of CYP<sub>450</sub>, and modulates the HO-1 and Hsp70 expression. (**Adapted from Bryan, 2005**). ..... 22

**Figure 1.12** – Griess method for nitrite quantification. Griess reaction comprehends two steps in acidic conditions. First, nitrite ions from samples or standard solutions, react with sulfanilamide – a diazotizing reagent - and an intermediate diazonium salt is formed. Then, the salt couples with an aromatic amine N-(1-naphthyl)ethylenediamine dihydrochloride - coupling agent - forming a purple-colored azo dye that absorbs at a maximum of 540 nm. (**From Gassmann, 2016**) .... 23

**Figure 1.13** - Biosensor scheme. A specific analyte is recognized by the biological element that is immobilized in a molecularly recognizing material called biorecognitor. Signal Transducer converts biorecognition into a measurable signal detected by the detector quantifying the specific analyte present in a sample. (**From Lozano et al., 2019**). ..... 24

**Figure 1.14** - Cytochrome c Nitrite Reductase quaternary structure obtained with the program PyMOL. The Protein Data Bank Code of this protein is 1oah. The figure represents the principal chain of the protein with 519 amino acid residues (dark blue). The image shows 10 hemes c (red salmon) and other ligands: 2 zinc ions (grey), 4 calcium ions (red), and 4 Cl<sup>-</sup> ions (green). Using the X-ray diffraction technique to obtain this structure, water molecules (red dots) were detected. (**Adapted from Protein Data Bank and Cunha et al., 2003**). ..... 26

**Figure 1.15** – Schematic model of the enzymatic nitrite biosensor with direct electrochemical transduction. The electrochemically reduced enzyme ccNiR, transfers six electrons from the electrode to the nitrite, forming the product  $\text{NH}_4^+$ . (**From Almeida, 2010**). ..... 26

**Figure 1.16** - Thesis outline. All the figures in this work were prepared in Biorender. .... 27

**Figure 2.1** – Detailed scheme of an SPE/ccNiR/AOx/PVA. The working electrode is modified through the layer-by-layer deposition of two different enzymes. The first layer is composed of

ccNiR that converts  $\text{NO}_2^-$  into  $\text{NH}_4^+$ . The next layer is oxygen scavenger AOx which catalyzes the reduction reaction of  $\text{O}_2$  into water. On the top is a layer of PVA to enhance the enzyme  $k_m^{\text{app}}$  of ccNiR. .... 37

**Figure 2.2 - a)** is a screen-printed three electro system composed of a (1) carbon working electrode, a (2) carbon counter electrode, and a (3) Ag pseudo reference electrode. **b)** scheme of ccNiR/AOx/PVA/SPE. .... 38

**Figure 2.3** - ccNiR/AOx/PVA/SPE DropSens 110 connected with PalmSens SensitSmart portable potentiostat. .... 38

**Figure 3.1** - Nitrite calibration curve using the Griess Method. Each data point is the average of duplicates. The data were fitted to a straight line using the linear regression method, resulting in the following equation:  $\text{Abs.} = 0.965 [\text{NO}_2^-] + 0.039$ ,  $r^2 = 0.997$ . .... 44

**Figure 3.2** – Nitrite calibration curve using the electrochemical biosensor. SPEs were modified following SPE/ccNiR/GOx/Cat (triangles) and SPE/ccNiR/GOx/Cat/PVA (squares). Data was performed using a CV. Each data point is the average of duplicates. The data points were fitted to a straight line using the linear regression method, resulting in the following equations:  $\Delta I_{\text{cat}} = 0.0311 [\text{NO}_2^-] + 1.3991$  with  $r^2 = 0.978$  (SPE without PVA) and  $\Delta I_{\text{cat}} = 0.0135 [\text{NO}_2^-] + 1.009$  with  $r^2 = 0.993$  (SPE with 1.25% PVA). .... 45

**Figure 3.3** - Cyclic voltammograms ( $20 \text{ mV s}^{-1}$  scan rate) of the supporting electrolyte 0.1 M Tris-HCl buffer, pH 7.6, with 0.1M KCl, recorded with AOx/SPE (dark blue) and GOx/Cat/SPE (light blue) modified electrodes, in the presence of their substrates, i.e., 100 mM ascorbate, and 80 mM glucose, respectively. .... 46

**Figure 3.4 - A)** Cyclic voltammograms ( $20 \text{ mV s}^{-1}$  scan rate) of supporting electrolyte (0.1 M Tris-HCl buffer, pH 7.6, 0.1M KCl) containing the 100 mM ascorbate and nitrite (linear range, 20-200  $\mu\text{M}$ ). Measurements were recorded with ccNiR/AOx/PVA/SPE and the  $\Delta I_{\text{cat}}$  was measured at the cathodic peak height. **B)** Nitrite calibration curve using the CV electrochemical technique. Each data point is the average of duplicates. The data were fitted to a straight line using the linear regression method, resulting in the following equation:  $\Delta I_{\text{cat}} = 0.014 [\text{NO}_2^-] + 0.981$ ,  $r^2 = 0.982$ , and a linear range of 20 to 200  $\mu\text{M}$ . .... 47

**Figure 3.5 - A)** Amperograms at -0.5 V of supporting electrolyte (0.1 M Tris-HCl buffer, pH 7.6, with 0.1M KCl) containing the 100 mM ascorbate and nitrite (linear range of 2.5-300  $\mu\text{M}$ ). Measurements were recorded with ccNiR/AOx/PVA/SPE and the  $\Delta I_{\text{cat}}$  was measured at time = 60 s. **B)** Nitrite calibration curve using the CV technique. Each data point is the average of duplicates. The data were fitted to a straight line using the linear regression method, resulting in the following equation:  $\Delta I_{\text{cat}} = 0.015 [\text{NO}_2^-] + 0.802$ ,  $r^2 = 0.998$ , and a linear range of 5 to 300  $\mu\text{M}$ . .... 48

**Figure 3.6** - Influence of centrifugation on the biosensor (red circles) and Griess (blue circles) methods. Dispersion plot of nitrite concentration in saliva samples (freshly collected) before (y-axis), and after (x-axis) centrifugation. .... 52

**Figure 3.7** - Dispersion plot of nitrite concentration, measured using the biosensor, according to turbidity levels: 0 – clear samples, 1 – low turbid samples, 2 – turbid samples, 3 – very turbid samples. For that analysis, 38 samples were quantified. ....53

**Figure 3.8** – Dispersion plot of nitrite concentration, measured using the Griess method according to turbidity levels: 0 – clear samples, 1 – low turbid samples, 2 – turbid samples, 3 – very turbid samples. For that analysis, 44 samples were quantified. ....53

**Figure 3.9** – Characterization of the study populations accordingly to the health status. ...58

**Figure 3.10** - PD stages distribution. Of the 24 participants, 1 is on stage I, 3 in II, 8 in III, and 9 in IV. 3 of the patients have periimplantitis. ....59

**Figure 3.11** - Mean nitrite concentration in different PD Stages. Results were obtained with the ccNiR/AOx/PVA/SPE biosensors and using amperometric transduction. ....60

**Figure 3.12** - Mean nitrite concentration in different PD Grades. Results were obtained with the ccNiR/AOx/PVA/SPE biosensors and using amperometric transduction. ....61

**Figure 3.13** - Nitrite content according to the age group. This trial was performed using 24 PD different saliva samples. Results were obtained with ccNiR/AOx/PVA/SPE and using amperometric transduction. ....63

**Figure 3.14** - Nitrite content according to the smoke habits. This trial was performed using saliva samples from 24 persons with PD. Results were obtained with ccNiR/AOx/PVA/SPE and using amperometric transduction. ....63

**Figure 3.15** - Nitrite quantification according to food habits. This trial was performed using 24 PD different saliva samples (full), and 11 healthy individuals (stripes). Results were obtained with ccNiR/AOx/PVA/SPE and using amperometric transducing. ....65



## Table Index

<b>Table 1.1</b> - Periodontal Disease is subdivided into four stages with a focus on severity and complexity. (Adapted from Steffens, 2018; Tonetti, 2018; Costa, 2019).....	3
<b>Table 1.2</b> - Periodontal Disease is subdivided into three grades. (Adapted from Tonetti, 2018; Rita Costa, 2019). .....	4
<b>Table 1.3</b> - The three different isoforms of NOS enzymes and correspondent expression sites and functions. ....	10
<b>Table 1.4</b> - Vegetable and fruits' typical nitrite concentrations in mg per Kg of fresh/pickled vegetable, according to different authors. ....	16
<b>Table 1.5</b> - Nitrite concentrations in the salivary fluid of healthy, gingivitis, and periodontitis patients, according to different authors. ....	19
<b>Table 3.1</b> - Analytical parameters of the calibration curves obtained with SPE/ccNiR/GOx/Cat and SPE/ccNiR/GOx/Cat/PVA. ....	45
<b>Table 3.2</b> - Analytical parameters of the calibration curves obtained with the SPE/ccNiR/AOx/PVA biosensor and the Griess methods. ....	48
<b>Table 3.3</b> - Centrifugation influence on the NO <sub>2</sub> <sup>-</sup> quantification in saliva specimens by the Griess method. ....	49
<b>Table 3.4</b> - The influence of sample freezing on nitrite quantification in saliva samples by the Griess method. All the samples were centrifuged prior to measurements.....	50
<b>Table 3.5</b> - Statistical analysis of the nitrite levels obtained from the Griess method, before and after centrifugation, and from the biosensor approach, before and after centrifugation. The hypotheses tested are the following: “Griess method is affected by centrifugation” and “Biosensor performance is affected by centrifugation”. ....	52
<b>Table 3.6</b> - Influence of turbidity in both methods before and after centrifugation considering turbidity levels: 0 – clear samples, 1 – low turbid samples, 2 – turbid samples, 3 – very turbid samples. ....	54
<b>Table 3.7</b> - Freezing effect on saliva samples. ....	55
<b>Table 3.8</b> - Nitrite concentration in salivary fluid samples of fourteen volunteers to evaluate two important parameters: the influence of centrifugation in both methods and the nitrite stability in frozen samples. ....	55
<b>Table 3.9</b> - Comparison of nitrite concentrations obtained with both techniques (Griess and biosensor).....	56
<b>Table 3.10</b> – Nitrite content in two saliva samples, quantified by Griess, biosensor, and HPLC techniques. ....	57
<b>Table 3.11</b> - Pros and cons of the new nitrite biosensor (SPE/ccNiR/AOx/PVA) and the Griess method.....	57
<b>Table 3.12</b> - Sample trial genre distribution according to female and male. ....	58
<b>Table 3.13</b> - Sample trial age distribution according to different age groups. ....	58

<b>Table 3.14</b> - Nitrite concentrations according to periodontitis participants' genre.....	61
<b>Table 3.15</b> - Nitrite concentrations according to periodontitis participants' age group. ....	62
<b>Table 3.16</b> - Food habits participants' distribution.....	64





## List of Abbreviations and Symbols

AHT – Arterial Hypertension

AOx – Ascorbate Oxidase

ASAE – Autoridade de Segurança Alimentar e Económica

BOD – Bilirubin Oxidase

CAL – Clinical Attachment Loss

Cat – Catalase

ccNiR - cytochrome c Nitrite Reductase

CNS – Central Nervous System

CYP<sub>450</sub> – Cytochrome P450

DET – Direct Electron Transfer

eNOS – Endothelial Nitric Oxide Synthase

ET – Electron Transfer

FAD – Flavine Adenine Dinucleotide

FMN – Flavine Mononucleotide

GCF – Gingival Crevicular Fluid

GOx – Glucose Oxidase

HO-1 – Heme Oxygenase-1

Hsp70 – Heat shock protein

IL-1 $\beta$  – Interleukin 1 $\beta$

iNOS – Inducible Nitric Oxide Synthase

MetHb - Methemoglobin

NADPH – Nicotinamide Adenine Dinucleotide Phosphate

NaR – Nitrate Reductase

NED - N-(1-naphthyl)ethylenediamine dihydrochloride

NiR – Nitrite Reductase

nNOS – Neuronal Nitric Oxide Synthase

NOS – Nitric Oxide Synthase

PNS – Peripheral Nervous System

POCT – Point-of-care test

PVA - Poly(vinyl alcohol)

RBC – Red Blood Cell

RBL – Radiographic Bone Loss

ROS – Reactive Oxygen Species

Ser – Serina amino acid

sGC – soluble Guanylyl Cyclase

SPE – Screen-printed elctrode

WHO – World Health Organization



**Chapter**

**1**

# Introduction



# 1. INTRODUCTION

## 1.1. Periodontal Disease

### 1.1.1. Definition and Classification

According to WHO, oral diseases affect 3.5 billion people in the world and Periodontal Disease (PD) covers 1 billion cases in the global adult population (**WHO, 2022**). About, 10 to 15% of the world's population, were diagnosed with advanced periodontitis stages (**Lindhe, 2003**). In general, this disorder occurs in adults. For example, in the United States of America, about 47.2% of the adults in the 30-64 age group have PD, and above 65 years old, the percentage rise to 70.1% (**GDB compare**).

PD is known for about 5000 years and is described as a condition that affects the tissues around the teeth, namely the bone and gingival gums (**WHO, 2022**). Briefly, PD is an oral disease caused by bacterial biofilms involving the immunity system for infection control (**Highfield, 2009**).

This disease is characterized by two main phases (Figure 1.1). It begins with gingivitis, where the gums become red and swollen and bleeding can occur. After this stage, if there are no treatments to stop the disease progression, the disorder evolves into the periodontitis disease phase:

- Gingivitis – characterized by the slight swell of the gums, red gingiva, and bleeding.
- Periodontitis – characterized by the gums pulling away from the teeth, bleeding, and sometimes bone and teeth loss.

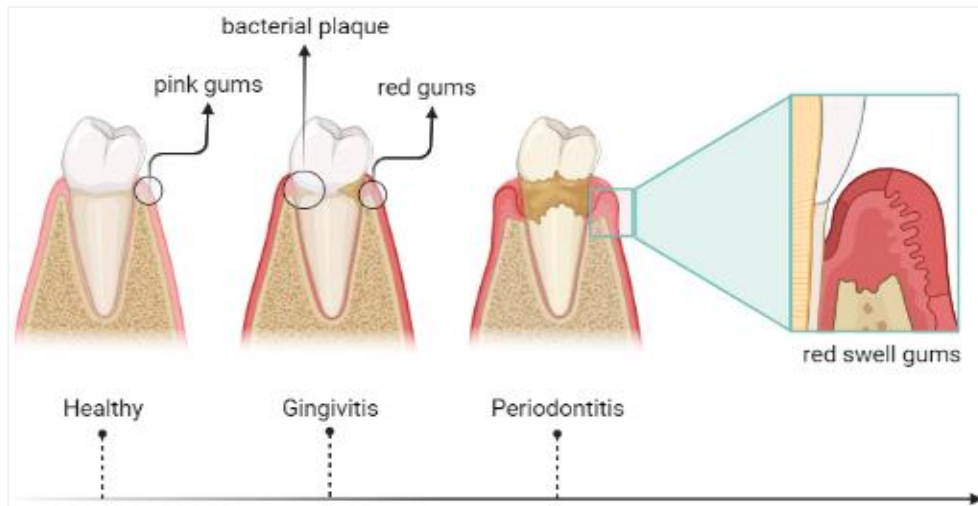


**Figure 1.1** - Scheme of periodontal disease evolution. Healthy gingiva is characterized by the pink/coral color and absence of bacterial plaque. The first phase of PD is gingivitis which is characterized by red gums, bleeding, and the presence (or not) of bacterial plaque. Periodontitis is distinguished from gingivitis because of the presence of gums pull away, bacterial plaque presence, bleeding, and sometimes accompanied by bone and teeth loss. (Adapted from Highfield, 2009).

Many modifications have been done over time to the disease classification. As proposed in 1982 by Page and Schroeder, one can identify five different forms of periodontitis in the human oral cavity. Currently, periodontitis can be specifically classified into different stages and grades (Tables 1.1 and 1.2). These two important parameters were defined according to the American Academy of Periodontology (AAP) and European Federation Periodontology (EFP) extensive knowledge (AAP, 2022).

- **Stage** classifies the severity and extension of a patient's disease. This classification is based on the measurable amount of destroyed and/or damaged tissue due to periodontitis considering the disease complexity of long-term management.
- **Grade** aims to indicate the periodontitis progression rate, awareness of the standard therapy, and systemic health potential impact.

**Table 1.1** - Periodontal Disease is subdivided into four stages with a focus on severity and complexity. (Adapted from Steffens, 2018; Tonetti, 2018; Costa, 2019).

Periodontal disease Stage		Stage I	Stage II	Stage III	Stage IV
Characteristics – Severity	<b>CAL*</b> <b>Interproximal</b>	1 – 2 mm	3 – 4 mm	≥ 5 mm	≥ 5 mm
	<b>RBL**</b>	1/3 coronal (<15%)	1/3 coronal (15 - 30%)	Until ½ or until 1/3 root apical	Until ½ or until 1/3 of the root
	<b>Tooth Loss</b>	Does not exist tooth loss due to periodontitis		≤ 4 teeth loss due to periodontitis	≥ 5 teeth loss due to periodontitis
Characteristics – Complexity	<b>Local</b>	PS maximum ≤ 4 mm  Predominantly horizontal bone loss	PS maximum ≤ 5 mm  Predominantly horizontal bone loss	<b>In addition to the complexity of stage II:</b>  - PS ≥ 6 mm - Vertical bone loss ≥ 3 mm - Furcal defects - Moderate crest defects	<b>In addition to the complexity of stage II:</b>  The necessity of complex rehabilitation by: - Masticatory dysfunction - Occlusal trauma 2 <sup>nd</sup> (mobility ≥ 2) - Severe crest defects - Bite collapse, tooth malposition, and pathological migration - < 20 teeth remain
<b>Extension and Distribution</b>	From each stage, describe the extension as <b>LOCAL</b> (< 30 % of involved teeth), <b>GENERALIZED</b> , or <b>MOLAR/INCISOR PATTERN</b>				

\*CAL - Clinical attachment loss

\*\* RBL - Radiographic Bone Loss



**Table 1.2** - Periodontal Disease is subdivided into three grades. (Adapted from Tonetti, 2018; Rita Costa, 2019).

Periodontal disease Grade			Grade A Slow progression	Grade B Moderate progression	Grade C Rapid progression
Characteristics	Determinant	Direct Evidence	No evidence of bone loss or CAL in 5 years	Bone loss or CAL < 2 mm in 5 years	Bone loss or CAL ≥ 2 mm in 5 years
		Indirect Evidence	% bone loss / age = < 0.25	% bone loss / age = 0.25 - 1	% bone loss / age = > 1
	Secondary		Existence of dense biofilm deposits with a low level of destruction	Proportional destruction with biofilm deposits	Bone destruction exceeds the expectations for the quantity of present biofilm; Suspicion of rapid progression periods and/or early disease progression
Grade Modifiers Risk Factors			Normoglycemic or non-diabetes diagnosis	HbA1c* < 7% in diabetes patients	HbA1c* ≥ 7% in diabetes patients
			Non-smoker	<10 cigarettes per day	> 10 cigarettes per day

\* HbA1c – Glycated Hemoglobin (Pinheiro, 2022)

Diabetes is an important grade modifier. People with this condition cannot be submitted to periodontal surgery or other treatments for PD. As well as smoking habits that can enhance the disease grade.

The disease progression can affect the bone tissues. Before the 20<sup>th</sup> century, the bone in the infected area was removed by a flap surgery (**Highfield, 2009**), but nowadays, the approaches are focused on bacterial-plaque control, and hygiene care. In severe cases, periodontal surgery is done to remove the gingival gums (**Jain, 2021**). The grade and stage of a patient are established in the diagnosis appointment and never go back for lower disease levels (only for higher levels). Nevertheless, in the early PD stage, the currently available treatments can retard the condition's progress (**Jain, 2021**).

### 1.1.2. Causes

Before the 19th century, only systemic factors were pointed out as the PD cause. During this century, A. Witzel (1847-1906) and W.D. Miller (1853-1907) recognized periodontal disease as a disorder originating from the presence of oral bacteria in the periodontium (**Highfield, 2009**). Nowadays, evidence points out that plaque-induced gingivitis is formed by a lack of oral hygiene, malnutrition, and some medications. On the other hand, non-plaque-induced gingivitis could be

caused by specific viral, bacterial, or fungal infections, lesions caused by trauma, or even systemic conditions (allergic reactions), among others (**Highfield, 2009**) that can evolve into PD.

Naturally existing bacteria on dental surfaces, such as gram-negative bacteria – *Prevotellae* and *Fusobacteria* – and aerobic commensal gram-positive bacteria – *Actinomyces* and *Streptococci* – can form oral biofilms, commonly known as dental plaque (**Mariotti, 2015**). This dental bacterial biofilm has a recognizable red color due to the presence of *Porphyromonas gingivalis*, *Actinobacillus actinomycetemcomitans*, *Treponema denticola*, and *Prevotella intermedia* (**He, 2018**). Gingival inflammation is the result of endogenous microflora present in the gingival crevice. The bacterial species and pathogens present in the biofilm affect the tissues and their functions, causing inflammation, tissue destruction, and ultimately, the loss of teeth by one or two of the following mechanisms (**Lindhe, 2003**):

- **Mechanism 1:** direct action of microorganisms and their products on tissues.
- **Mechanism 2:** the result of microorganisms evoking a tissue-damaging inflammatory response.

Besides the activity of microbial flora, other risk factors contribute to the development of PD, such as tobacco, malnutrition, or poor oral hygiene habits (see **Risk Factors** section).

### 1.1.3. Periodontitis prevalence and incidence<sup>1</sup>

Despite the improvements in oral hygiene and health care, PD has a big impact on the population affecting both developed and developing countries, where it raises health concerns (**Nazir, 2017**).

The prevalence of PD in both sexes and all ages is shown in figure 1.2. for different countries. In developed countries, such as Portugal, Germany, and the United States of America the number of active cases per 100 000 residents, in 2019 was 15, 23, and 12 thousand, respectively (**GDB compare**). In less developed countries, such as India, the Republic of Korea, or Sub-Saharan Africa, the prevalence, per 100 000 residents, in 2019 was 15, 15, and 13 thousand, respectively. In less developed countries, lack of information could compromise these data, considering higher PD numbers. Germany and the United States of America presented decreased tendency

---

<sup>1</sup> Prevalence and incidence are two different concepts. Prevalence refers to the number of active cases at a specified point in time in the population at the same point in time (**from CDC, 2013**). The Incidence determines the new cases of a disease during a specified time window in a risk population at the start of the time interval (**Fajardo-Gutiérrez, 2017**).

whereas, in Portugal and developing countries, the tendency is to have more active cases per 100 000 residents (**GDB compare**).

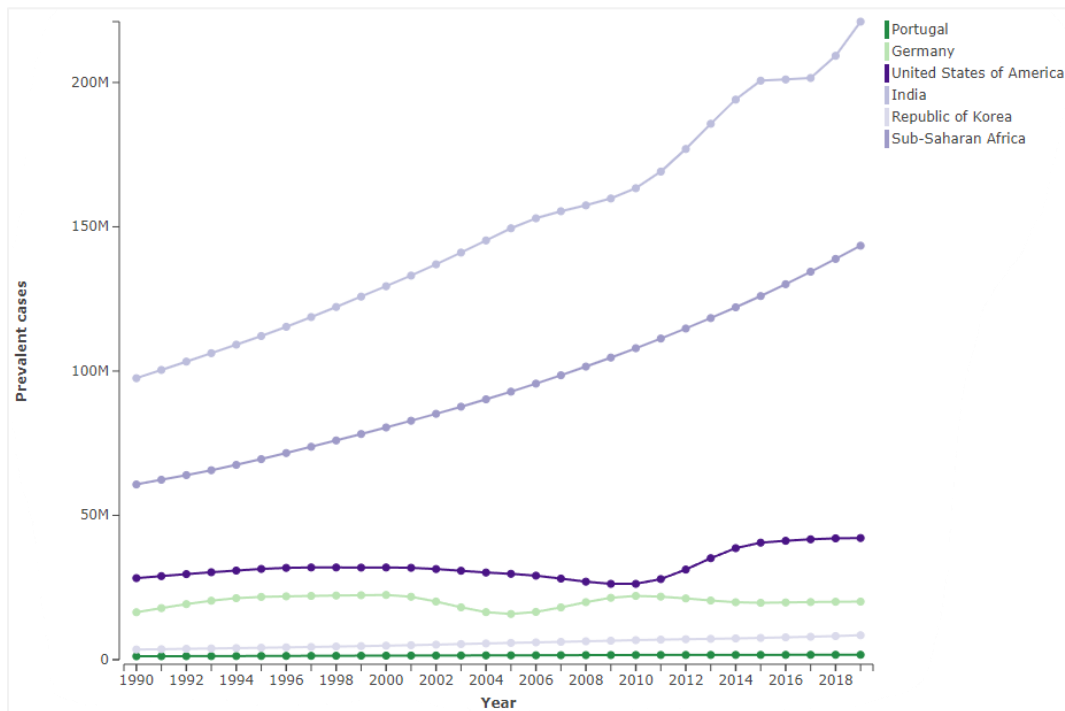


**Figure 1.2** - Periodontitis population prevalence (both genders), in developed (Portugal, Germany, and the United States of America) and less developed countries (India, Republic of Korea, and Sub-Saharan Africa). (**From GDB compare**)

In 2019, 27% of the active cases were found within the 50 to 69 age group, which is the predominant periodontitis group. This means that the disease prevalence tendency is to increase in the older population. The incidence has been increasing over time in all age groups (Figure 1.3), more in the 25-49 and above 70 years old groups (**from GDB compare**).



**Figure 1.3** - Periodontitis prevalence (left), and incidence (right), in the population of both genders, in Portugal (**adapted from GDB compare**). Data collected for different age groups: 10-24 (green), 25-49 (blue), 50-69 (purple) and >70 (coral) years old. Prevalence refers to the number of active cases in the population. The Incidence determines the number of cases in a risk population in a determined time window (**Fajardo-Gutiérrez, 2017**).

### 1.1.4. Symptoms and Clinical Diagnosis

During periodontitis progression, oral tissues are injured compromising their integrity. The injuries are characterized by gingiva color changes, bone loss, and bleeding (**Jain, 2021**). The clinical diagnosis of PD is based on the recognition of the symptoms and the evaluation of the gingival tissue morphology, namely:

- Gingival crevice out of 1-3 mm deep range.
- Gingival tissue with changes in color, contour, and texture.
- Bleed.
- Pain.
- Presence of deeper pockets with high volumes of gingival crevicular fluid (GCF<sup>2</sup>).
- The low resistance of the tissue to the periodontal probe.

For the diagnosis, a periodontal chart is filled with the gingival tissue morphology parameters. The size of commonly formed pockets has the same horizontal and vertical dimensions. The color-altered pockets and gums formed are a bleed indicator. Tooth migration and mobility are relevant but are not exclusive factors for periodontal disease diagnosis since previous trauma could cause migration. The pain felt is also a symptom to consider (**Highfield, 2009**). If necessary, the clinician uses complementary techniques, such as radiographs. The diagnosis is also a result of the patient's clinical history.

As an inflammatory disease, for PD diagnosis, biomarkers hold an important role to evaluate inflammatory mediators released in an immune process (**Jain, 2021**), as explained in detail in the ***Periodontal disease biomarkers*** section.

### 1.1.5. Risk Factors

A risk factor is described as a characteristic or occurrence that has been associated with a high rate of disease occurrence, for example, PD occurrence could be increased if the patient has smoking habits. A risk factor does not necessarily cause the disease but is associated with the disease (**Nazir, 2017**). PD has several risk factors with both environmental (modifiable risk) and systemic causes (non-modifiable risk). Environmental factors are modifiable by individuals' habits that, when modified, can decrease the disease risk (**Van Dyke, 2005**). These risk factors are explained below:

---

<sup>2</sup> GCF is a serum exudate fluid, collected from the gingival sulcus surrounding natural teeth (**Topcu, 2014**).

- **Smoking:** smokers have a higher probability of having periodontal attachment and bone loss which, culminates in the progression of destructive PD (**Mariotti, 2015**).
- **Medications:** affect the periodontium with overgrowth of gingival tissue and a reduction of salivary flow (dry mouth sensation) (**Nazir, 2017**).
- **Nutrition:** malnutrition culminates in an exacerbated response of the periodontal tissues to biofilm bacteria (**Mariotti, 2015**).
- **Stress:** stress contributes to pathogenic infection through salivary fluid reduction and, consequently, bacterial biofilm formation (**Mariotti, 2015**).
- **Pre-existing periodontal pockets:** the presence of residual pockets >4 mm with bleeding (**Mariotti, 2015**).
- **Pre-existing biofilm:** biofilm could induce inflammation (**Mariotti, 2015**).
- **Occlusion:** occlusal forces cause progressive mobility of the tooth with conjugation of biofilm-induced inflammation-provoking periodontitis (**Mariotti, 2015**).
- **Hygiene:** the presence of supragingival plaque and consequently the presence of bacterial biofilm (**Mariotti, 2015**).
- **Diabetes:** has direct and negative effects on inflammation when not controlled (**Jain, 2021**).
- **Age:** older groups are affected by the prevalence and disease severity (**Nazir, 2017**).

## 1.2. Nitrites in human physiology

### 1.2.1. NO<sup>-</sup> physiological paper

Nitric Oxide (NO<sup>-</sup>) is an intracellular messenger acting as a physiological mediator when in low concentrations, playing immune, cardiovascular (blood flow regulator), and neurological functions (**Sundar, 2013**). The inorganic nitrite anion is present in the human organism as a product of two endogenous pathways, the L-arginine path, and the nitrate-nitrite-nitric oxide (NO<sub>3</sub><sup>-</sup>-NO<sub>2</sub><sup>-</sup>-NO) route. Furthermore, nitrite could be provided from the diet, corresponding to the exogenous source.

The classic L-arginine pathway is dependent on enzymes that synthesize NO<sup>-</sup> from this amino acid, in presence of the oxygen, the nitric oxide synthases (NOS), which were first found in 1980 by Tannenbaum (**Gladwin et al., 2005**). The exaggerated action of NOS enzymes culminates in the overproduction of NO<sup>-</sup>, consequently, in nitrosative stress that can cause cellular and DNA damage (**Karwowska, 2020**).

An alternative  $\text{NO}\cdot$  source is the  $\text{NO}_3^-$ - $\text{NO}_2^-$ - $\text{NO}\cdot$  via. In hypoxia conditions, the NOS-dependent pathway (L-arginine route) is unable to keep up the  $\text{NO}\cdot$  production, so nitrite is reduced to  $\text{NO}\cdot$  as a backup pathway (Lundberg et al., 2008).

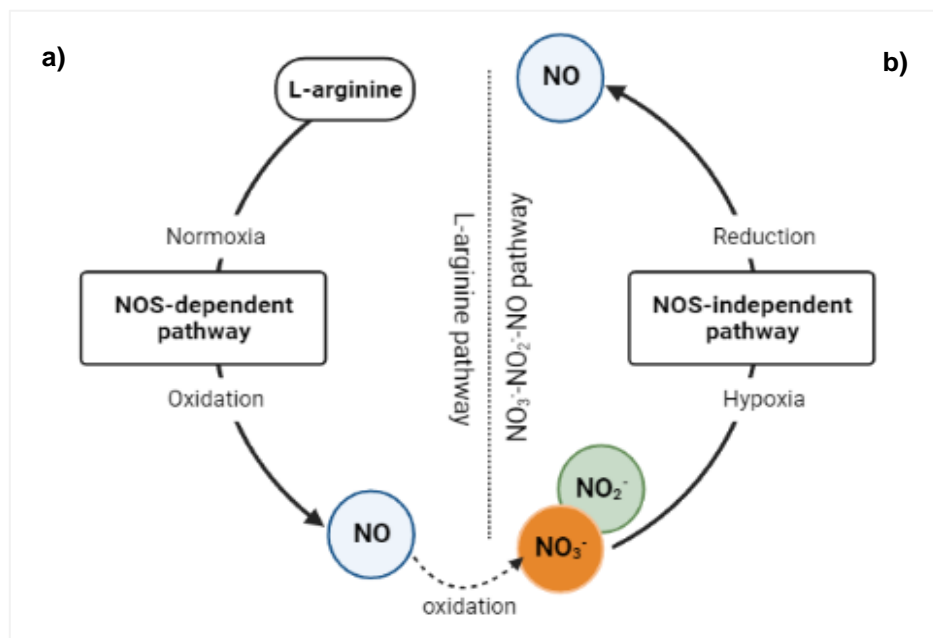
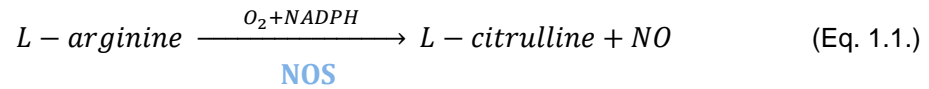


**Figure 1.4** - The two physiological pathways to obtain  $\text{NO}\cdot$ . a) The L-arginine pathway uses this amino acid as the substrate of NOS enzymes in Normoxia conditions, to obtain  $\text{NO}\cdot$ . b) Nitrate-nitrite- $\text{NO}\cdot$  pathway occurs without the presence of oxygen (hypoxia conditions). In this case,  $\text{NO}_3^-$  is reduced to  $\text{NO}_2^-$  which in turn is reduced to  $\text{NO}\cdot$ . The two pathways have a connection point since  $\text{NO}\cdot$  provided from the L-arginine route can be oxidized to  $\text{NO}_2^-$  and  $\text{NO}_3^-$ . (Adapted from Lundberg, 2008).

In addition to the physiological sources of nitrite in the organism, this ion can be ingested from green vegetables and cured meats, where nitrite salts are used as preservatives, and to give the meat a brighter red color (Gladwin et al., 2005). Human exposure to nitrite can also result from the consumption of contaminated water from bad agricultural practices or fish decomposition contributing to water's higher nitrite concentration (Almeida, 2010).

### 1.2.2. L-arginine pathway

As mentioned above, the L-arginine pathway is enzymatically dependent on the NOS enzyme and uses the L-arginine amino acid as substrate, which is converted to L-citrulline, with  $\text{NO}\cdot$  release. This reaction is  $\text{O}_2$ , and NADPH (co-substrate) dependent as shown in Equation 1.1 (Karwowska, 2020).



Depending on the tissue and function, different isoforms are expressed, denominated as nNOS, iNOS, and eNOS, as presented in table 1.3 (Förstermann, 2012; Kevil et al., 2011) since they are expressed in the brain, macrophages, and in the endothelium, respectively (Karwowska, 2020).

**Table 1.3** - The three different isoforms of NOS enzymes and correspondent expression sites and functions.

Isoform	Expression site	Function(s)
Neuronal NOS (nNOS)	- Specific neurons of the central system (CNS) - Peripheral nervous system (PNS)	(CNS) Synaptic plasticity and blood pressure regulation. (PNS) Atypical neurotransmission and penile erection.
Inducible NOS (iNOS)	- Macrophages	Nonspecific immune defense against bacterium and parasites, mediation of inflammation, and septic shock control.
Endothelial NOS (eNOS)	- Endothelium	Vasodilatation, vasoprotection, and prevention of atherosclerosis.

The NOS enzyme from *Homo sapiens* is classified as an oxidoreductase (E.C.1.14.13.39) with 102.37 kDa (from RCBSPDB and Genomenet). The three isoforms have a similar heme co-factor localized in the N-terminal domain, close to the catalytic center (Liu, 2019). NOS also binds the BH<sub>4</sub> cofactor, as seen in figure 5. The C-terminal reductase domain binds to FMN, FAD, and NADPH (H. Li, 2014).

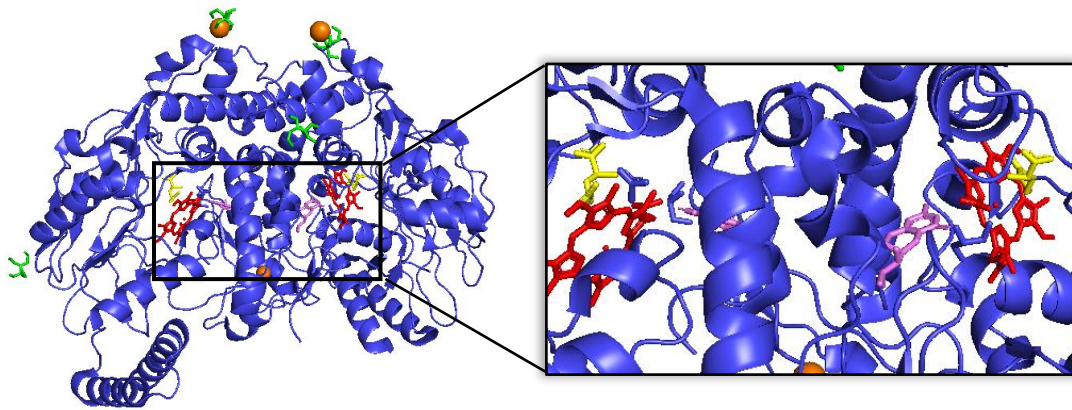


**Figure 1.5** - Human endothelial NOS enzyme (PDB 4D1O). The figure represents the principal chain of the heme domain of the protein with 440 amino acid residues (dark blue). L-arginine (yellow) has a specific binding site, near protoporphyrin IX containing Fe (red). The image shows other ligands: two tetrahydrobiopterin (pink), and three gadolinium ions (orange). The structure was prepared with the PyMOL program.

Following the formation of  $\text{NO}\cdot$  and L-citrulline, the latter goes to the urea cycle to form arginine in the kidneys, whereas the former can go through different pathways (the formation of nitrite is the most important one for this work) (H. Li, 2014). At last,  $\text{NO}\cdot$  is oxidized to nitrite, which is oxidized to  $\text{NO}_3^-$  through interaction with oxyheme proteins (Kevil et al., 2011).

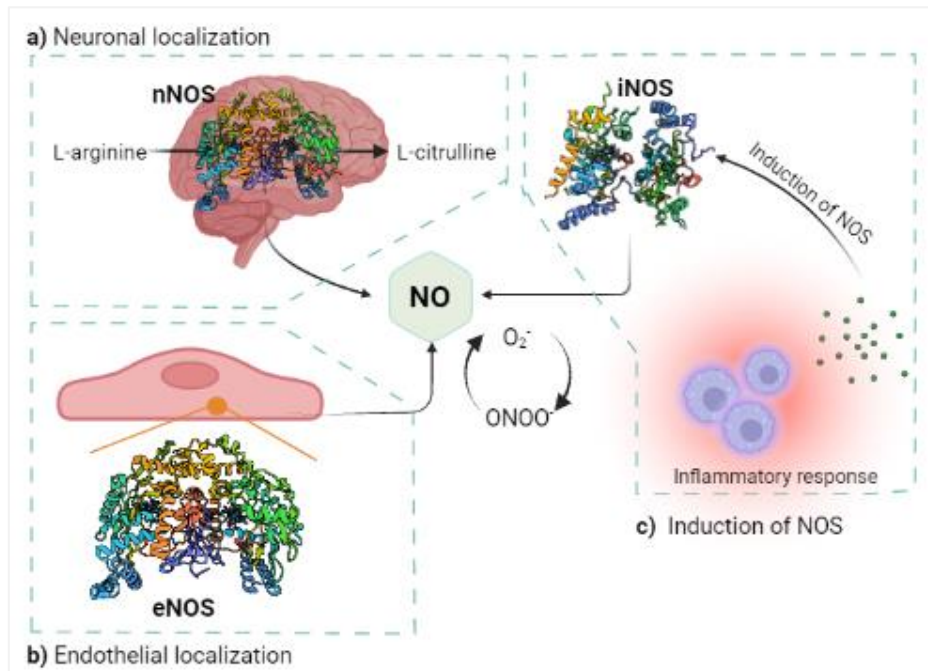


**Figure 1.6** - L-arginine pathway and the three NOS enzyme isoforms. a) nNOS is located in the neuronal tissue and converts L-arginine into L-citrulline. b) eNOS is localized in endothelial cells. c) iNOS is inducible, in macrophages, by an inflammatory reaction mediated by cytokine release (Adapted from Kleinbongard, 2006; Kevil et al., 2011).



The regulation of nNOS and eNOS isoforms depends on two different mechanisms: calcium-dependent activation, and calcium-independent activation. The iNOS is activated in macrophages, induced by the cytokines released in inflammatory processes, and needs large amounts of  $\text{Ca}_2^+$  (Bejeh-Mir et al., 2014; Zhao, 2015).

The eNOS enzyme is expressed constitutively, being responsible for 70 to 90 % of nitrite in human plasma (Kevil et al., 2011). nNOS is also expressed constitutively but the overproduction of  $\text{NO}\cdot$  by neuronal NOS is associated with neurological complications (Kevil et al., 2011). As for iNOS, it is expressed in the human body, as an inflammatory response, like the case of PD. Consequently,  $\text{NO}_3^-$  and nitrite are above the normal values (200 to 600 nM) in an inflammatory condition (Kevil et al., 2011).

The physiological role of nitrite and the consequences of their high/low concentrations will be discussed in the *Physiological role of Nitrite* section.

Nitrite is present in the endothelium, consequently in the vascular lumen. In the presence of oxygen,  $\text{NO}\cdot$  has a relatively short life (Almeida, 2010) and the endothelium-derived  $\text{NO}\cdot$  is oxidized to nitrite into nitrate. According to Gladwin et al., the nitrite concentration in vital organs is in the range of 0.3 to 20  $\mu\text{M}$ .

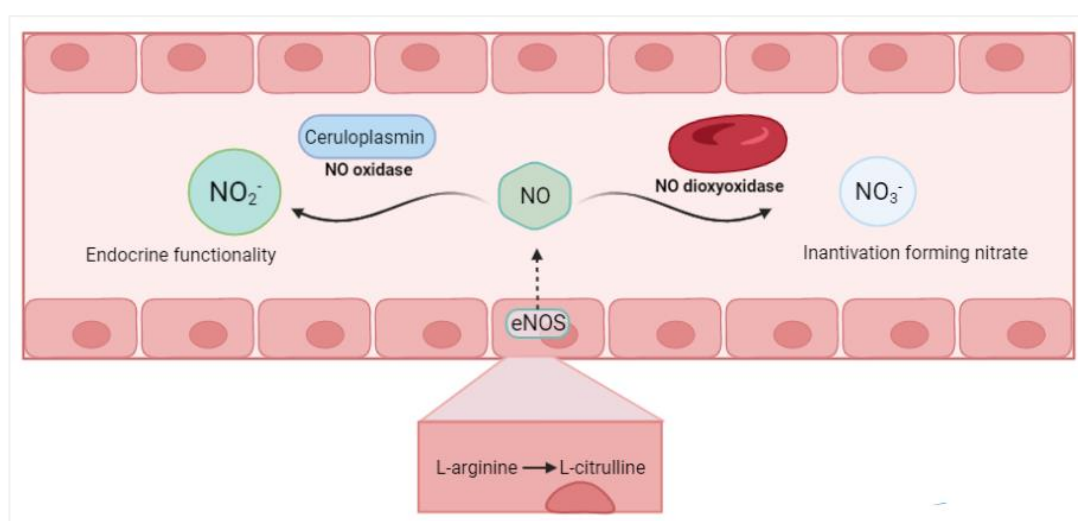


**Figure 1.7** - Endothelium distribution of nitrite. In endothelial cells, the eNOS enzyme is present and promotes the enzymatic conversion of L-arginine into L-citrulline resulting in NO production. The NO can cross through the plasmatic cell membrane, which will be converted into nitrate, mediated by NO dioxygenase present in red blood cells (RBC), and oxidized into nitrite – by NO oxidase action accompanied by ceruloplasmin (Adapted from Shiva, 2010).

Nitrite is also present in brain tissue produced via nNOS, where it plays a relevant role in certain forms of synaptic plasticity, memory, learning functions, and the process of sensorial information (Salter, 1996).

### 1.2.3. $\text{NO}_3^-$ - $\text{NO}_2^-$ -NO pathway

The NO $\cdot$  pathway was found in the 80s of the 20th century, by Hibbs. While the L-arginine NOS-dependent pathway is O $_2$  dependent,  $\text{NO}_3^-$ - $\text{NO}_2^-$ -NO occurs in hypoxia conditions and contributes to the largest levels of nitrite in our organism. Furthermore, is a backup NO $\cdot$ -producing system when the L-arginine pathway is blocked (Kevil et al., 2011). Therefore, when its biosynthesis decreases, the risk of cardiovascular diseases is enhanced (Tang, 2011).

This pathway starts with the load of the electron acceptor  $\text{NO}_3^-$  (from endogenous and/or exogenous sources), which is reduced to nitrite by oral facultative anaerobic bacteria since mammalian cells cannot directly metabolize nitrate into nitrite. Nitrite is then taken to the stomach through the salivary fluid where the low pH facilitates the protonation of nitrite forming nitrous acid ( $\text{HNO}_2$ ). In the gastric lumen (stomach), some reactions after, nitrate and nitrite were formed, going to the intestine. Then, in the intestinal mucus, nitrite is absorbed and transported through the blood flow to two different destinations: to be absorbed in salivary glands or to be excreted by kidneys (Lundberg, 2008).

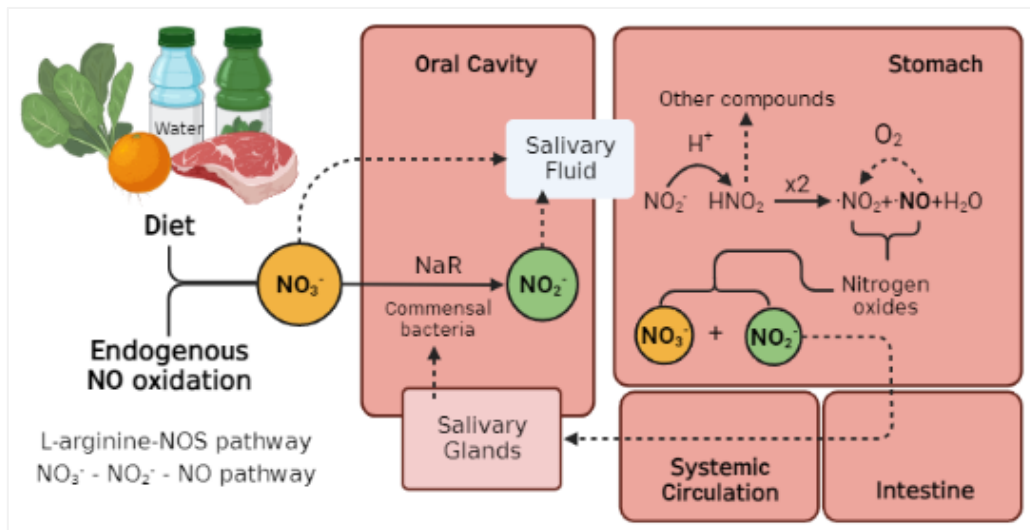


**Figure 1.8** - The  $\text{NO}_3^-$ - $\text{NO}_2^-$ -NO pathway starts with  $\text{NO}_3^-$  loading from exogenous (diet) and endogenous oxidation of NO $\cdot$ . In the oral cavity,  $\text{NO}_3^-$  is reduced into  $\text{NO}_2^-$  by facultative anaerobic bacteria. The salivary fluid goes to the stomach and  $\text{NO}_2^-$  is protonated into  $\text{HNO}_2$ , in acidic conditions. Several reactions later,  $\text{NO}_3^-$  and  $\text{NO}_2^-$  are formed. In the intestine,  $\text{NO}_2^-$  is absorbed and transported through the blood flow for two different routes: to be stored in salivary glands or be excreted by kidneys. The cycle starts again with the presence of nitrite in salivary glands returning to the oral cavity (Adapted from Rocha, 2011).

#### 1.2.3.1. Nitrite and the enterosalivary circulation

The concentration of nitrite in the saliva is closely related to the enterosalivary pathway combining endogenous and exogenous nitrite sources. Saliva is a biological fluid composed of

proteins ( $\alpha$ -Amilase protein and mucins) (Osório, 2020), other compounds, and bacteria, such as the commensal nitrate-reducing ones present in the tongue backside (Kevil et al., 2011).

The salivary microbiome has been studied and some of the nitrate-reducing bacteria are *Prevotella*, *Granulicatella*, *Rothia*, *Veillonella*, *Neisseria*, *Actinomyces*, *Haemophilus*, *Fusobacterium*, *Leptotrichia*, and *Campylobacter* (Pignatelli, 2020), facultatively anaerobic bacteria (Lundberg, 2008). The abundance of commensal bacteria in the mouth decreases significantly when antibiotics and antiseptic mouthwashes were used, consequently, the nitrite concentration decreases (Kevil et al., 2011). The influence of dietary nitrate in the oral cavity depends on bacterial microflora. The higher the  $\text{NO}_3^-$  concentration in aliments, the higher the nitrite in saliva (Bryan, 2016). Even though, only 5 to 7% of nitrates from the diet are reduced to nitrite by oral bacteria.

Nitrate is reduced to nitrite by nitrate reductases (NaR) (Lundberg, 2008) which goes to the stomach where it is converted to  $\text{NO}$ , as explained in previous **subsection 1.2.3**. Then,  $\text{NO}$  goes to blood flow enhancing plasma concentration. This pathway is a cycle of nitrite that can be reabsorbed, returning to the oral cavity (via enterosalivary circulation, from plasma to saliva), or excreted by kidneys (Kevil et al., 2011).

Besides the exogenous sources, the saliva nitrite concentration is affected by two factors: the common nitrate intake from diet or, the endogenous overproduction of  $\text{NO}$  in pathological situations. In pathological situations, the L-arginine route, mediated by the iNOS enzyme (inducible in an inflammatory process), produces high amounts of  $\text{NO}$  which is rapidly oxidized into nitrite, as an answer to the inflammatory stimulus (Kevil et al., 2011).

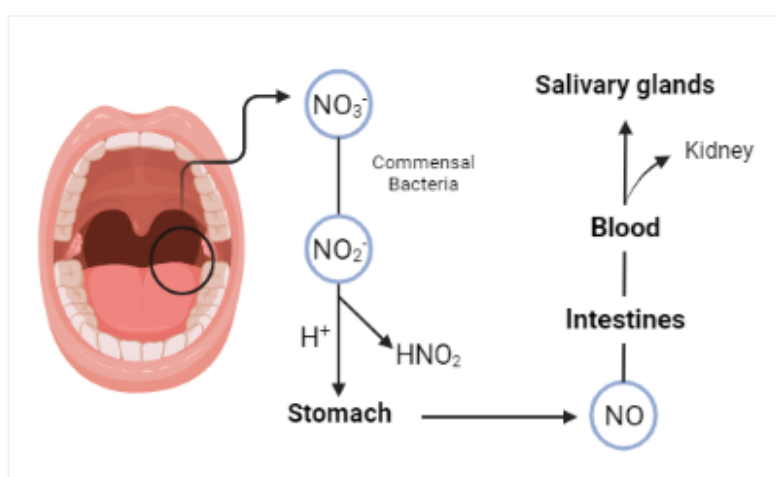


**Figure 1.9** - Enterosalivary pathway. This pathway starts with  $\text{NO}_3^-$  from the diet. Commensal bacteria are nitrate-reducing and intervene to produce  $\text{NO}_2^-$  which is reduced into  $\text{NO}$  and, part of the  $\text{NO}$  is reconverted into  $\text{NO}_2^-$  in the intestines, enhancing the latter concentration in blood. Finally,  $\text{NO}_2^-$  goes to the kidneys to be expelled from the organism or turns to the salivary glands to be stored (Adapted from Kevil et al., 2011).

## 1.2.4. External sources

Nitrite is a flavorless and odorless compound, present in vegetables, meat, fish, processed food, and drinking water (**Almeida, 2010; Hickey, 2021**). According to the literature, diet nitrates mostly come from vegetables and drinking water. However, nitrite comes from vegetables, fruits, and meat (**Hord, 2009**).

Nitrite is present in foodstuffs as nitrite salts ( $\text{NaNO}_2$ ) that are used as preservatives in the food industry, i.e., in fresh or smoked meat products (**Gladwin et al., 2005**). These salts give a strong red color to meat (**Gladwin et al., 2005**) and can also inhibit the growth and proliferation of pathogenic microorganisms such as *Clostridium botulinum* (**Ma, 2017**) and *Helicobacter pylori* (**Pereira, 2013**). This microorganism control is nitrite and  $\text{O}_2$ -dependent. Fundamentally it is a consequence of the inhibition of the active transport of glucose since the nitrite occupies the electron-accepting site where the oxidative phosphorylation occurs (**Rowe, 1979**). In addition to the glucose apport, also oxygen intake is inhibited.

Nitrate and nitrite are naturally present in vegetables, fruits, and water. Sometimes, considering bad agriculture practices, nitrogen fertilizers contribute to higher nitrite concentrations in underground waters near drinking water sources (**ASAE, 2007**).

Nevertheless, nitrite could be prejudicial to the organism if the concentrations are higher than the basal ones, which commonly can provoke methemoglobinemia and *N*-nitroso compounds production (**Bryan, 2005**). Because of the higher nitrite concentrations in fertilizers and drinking water, the World Health Organization (WHO), the European Union Regulation (EUR), and the Food and Drug Administration (FDA) established maximum admissible nitrite values. For drinking water (3 mg/mL) (**WHO, 2014**), and meat (100 mg/kg) (**EUR, 2008**). In Europe, the legislation is more restricted compared with the USA (**Ledezma-Zamora, 2021**).

Nitrite content in vegetables and fruits is influenced by plant species, soil nitrite concentration, osmotic stress, and other factors (**Muhaidat, 2019**). However, fertilizers' can influence nitrite concentrations being important to monitor the limit values.

**Table 1.4** - Vegetable and fruits' typical nitrite concentrations in mg per Kg of fresh/pickled vegetable, according to different authors.

	Product	[NO <sub>2</sub> <sup>-</sup> ] (mg kg <sup>-1</sup> )	Reference
Vegetables and Fruits	Spinach	0.73	Muhaidat, 2019
		0.2	Hord, 2009
	Lettuce	2.15	
	Cabbage	0.41	
		0.26	Muhaidat, 2019
	Cauliflower	0.25	
	Onion	0.42	
	Vegetable juice *	0.092	Hord, 2009
	Banana	0.09	
	Orange	0.2	
	Fruit salad	0.8	
	Pomegranate juice *	0.069	
	Cured meat	Pickled cabbage	3.08
Pickled turnip		2.68	
Bacon **		40	Ledezma-Zamora, 2021
Sausage **		90	
Ham **		45	
Cured meat		Bacon	3.8
	Sausage	0.5	
	Ham	8.9	

\* NO<sub>2</sub><sup>-</sup> concentration in mg/L

\*\* Nitrite concentration represented as NaNO<sub>2</sub> in mg kg<sup>-1</sup>

### 1.3. Health risks

Although nitrite presence is natural in food, its consumption in high amounts has health effects. Thus, it represents a health concern. According to some international organizations (WHO and FDA), the presence of higher nitrite concentration in food is associated with an increase in gastrointestinal cancer and methemoglobinemia cases (**Hord, 2009**).

### 1.3.1. Cancer

The consumption of fresh or preserved meat and fish is associated with an increase in cancer. Nitrite is recognized as a carcinogenic potentiator since, after its oxidation, can react with secondary amines to produce carcinogenic compounds, namely, carcinogenic *N*-nitrosamides (**Hord, 2009**). This process occurs in acidic conditions, i.e., in the stomach (the common cancers are gastric, colon, and esophageal). Because of this carcinogenic potential, the WHO established a maximum daily nitrite consumption of 0.06 to 0.07 mg/kg (**Ma, 2017**). Due to the use of nitrite salts to preserve meat and other foods, the American Institute for Cancer indicates that the consumption of 500 g of meat (fresh or processed) per week does not necessarily imply an associated risk of cancer (**Hord, 2009**). Nonetheless, smoking or drinking beer can contribute to 100 to 1000 times more nitrosamines than the daily diet (**Ma, 2017**).

According to some authors, the conversion of nitrite into nitrosamines in the stomach can reduce the inhibition of secondary amine nitrosylation, enhancing the latter concentrations. Nevertheless, the relationship between the endogenous production of nitrite and cancer in humans is still inconclusive (**Hord, 2009; Ma, 2017**).

### 1.3.2. Methemoglobinemia

Methemoglobinemia, also called the “blue baby syndrome”, is a disease that affects, not exclusively, infants. It occurs, mostly, from two sources: due to bacterially contaminated water sources which are rich in nitrates, or from the  $\text{NaNO}_2$ , present in fresh and processed meat and other foods. The iNOS-mediated production of the  $\text{NO}\cdot$  is activated by the presence of bacteria from contaminated water sources (**Hord, 2009**).

This condition is a result of the nitrite-mediated oxidation of the ferrous iron ( $\text{Fe}^{2+}$ ) in oxyhemoglobin into ferric iron ( $\text{Fe}^{3+}$ ) in methemoglobin (MetHb) (**Hord, 2009**). Methemoglobin is the oxidized form of hemoglobin and the capacity to bind oxygen is compromised culminating in systemic tissue hypoxia and cyanosis and, if untreated, can cause death (**Hickey, 2021**).

Recent studies revealed a new intentional sodium nitrite poisoning trend using nitrite and nitrate salts (**Khan, 2019; Mudan, 2020, Hickey, 2021**).

### 1.3.3. Current Perspectives

The relationship between NO· and gastrointestinal cancer and methemoglobinemia is a controversial topic that has been prompting a great deal of discussion among the scientific community. Some authors, such as Lundberg and Laranjinha, have shown that the consumption of green leafy vegetables can generate large amounts of NO· in the human stomach (**Lundberg, 1994**) through the nitrate-nitrite-NO via. This pathway needs acidic conditions to reduce nitrite into NO·, which is physiologically found in the stomach. The uptake of nitrate to the oral cavity from the enterosalivary circulation and diet contributes to the constant presence of nitrite in the stomach, which is at much higher levels than the systemic concentrations (**Laranjinha, 2021**).

Some biological effects have been attributed to NO· such as the increase in mucosal blood flow and mucus formation (preventing gastric damage), protection against hepatic and cardiac ischemia, and improvement of systemic vascular functions (**Laranjinha, 2021**), emphasizing the importance of the NO<sub>3</sub><sup>-</sup>-NO<sub>2</sub><sup>-</sup>-NO pathway in human physiology.

## 1.4. Physiological role

### 1.4.1. Periodontal disease biomarkers

As mentioned in section 1.2.2, the iNOS activity is induced in several inflammatory conditions, including PD. According to several reports, the consequent production of NO·, increases the concentration of its oxidation metabolite, nitrite, in the salivary and gingival crevicular fluids, compared to healthy patients (**Topcu et al., 2014**). Therefore, the role of nitrite as a PD biomarker in advanced diagnosis techniques has been gaining interest. The saliva stimulation or non-stimulation, during sampling, can vary the nitrite concentration (**Sánchez, 2014**) so strict protocols are needed for the saliva fluid collection. Not surprisingly, different authors reported different nitrite concentrations (Table 1.5); in some studies, periodontal patients have lower nitrite concentrations in saliva and CG fluids. This could mean that the sampling and analytical conditions could affect the concentration of this metabolite.

**Table 1.5** - Nitrite concentrations in the salivary fluid of healthy, gingivitis, and periodontitis patients, according to different authors.

Disease stage	Salivary Fluid ( $\mu\text{M}$ )	Quantification Method	Obs.	Ref.
<b>[Nitrite] Healthy</b>	Unstimulated saliva $8.67 \pm 8.68$	Griess Method	Chronic Periodontitis. 147 patients. Sampling between 10 to 11 a.m. Freeze ( $-80^{\circ}\text{C}$ ) and centrifuge samples.	Topcu, 2014
	Unstimulated saliva 300	Griess Method	Freeze ( $-20^{\circ}\text{C}$ ) and N/centrifuged samples. With the influence of food or fluid intake.	Sánchez, 2014
	Stimulated saliva $5.86 \pm 1.58$	Griess Method	Stimulated saliva. 10 individuals in the control group. Sampling between 10 and 11 a.m. Freeze ( $-20^{\circ}\text{C}$ ) and Centrifuged samples	Reher, 2007
	Stimulated saliva $92.5 \pm 13.6$	Chemiluminescence assay	Stimulated saliva. Freeze ( $-80^{\circ}\text{C}$ ). Sampling between 7 to 9 a.m.	Meschiari, 2015
	Unstimulated saliva $43 \pm 14$	Chemiluminescence assay	Centrifuge and Freeze ( $-20^{\circ}\text{C}$ ) samples	Bjorne, 2004
<b>[Nitrite] Gingivitis</b>	Unstimulated saliva $5.56 \pm 4.53$	-	Chronic Periodontitis. 183 patients. Sampling between 10 and 11 a.m. Freeze ( $-80^{\circ}\text{C}$ ) and centrifuge samples.	Topcu, 2014
<b>[Nitrite] Periodontitis</b>	Unstimulated saliva $5.55 \pm 5.39$	Griess Method	Chronic Periodontitis. 150 patients. Sampling between 10 and 11 a.m. Freeze ( $-80^{\circ}\text{C}$ ) and centrifuge samples.	Topcu, 2014
	Unstimulated saliva 500	Griess Method	Severe Chronic Periodontitis. Freeze ( $-20^{\circ}\text{C}$ ) and non-centrifuged samples. With the influence of food or fluid intake.	Sánchez, 2014
	Stimulated saliva $7.78 \pm 3.02$	Griess Method	Stimulated saliva. 10 individuals in the moderated chronic periodontitis group. Sampling between 10 and 11 a.m. Freeze ( $-20^{\circ}\text{C}$ ) and Centrifuged samples	Reher, 2007
	Stimulated saliva $15.79 \pm 5.59$	Griess Method	Stimulated saliva. 10 individuals in the severe chronic periodontitis group. Sampling between 10 and 11 a.m. Freeze ( $-20^{\circ}\text{C}$ ) and Centrifuged samples	Reher, 2007
	Stimulated saliva $57.3 \pm 9.8$	Chemiluminescence assay	Stimulated saliva. Freeze ( $-80^{\circ}\text{C}$ ). Sampling between 7 to 9 a.m.	Meschiari, 2015

The mechanism behind the Periodontitis onset is based on the response of the immune system to infection. In the presence of pathogenic microorganisms, pathogen-associated molecular patterns (PAMPs) are released to bind host cells, thus starting the inflammatory



cascade, and recruiting immune phagocytic and apoptotic cells. In uncontrolled situations, the inflammatory cascade fails which culminates in an advanced periodontitis state (Jain, 2021).

The bacterial biofilm (pathogens) PAMPs, induces immune cells, such as macrophages, dendritic cells, neutrophils, natural killer cells, and other phagocytic cells (Jain, 2021). This process promotes the release of cytokines for macrophage recruitment: interleukin-1 $\beta$  (IL-1 $\beta$ ) and tumor necrosis factor- $\alpha$  (TNF- $\alpha$ ) (He, 2018). By activating macrophages functions, iNOS is induced and NO $\cdot$  is produced being rapidly converted to nitrite. When nitrite levels are higher, the leukocyte recruitment is inhibited, and, as mentioned above, conjugated with an inflammatory cascade switch-off, the infection resolution fails (Topcu, 2014 and He, 2018).

For these reasons, nitrite, inflammatory cytokines (IL-1 $\beta$ , TNF- $\alpha$ ), and proteinases (MMP-8) related to soft tissue destruction, are also recognized as disease biomarkers.

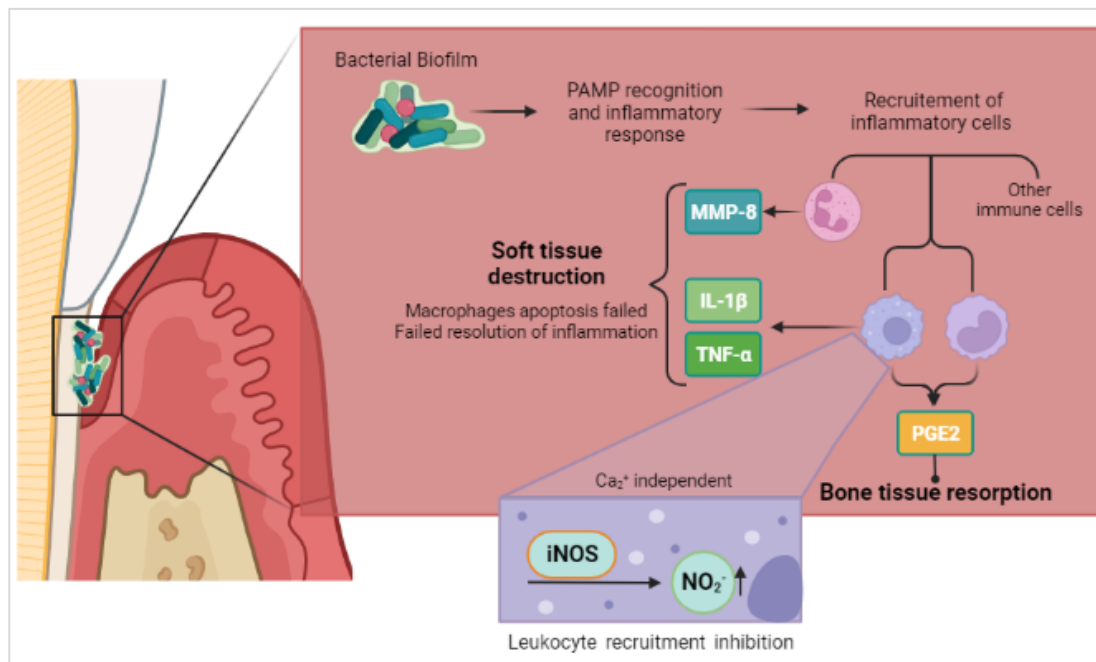


**Figure 1.10** – Periodontitis disease mechanism starts with the presence of bacterial biofilm that has recognition patterns – PAMPs – that induce an inflammatory response. In this process are involved immune cells – neutrophils, macrophages, monocytes, and others – that release important biomolecules, such as MMP-8 (a protease), IL-1 $\beta$ , and TNF- $\alpha$  (interleukins) known as bacterial killers. The PGE2 is a prostaglandin, associated with bone tissue resorption. Soft tissue destruction is caused by collagen and fibronectin degradation. In addition, iNOS expression increases in macrophages, and the NO $_2^-$  concentration is higher, inhibiting leukocyte recruitment. Consequently, the inflammation resolution failed without the macrophages' apoptosis (Adapted from He, 2018; Jain, 2021).

The presence of NO $\cdot$  and its metabolites contribute to nitrosative stress, which is toxic to the human organism (Laranjinha, 2021). If the iNOS activity is inhibited, the nitrosative stress drops, enabling periodontitis to recede (He, 2018).

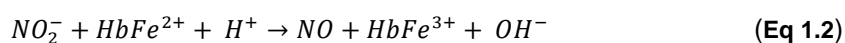
## 1.4.2. Hypoxia and vasodilatation

Hypoxia is commonly known as a condition where the oxygen concentration ( $pO_2$ ) in the organism decreases (**Gladwin et al., 2005**) as well as pH, causing medium acidification (**Cosby, 2003**). In this condition, the L-arginine pathway is inhibited while the  $NO_3^-$ - $NO_2^-$ -NO is activated as a backup pathway to produce the rNO $\cdot$  (**Gladwin et al., 2005; Ma, 2017**) required for the NO $\cdot$ -dependent vasodilatation (inducing hypotension), blood flow regulation, mitochondrial respiration and, tissue cytoprotection in ischemic episodes (**Ma, 2017**).

When a cardiovascular condition occurs, such as in a hypoxia episode, the nitrite levels in plasma decrease, with a consequent increase in cardiovascular risk (**Kleinbongard, 2006**). Because of that, maintaining vasodilatation is truly important against oxidative stress.

In Portugal, cardiovascular diseases lead to 32% of deaths, with 42% of cardiovascular patients having arterial hypertension (HTA) (**Portuguese Health General Direction website**) caused by both environmental (salty food, fatty reached alimentation, stress, and others) and homeostatic (genetic prevalence, kidney problems, endothelial dysfunction, and others) factors (**Ling, 2020**).

In hypoxia conditions, the vasodilatation process starts with the nitrite/hemoglobin ( $NO_2^-/Hb$ ) or nitrite/myoglobin complex formation, in their deoxygenated states (**Lundberg et al., 2008**), and the nitrite is enzymatically reduced to NO $\cdot$  by xanthine oxidase, and heme and thiol groups enzymes (**Förstermann, 2012**) (Equations 1.2 and 1.3). Then, the NO $\cdot$  produced reacts with other deoxyhemoglobin forming an iron-nitrosyl-hemoglobin complex ( $HbFe^{3+}$ -NO $\cdot$ ) (**Shiva, 2010**). In hypoxia, deoxyhemoglobin is more available to bind nitrite in heme sites, and consequently the production of NO $\cdot$  increases. The formation of the  $HbFe^{3+}$ -NO $\cdot$  complex facilitates the oxidation of NO $\cdot$  to nitrite in plasma contributing to vasodilatation (**Shiva, 2010**).



As mentioned above, endothelial dysfunction is one of the consequences of hypertension and it is due to the decline of NO $\cdot$  bioavailability (**Ling, 2020**), an important vasomotor control.

Several studies demonstrated an advantageous relationship between nitrite and the physiopathological effects of hypertension. These studies revealed that the mammalian tissues can reduce nitrite into NO $\cdot$  not also in HTA situations, but also in hypoxia and ischemic episodes (**Ling, 2020**). In pharmacological doses, nitrite has been seen as a potential therapeutic agent to normalize the increase in blood pressure (**Dalsgaard, 2007**).

### 1.4.3. Signaling molecule

Signaling molecules have different functions: act as ligand binding to a specific cell receptor (in cytoplasm or nucleus, or on the surface of plasmatic membrane) and module the signal to transmit a message. Signaling molecules can cross the plasma membrane of cells.

Nitrite is an important hallmark as a signaling molecule. For example, contribute to the stimulation of soluble guanylyl cyclase (sGC), inhibition of CYP<sub>450</sub> activity, and the modulation of expression of two important proteins, the heme oxygenase-1 (HO-1) and heat shock protein 70 (Hsp70) (Bryan, 2005). These signaling roles occur in physiological concentrations (Gladwin, 2005).

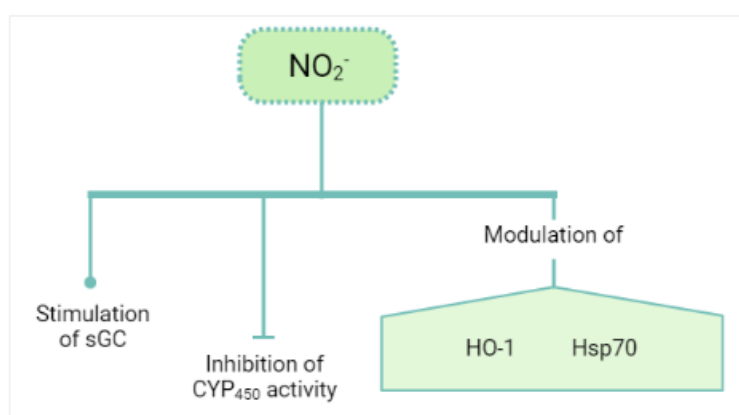


**Figure 1.11** - Nitrite as a signaling molecule. Acting as an sGC stimulator, inhibitor of CYP<sub>450</sub>, and modulates the HO-1 and Hsp70 expression (Adapted from Bryan, 2005).

## 1.5. Nitrite determination Methods

### 1.5.1. Traditional methods

Many nitrite quantification methods are described in the literature, such as ion chromatography, gas chromatography, UV-Vis spectrophotometry, fluorescence spectrophotometry, electrophoresis, and chemiluminescence, among others, to evaluate the concentration of this ion in environmental and food samples (Almeida, 2010; Azmi, 2017; Li, 2018).

Due to the high instability of  $\text{NO}\cdot$ , with a half-life of a few ms (Almeida, 2010), and its rapid oxidization into nitrite, a stable metabolite and is an easier specie to be measured. The latter has been also used as an  $\text{NO}\cdot$  index in physiological samples (Wang, 2019).

The most popular technique is the Griess Method, which is based on a colorimetric reaction followed by spectrophotometric measurements, proposed for the first time by Johann Peter Griess, in 1879 (Silva, 2018). The detection principle is based on the determination of an absorbance peak at 540 nm that is proportional to the nitrite concentration in the solution. Because this is an optical method, depending on the sample, it may need preparation steps, such as centrifugation, since measurements could be affected by turbidity. The reagents are Sulfanilamide (SA) and N-(1-naphthyl)ethylenediamine dihydrochloride (NED). First, in acidic conditions, nitrite reacts with SA, and a diazonium salt is formed (Figure 1.12). After that, NED reacts with the salt forming a purple azo compound, which tonality is proportional to the nitrite concentration (Li, 2018, Gassmann, 2016, Vishwakarma, 2019).

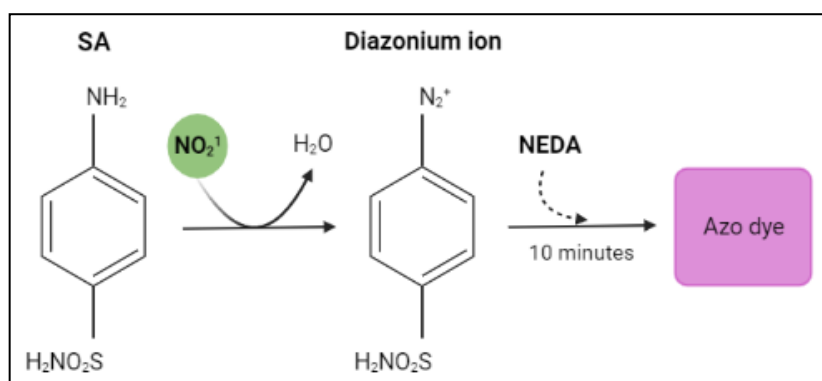


**Figure 1.12** – Griess method for nitrite quantification. Griess reaction comprehends two steps in acidic conditions. First, nitrite ions from samples or standard solutions, react with sulfanilamide – a diazotizing reagent - and an intermediate diazonium salt is formed. Then, the salt couples with an aromatic amine N-(1-naphthyl)ethylenediamine dihydrochloride - coupling agent - forming a purple-colored azo dye that absorbs at a maximum of 540 nm. (From Gassmann, 2016)

Some disadvantages of colorimetric assays are the need for bulky and specialized equipment and higher volumes of reagents and samples, making the routine analysis of nitrite a complex task. Besides, optical methods are affected by matrix interferences, long-time analysis, and lack of portability, forbidding real-time measurements (Almeida, 2010).

Our group proposed a different approach that aims to tackle these obstacles by producing a miniaturized, point-of-care test based on an electrochemical biosensor (Almeida, 2007; Monteiro, 2019; Monteiro, 2022).

## 1.5.2. Biosensors

The biosensing technology is focused on diverse areas of application such as agriculture, healthcare, the food industry, and water control and air control, aiming at reducing the impact of chemicals on the environment and human health. By definition, a biosensor combines a biological element, able to recognize the analyte with a physicochemical transducer that transduces the biorecognition process into an electronic signal which is proportional to the analyte concentration (Monteiro, 2018).

Biosensors provide important information on the analyte (Mehrotra, 2016). Despite having the same quantification principle, they are different from sensors which do not have a biological component. As for the biological element, biosensors can be modified with macromolecules (enzymes, nucleic acids, antigens/antibodies), cell fragments (organelles, membrane receptors), or whole cells (tissues, MO) (Monteiro, 2018; Lozano et al., 2019). According to the type of transducing method, biosensors can be classified as electrochemical, optical, piezoelectric, calorimetric, and scanning probe microscopies (Monteiro, 2018; Lozano et al., 2019).

To develop a biosensor, it is important to choose and optimize the materials, the immobilization methods of the biological component, and the transducing devices (Lozano et al., 2019). Biosensors can be divided into biocatalytic or bioaffinity systems. The biocatalytic ones comprise enzymes and microorganisms as biorecognition elements. On the other hand, a bioaffinity system includes antibodies, nucleic acids, and biological receptors forming stable complexes between the biological element and the analyte (Monteiro, 2018).

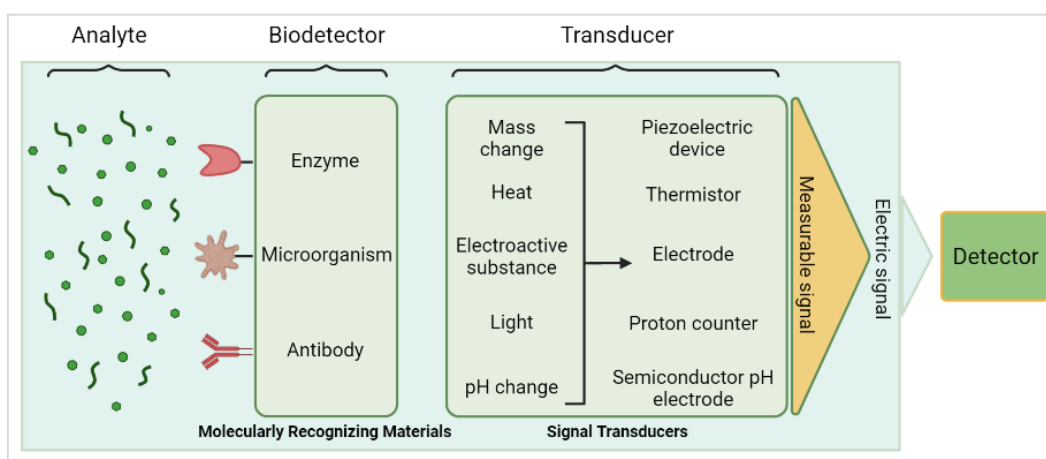


**Figure 1.13** - Biosensor scheme. A specific analyte is recognized by the biological element that is immobilized in a molecularly recognizing material called biodetector. Signal Transducer converts biorecognition into a measurable signal detected by the detector quantifying the specific analyte present in a sample. (From Lozano et al., 2019).

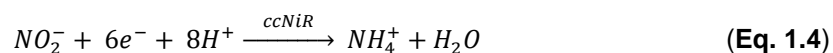
The advantages of biosensors are the no need for sample pre-treatment, including no reagent addition, low sample volumes, high selectivity to the analyte, and no interference from the sample matrix (Almeida, 2010), like the viscosity and solid residues present in salivary fluids, for instance. Real-time analysis and fast point-of-care testing (POCT) are truly important for novel and better approaches (Monteiro, 2018).

In our group, the nitrite biosensor is modified with enzymes and the transducer method is electrochemical (voltammetry and/or amperometry) (Almeida, 2010). This topic will be thoroughly discussed in the next section.

### 1.5.2.1. Enzyme-based electrochemical biosensors for nitrite determination

In this work, we tested a new enzyme-based nitrite biosensor using both voltammetric and amperometric techniques as transducing systems. The commercial unmodified carbon-based screen-printed electrodes (SPE) were modified with a redox enzyme called cytochrome *c* Nitrite Reductase (ccNiR).

The enzyme cytochrome *c* nitrite reductase (ccNiR) (E.C. 1.7.2.2) catalyzes the six-electron reduction reaction of nitrite into  $\text{NH}_4^+$  (Equation 1.4) when is electrochemically activated at negative potentials (Monteiro, 2022).



It is produced by the proteobacterium *Desulfovibrio desulfuricans*, during anaerobic respiration in the presence of the electron receptor substrate, nitrate. The catalytic subunit (NrfA) is anchored to the cell membrane through its electron donor (NrfH). Each monomer is composed of 519 amino acid residues, with 61 kDa, and 5 *c*-types hemes, one as the catalytic site and the remaining four, as electron-transfer centers (from *Protein Data Bank* and *Genomenet*).

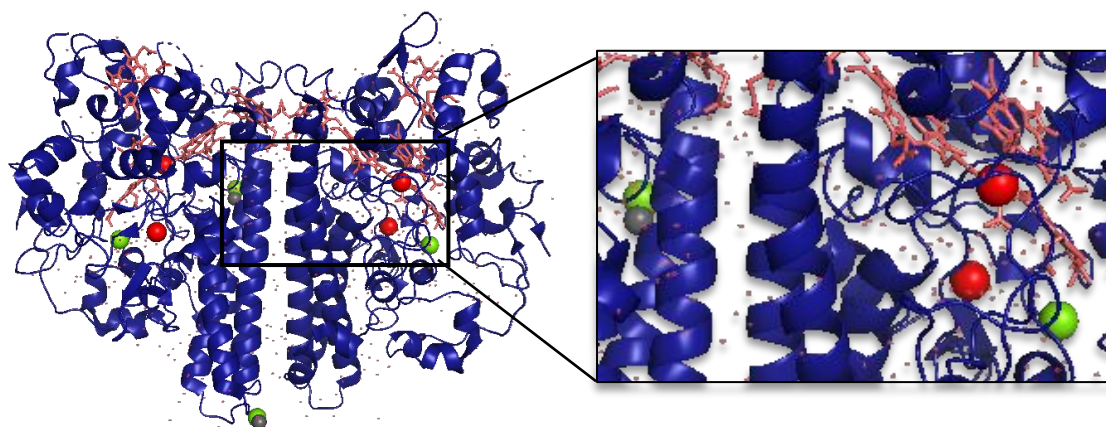


**Figure 1.14** - Cytochrome c Nitrite Reductase quaternary structure obtained with the program *PyMOL*. The Protein Data Bank Code of this protein is 1oah. The figure represents the principal chain of the protein with 519 amino acid residues (dark blue). The image shows 10 hemes c (red salmon) and other ligands: 2 zinc ions (grey), 4 calcium ions (red), and 4 Cl<sup>-</sup> ions (green). Using the X-ray diffraction technique to obtain this structure, water molecules (red dots) were detected. (Adapted from *Protein Data Bank* and Cunha et al., 2003).

Enzyme immobilization is a fundamental aspect of the biosensor configuration, considering the interactions between the enzyme and the material. In this study, the protein was adsorbed directly in contact with the carbon (Figure 1.15) (Almeida, 2010). So, a direct electron transference (DET) is established, following an EC' mechanism. The catalytic current is thus directly correlated to the analyte amount (enzyme substrate) being processed (Almeida, 2010). To avoid electrochemical interferences, the working potential is close to the reduction potential of the catalytic heme (Almeida, 2003). In this study, the working potential was established at -0.5 V (Monteiro, 2019)

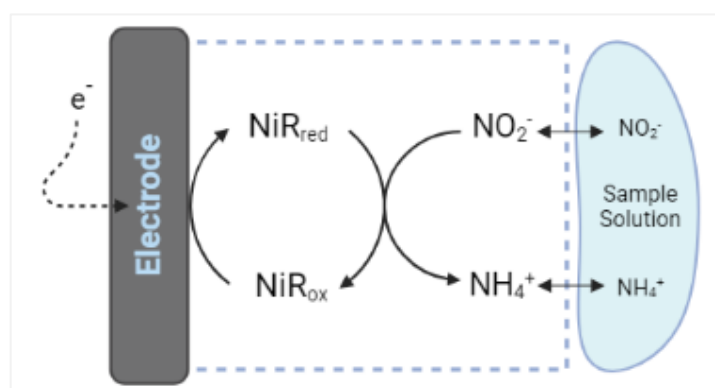
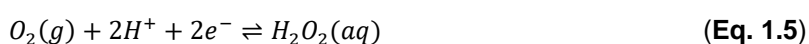


**Figure 1.15** – Schematic model of the enzymatic nitrite biosensor with direct electrochemical transduction. The electrochemically reduced enzyme ccNiR, transfers six electrons from the electrode to the nitrite, forming the product NH<sub>4</sub><sup>+</sup>. (From Almeida, 2010).

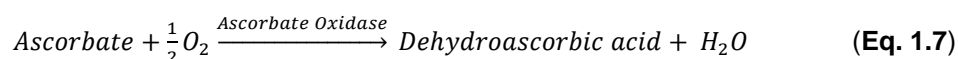
Through decades, other elements have been incorporated into the biosensor configuration to avoid interferences and enhance response stability.

The molecular oxygen dissolved in the samples is an interfering specie, compromising the redox processes between -0.2 V and -0.8 V (**Monteiro, 2022**). This interference is felt by both oxidase and reductase enzymes. So, its depletion is needed before measurements. For oxidase proteins, the O<sub>2</sub> interference is due to the electron acceptor's ability to react with this gas (mediated electrochemistry). Similar to reductases, where occurs the cathodic reduction of oxygen into hydrogen peroxide or water (**Plum re, 2013**) (Equations 1.5 and 1.6), generating a broad wave (intense cathodic current) that masks the analytical signal, with dramatic interference consequences.



To deoxygenate the samples, some techniques have been applied, i.e., chemical compounds, usually used in packaged foods, such as ascorbic acid, sodium sulfate, and gallic acid among others (Monteiro, 2022), reacting directly with the oxygen. Another technique, frequently used in a laboratory setting, is bubbling an inert gas while measurements were conducted. Since this method is not usable in a portable analysis, another technique, based on the use of biochemical approaches, uses a bi-enzymatic system composed of glucose oxidase and catalase enzymes or the mono-enzyme strategy using the bilirubin oxidase (BOD) enzyme (**Monteiro, 2022**). Since these methods could have some issues related to enzyme impurities, and ROS formation, our group developed a new enzymatic strategy.

To solve this limitation, our group developed a new enzymatic scavenger system based on the reaction of copper oxidase capable to convert O<sub>2</sub> into water, in the presence of the respective substrate, promoting oxygen reduction (Equation 1.7) (**Monteiro, 2022**).



One of the advantages of the proposed biosensor is the use of a single enzyme without releasing any reactive species and the great effectiveness of oxygen depletion. One of the disadvantages of this deaerated method is related to the substrate concentration since normally is higher than the analyte, which could result in a lower or complete absence of cathodic currents (**Monteiro, 2022**). Another reported disadvantage is the partial ccNiR reduction by ascorbate, avoided by the AOx fast ascorbate oxidation (**Monteiro, 2022**). This mono-enzymatic oxygen scavenger system was never tested in real samples.



## 1.6. Hypothesis

Our working hypothesis assumes that nitrite present in human saliva is a biomarker of periodontal disease. Thus, the hypothesis tested in this work is the following "Is the concentration of nitrite quantified in saliva samples correlated with the degree and severity of periodontal disease?".

## 1.7. Objectives

The present Master Thesis dissertation focus on nitrite as a periodontal disease biomarker, important for clinical diagnosis. Thus, to follow the established hypothesis we aim to develop an enzymatic biosensor for nitrite quantification in a clinical pilot study. For that, the ccNiR, a multihemic reductase that catalysis the conversion of nitrite to ammonia is the main biosensor layer that is immobilized in the working electrode. Also, an oxygen scavenger system is important to add to our biosensor, due to the sample's dissolved oxygen depletion.

Since periodontal disease is a condition that affects the oldest population, we aim to create this POC test to facilitate the diagnosis, retarding the disease progression.

Thus, the main objectives of this study are:

- 1) to study the relationship between nitrite concentration in saliva and periodontal disease.
- 2) the implementation of a new point-of-care test (biosensor) to evaluate the nitrite concentration in saliva samples.

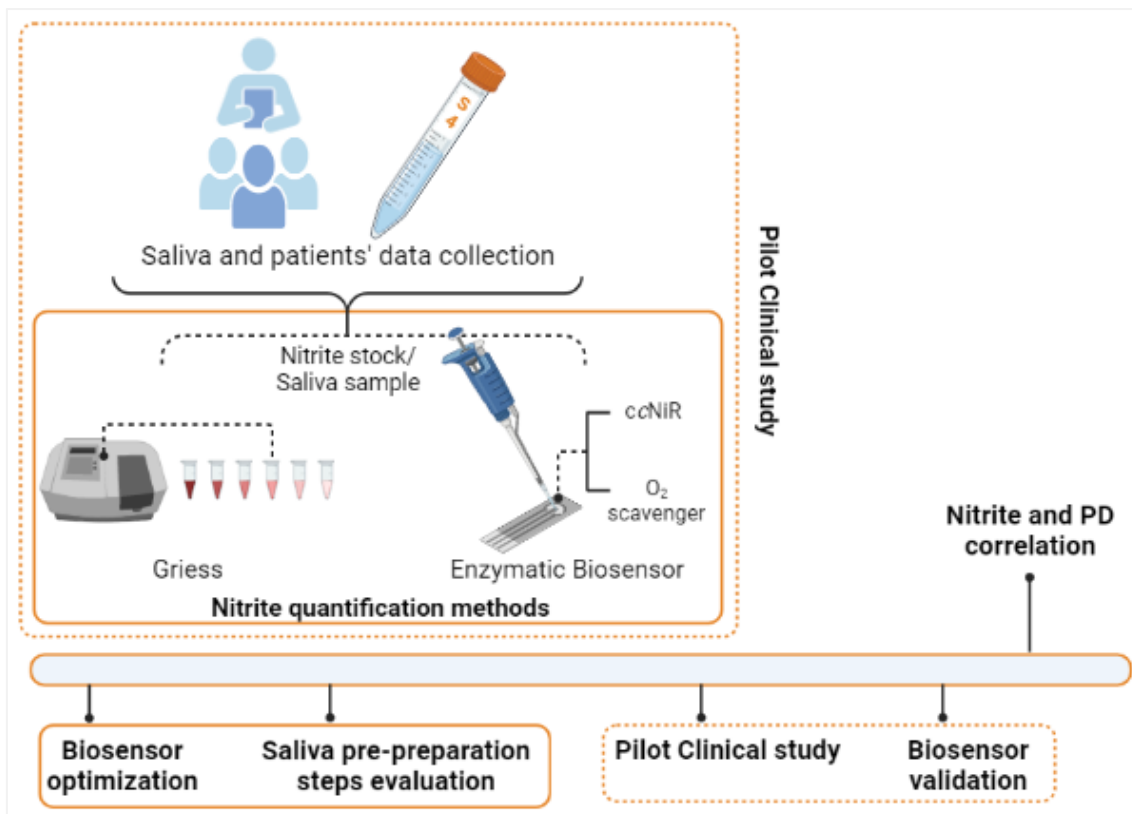


**Figure 1.16** - Thesis outline. The saliva samples were treated using both Griess and the new Biosensor. These techniques help us to evaluate the biosensor, comparing the results obtained with both techniques and evaluating the saliva pretreatment steps. In a clinical context, nitrite present in patients' saliva samples were quantified validating the biosensor method, at the same time. All figures in this work were prepared in the Biorender platform.



Chapter

2

Materials and  
Methods



## 2. MATERIALS AND METHODS

### Experimental section

To meet the objectives of this study, we followed the following plan:

- The electrode preparation and characterization were carried out in the GB2 – Group of Biomarker and Biosensors' Labs. At UCIBIO (FCT-NOVA) and CiiEM (Coop. de Ensino Superior Egas Moniz). The pre-clinical and clinical studies were carried out at the Egas Moniz Dental Clinic.
- Biological Model: Human Saliva.
- Parameters to be analyzed: Nitrite concentration.
- Previous procedures: Patient data collection, sampling of saliva, and nitrite quantification with the Griess method.

### 2.1. Reagents and Solutions

Sodium Nitrite ( $\geq 99\%$ ) was purchased from *Normapur®*. Sodium hydroxide 0.02% ( $\geq 98\%$ ) was obtained from *Sigma-Aldrich®*. Sulfanilamide ( $\geq 98\%$ ), Hydrochloric acid 37%, and NED ( $\geq 98\%$ ) were purchased from *Sigma-Aldrich®* for Griess quantification and were prepared using distilled water. Solutions were prepared with deionized water (18 M $\Omega$  cm) from the Millipore MilliQ purification system.

Ascorbate oxidase (from *Curcubita sp.* 1000-3000 units mg<sup>-1</sup>) and L-ascorbate (prepared with 0.1 M Tris-HCl, 0.1 M KCl, pH 7.6) were purchased from *Sigma-Aldrich®*. Enzyme solutions were prepared with PB buffer made with Sodium Chloride and Potassium Chloride purchased from *Fluka®* and Sodium phosphate monobasic and Potassium phosphate dibasic trihydrate purchased from *Sigma-Aldrich®*. Hydrochloride acid 37% and Trizma were obtained from *Sigma-Aldrich®*, and Potassium chloride was purchased from *Fluka®*.

ccNiR (300 U mg<sup>-1</sup>) from *D. desulfuricans* ATCC 27774 cells was purified in-house: the cells were grown in a nitrite-rich medium, as described by Almeida et al. (**Almeida et al., 2003**).

Polyvinyl alcohol was purchased from *Sigma-Aldrich®* and previously prepared by Tiago Monteiro.

All the solutions were prepared with deionized water (18 M $\Omega$  cm), from a MilliQ purification system.

## 2.2. Equipment

All solid reagents were weighed on a digital scale *Ohaus®* Pioneer Px. Samples were centrifuged in an *Eppendorf® Minispin®* centrifuge. The unmodified DropSens® SPEs DS-110 were obtained from Potential Zero Lab Technology. To store the sensors, aluminum thermos-sealable pouches were purchased from Amcor Flexibles. For electrochemical measurements, a *SensitSmart®* portable potentiostat from PalmSens®, and the PStouch software app for data acquisition were used. The bioelectrodes were dried in a Memmert® UNB100 oven. Spectrophotometric measurements were performed using a *THORLabs®* portable spectrophotometer and a Thermo Scientific® Helios Omega UV-Vis bench spectrophotometer. The pH measurements were made with BANTE Instruments® 210 Benchtop.

## 2.3. Clinical Study

### 2.3.1. Ethical Considerations

This study was approved by the Egas Moniz Ethics Committee where the Clinical Study was conducted. All participants were informed about the objectives of the study and their anonymous participation and were asked to sign an informed consent. The collected data were used exclusively for statistical analysis.

### 2.3.2. Inclusion and Exclusion criteria

#### **Inclusion Criteria**

- Age 18 years or older;
- At least 10 teeth present or with implants;
- Signature of informed consent.

## Exclusion Criteria

- Pregnant women;
- Patients suffering from autoimmune diseases, for example, have human immunodeficiency virus (HIV), hepatitis B, or hepatitis C;
- Patients with acute or chronic use of xerostomizing drugs;
- Patients under radiotherapy;
- Patients who had undergone periodontal treatments;
- Patients who have or have had any of the following pathologies: COPD, Respiratory apnea, or Covid-19;
- Patients with incomplete data.

## 2.3.3. Patient Data collection

### 2.3.3.1. Clinical Data

An early authorization from the Egas Moniz Dental Clinic was required for the collection of patient data. Information on diet habits, smoking habits, and the presence of other pathologies were collected from the questionnaire (see below). Other patients' information such as collected age, genre, periodontal disease grade, and severity information was taken from the patient's clinical diary.

### 2.3.3.2. Questionnaire

A total of 61 individuals were included in the study, 13 periodontal healthy people, and 48 patients with periodontal disease, following the inclusion criteria. Patient recruitment was performed during the mourning period to avoid interference from nitrate-rich aliments.

Prior to the collection of saliva fluid, participants were asked to sign an informed authorization and answer a questionnaire composed of questions like the following:

1. Do you smoke?
2. Have you had or have any of these pathologies?  
(Covid-19, COPD, Apnea Breath, Hypertension)
3. Do you drink alcohol often?
4. How much water did you ingest?
5. What is your weight?
6. Do you have a diet rich in vegetables and fruits?  
(spinach, beetroot, cabbage, vegetable juices, pomegranate, banana, and orange)



7. Do you have a diet rich in processed meat?  
(bacon, ham, and sausages)
8. Do you usually make a vitamin supplement?
9. Do you feel dry mouth?
10. Do you have any oral injuries?
11. Do you consider that you have high psychological stress, physical fatigue, or anxiety in your daily life?

The complete questionnaire is presented in the Appendices section.

### 2.3.4. Salivary fluid sampling and preparation

At the sampling moment, to avoid blood contamination, saliva sampling was the first procedure before the appointment with the Dentist. First, patients were gargled with water to clean their mouths and to help the salivation. After gargling, the individual salivated in a non-stimulated way without swelling. With the head tilted forward, the patient has guided the salivary fluid through a Falcon tube (previously identified). Falcons' lids were correctly closed and placed immediately on ice, for no longer than 10 minutes. Sample aliquots were also reserved at -20 °C, until other use.

Saliva samples were immediately analyzed to discard the time variable. For the turbidity influence study, samples were centrifuged and quantified again. On this end, samples were submitted to one centrifugation cycle at 13400 *rpm* for 10 minutes. After nitrite quantification, the supernatant was stored at -20 °C.

## 2.4. Nitrite quantification

### 2.4.1. Electrochemical Biosensor

The bare SPEs are composed of a carbon working electrode (WE), a carbon counter electrode (CE), and a silver (Ag) pseudoreference electrode. They were modified in-house by immobilizing enzymes (biorecognition component and oxygen scavenger) into the surface of the carbon WE, according to the following protocol.

A 5  $\mu\text{L}$  drop of ccNiR (1 mg mL<sup>-1</sup>) was drop-casted and oven-dried for 30 min. (40 °C). Then, the components of the mono-enzymatic oxygen scavenger system, recently developed in our

group, and never tested in real samples (Monteiro, 2022), were applied onto the SPE surface. To this end, the first ccNiR layer was coated with a 5  $\mu\text{L}$  drop of AOx (1000-3000 U  $\text{mg}^{-1}$ ) and dried in an oven (40  $^{\circ}\text{C}$ ) for 10 min. Finally, 10  $\mu\text{L}$  of 1.25% PVA solution was added to cover the enzymes and enhance the ccNiR's  $k_m^{\text{app}}$ . The PVA coat was dried at room temperature for 30 minutes and oven-dried (40  $^{\circ}\text{C}$ ) for 10 min. A scheme of the resulting test strips is shown in figure 2.1.

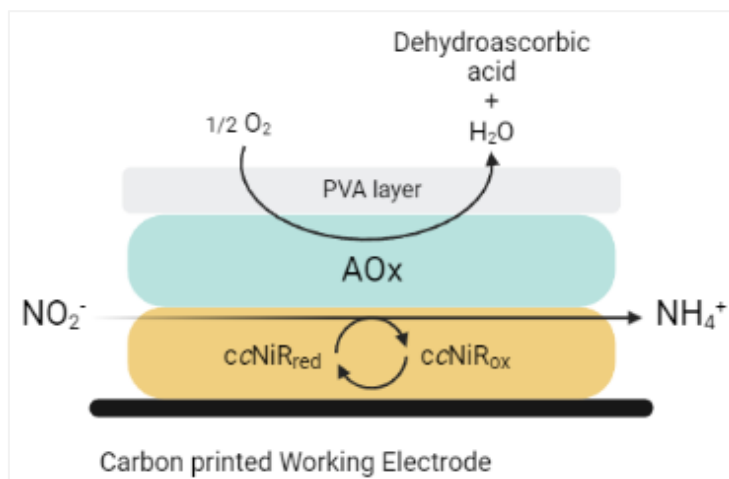


**Figure 2.1** – Detailed scheme of a SPE/ccNiR/AOx/PVA. The working electrode is modified through the layer-by-layer deposition of two different enzymes. The first layer is composed of ccNiR that converts  $\text{NO}_2^-$  into  $\text{NH}_4^+$ . The next layer is the oxygen scavenger AOx which catalyzes the reduction reaction of  $\text{O}_2$  into water. On the top, there is a layer of PVA to enhance the enzyme  $k_m^{\text{app}}$  of ccNiR.

The biosensors (disposable test strips) were used immediately after the preparation was completed or stored in small packages previously deaerated through Argon purging, and sealed at 4  $^{\circ}\text{C}$ , in dry conditions. After usage, the test strips were discarded.

The three-electrode system was covered with a 50  $\mu\text{L}$  drop of a freshly prepared solution of 100 mM ascorbate, in 0.1 M Tris-HCl, 0.1 M KCl, pH 7.6. mixed with the saliva sample or standard solution (1:1). Blank assays were run with a drop of 100 mM ascorbate in 0.1 M Tris-HCl, 0.1 M KCl, pH 7, only.

The electrochemical measurements were made two different techniques: cyclic voltammetry (CV) and Chronoamperometry. The cyclic voltammograms (CVs) were registered with a scan rate of 0.02  $\text{Vs}^{-1}$ , from 0.0 V to -0.6 V (vs Ag/AgCl pseudo reference). The catalytical currents ( $\Delta I_{\text{cat}}$ ) for each nitrite concentration were measured at the cathodic peak. The chronoamperograms were plotted using a fixed potential at -0.5 V (vs pseudoreference Ag) and the  $\Delta I_{\text{cat}}$  was measured after 60 s.

The biosensors were regularly calibrated using nitrite standards of 0, 2.5, 5, 10, 20, 40, 80, 160, 200, 250, and 300  $\mu\text{M}$  (one bioelectrode per concentration), in 100 mM ascorbate, 0.1 M

Tris-HCl, 0.1 M KCl (pH 7.6). The catalytic current was plotted against the nitrite concentration and the plot was fitted to a linear curve using the linear regression model.

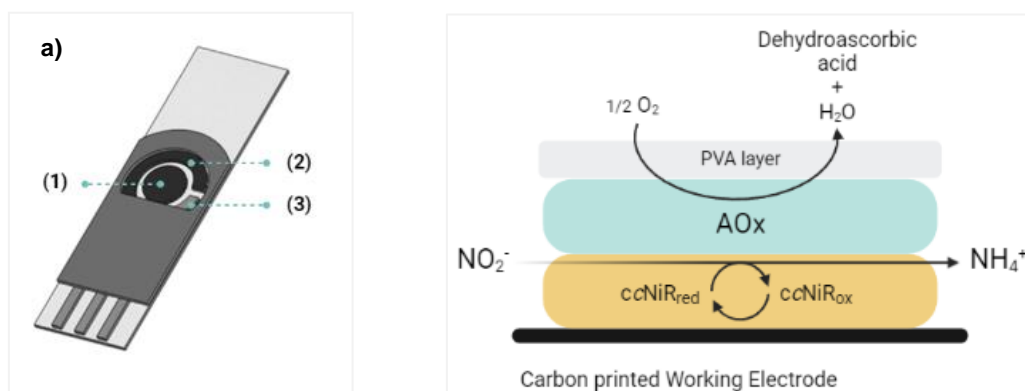


**Figure 2.2** - **a)** is a screen-printed three electro system composed of a (1) carbon working electrode, a (2) carbon counter electrode, and a (3) Ag pseudo reference electrode. **b)** scheme of ccNiR/AOx/PVA/SPE.

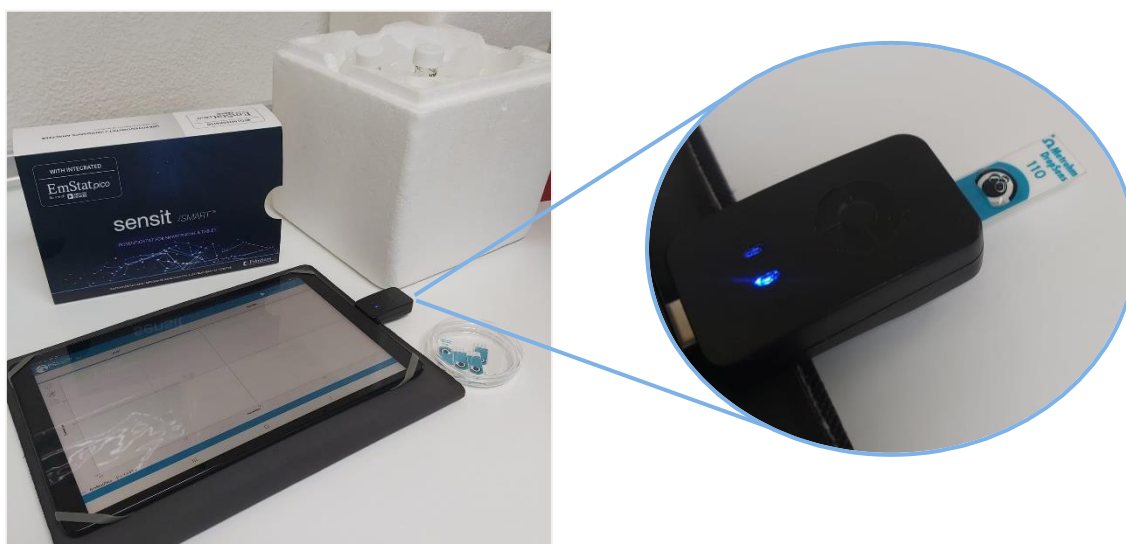


**Figure 2.3** - ccNiR/AOx/PVA/SPE DropSens 110 connected with PalmSens SensitSmart portable potentiostat.

## 2.4.2. Griess Method

The Griess Method is the classic protocol to quantify nitrite in different samples. To perform the calibration curve, 10 concentrations (2.5, 5, 7.5, 10, 12.5, 15, 17.5, 20, 22.5, and 25  $\mu\text{M}$ ), including a blank, were prepared, directly in a plastic cuvette using 10 mM nitrite stock solution in 0.02% sodium hydroxide. The stock solutions of the Griess reagents were prepared in the

following concentrations, 1% m/v SA and 0.02% m/v NED and stored in a dark flask for 1 month. A new calibration curve was prepared monthly with the new and fresh stock solutions of Nitrite, SA, and NED.

To plot the calibration curve, 25  $\mu$ L of standard, 475  $\mu$ L of deionized water, 250  $\mu$ L of SA, and 250  $\mu$ L of NED were added into a plastic cuvette, in this order. After 10 minutes, the absorbance was measured at 540 nm. For nitrite sample analysis the same protocol was used.

### 2.4.3. HPLC-ionic chromatography

The nitrite analysis was performed using a Thermo Ionpac AS18 250 mm x 4 mm column in a DIONEX ICS3000 equipment. This analysis was performed by the LAQV Requirnte Laboratory.

## 2.5. Statistical analysis

All data were recorded in *Microsoft Office Excel*® and analyzed using the software package *IBM SPSS Statistic 27.0*. Descriptive and inferential statistical analysis methodologies were applied. A 5% significance level was established for all inferential analyses.



Chapter

3

Results and  
Discussion



## 3. RESULTS AND DISCUSSION

The quantification of nitrite in saliva samples was performed with, two different methods. The first goal of the project was to test a novel approach based on an enzymatic electrochemical biosensor that was previously developed in our group and has proved to be highly selective for nitrite, easy to use, quick, and suitable for on-site testing (**Monteiro, 2019**). For validation purposes, we also utilized a colorimetric method based on the Griess reaction, which has been largely used to assess the nitrite levels in physiological samples such as saliva. For the latter, samples should be cleaned up first by centrifugation to avoid turbidity effects and then mixed with the Griess reagents for color development, and spectrophotometric analysis. Since this protocol requires the use of laboratory instruments, samples are often frozen after collection. Herein, we have first evaluated the influence of these two steps of sample preparation (centrifugation and freezing) on the analytical performance of the Griess method, and then compared the two methods' results "biosensor vs Griess method" in a small-scale clinical study, aiming at understanding the saliva nitrite levels variations with the periodontitis stage, a prevalent oral disease.

In the next sections, we will first present the analytical parameters of the nitrite quantification methods above mentioned, and then show the results of their application in saliva samples submitted to different pre-preparation steps. In the second part of this chapter, data from the clinical study will be presented and discussed.

### 3.1. Nitrite Quantification

#### 3.1.1. Griess Method

Following the application of the saliva collection protocol, the Griess method was applied by adding a couple of reagents to a sample aliquot, followed by the spectrophotometric analysis.

Figure 3.1 shows a typical calibration curve. The linear range goes from 2.5 up to 25  $\mu\text{M}$ , with a sensitivity of 0.965  $\mu\text{M}^{-1}$ .



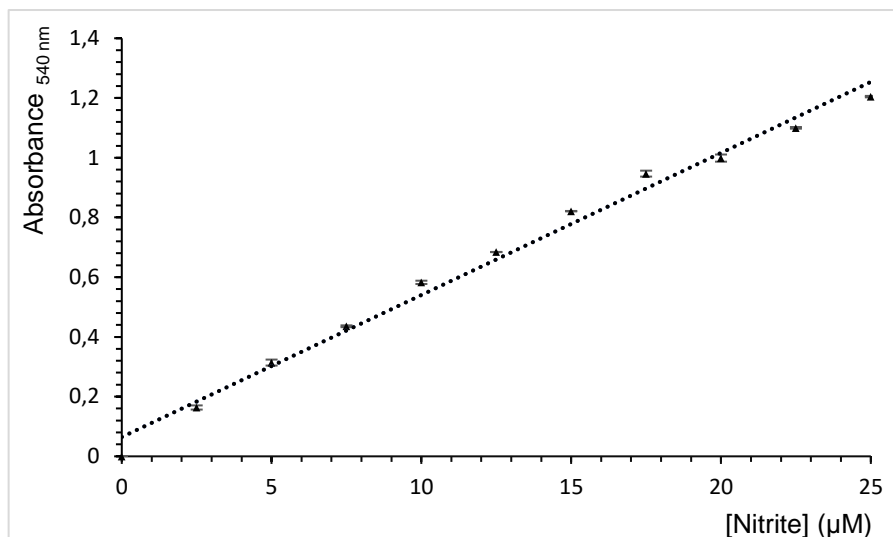


**Figure 3.1** - Nitrite calibration curve using the Griess Method. Each data point is the average of duplicates. The data were fitted to a straight line using the linear regression method, resulting in the following equation:  $\text{Abs.} = 0.965 [\text{NO}_2^-] + 0.039$ ,  $r^2 = 0.997$ .

To determine the nitrite concentration, the samples' absorbance was measured in the same way and interpolated from the standard curve. Regarding the protocol, one should emphasize that this optical method requires sample mixing with two reagents and waiting 10 minutes before running the spectrophotometric measurements.

### 3.1.2. Electrochemical Method – Biosensor Optimization

Before the electrochemical measurements, a 50 μL drop of a standard, or sample solution, was placed on top of the modified SPE and left for 4-5 minutes to allow complete oxygen depletion. The single-use bioelectrodes' response to nitrite, was then measured through electrochemical techniques (Cyclic Voltammetry (CV) and Amperometry) and were discarded after use. The catalytic current variation ( $\Delta I_{\text{cat}}$ ) for each nitrite concentration was determined at the cathodic peak (for CV) and at 60 s (for Amperometry), to which the background current was subtracted. All batches were previously calibrated using standard solutions (each assay was duplicated). The nitrite concentration in unknown samples was calculated by interpolation from a standard curve.

## Coating Polymer

To the biosensor, an external PVA layer was added coating over the enzymes to function as a diffusion barrier to the analyte, nitrite (Monteiro, 2018). Figure 3.2 shows two calibration curves for the nitrite testing strips prepared with and without PVA (in this case, CV was used as an electrochemical method). Despite decreasing the sensitivity, the PVA coat enhances the upper limit of detection (it increases the apparent Michaelis-Menten constant,  $K_m^{app}$ ), adjusting it to the nitrite concentrations initially observed in this study. For this reason, the nitrite analysis in real samples was performed with test strips coated with a PVA layer.

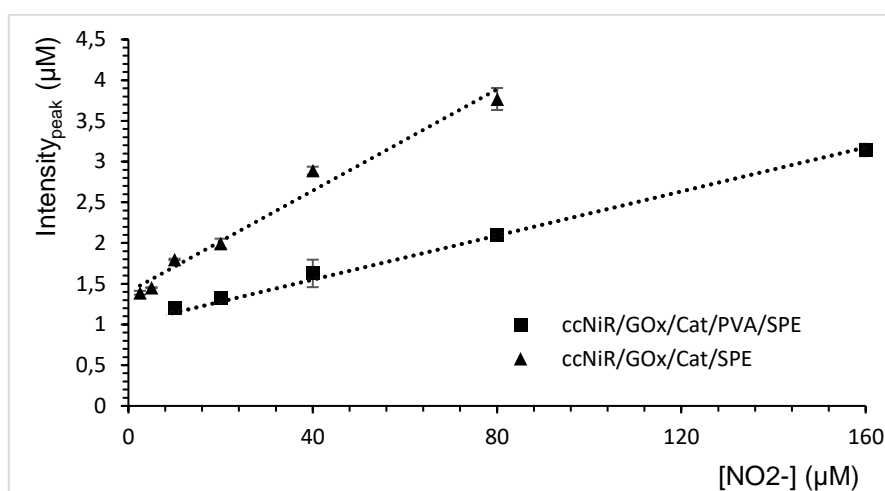


**Figure 3.2** – Nitrite calibration curve using the electrochemical biosensor. SPEs were modified following SPE/ccNiR/GOx/Cat (triangles) and SPE/ccNiR/GOx/Cat/PVA (squares). Data was performed using a CV. Each data point is the average of duplicates. The data points were fitted to a straight line using the linear regression method, resulting in the following equations:  $\Delta I_{cat}=0.0311 [NO_2^-] + 1.3991$  with  $r^2=0.978$  (SPE without PVA) and  $\Delta I_{cat}=0.0135 [NO_2^-] + 1.009$  with  $r^2=0.993$  (SPE with 1.25% PVA).

Table 3.1 compares the analytical performance of the nitrite biosensor, using biosensors with and without the PVA layer.

**Table 3.1** - Analytical parameters of the calibration curves obtained with SPE/ccNiR/GOx/Cat and SPE/ccNiR/GOx/Cat/PVA.

Parameters	Biosensor Method	
	Without PVA	With PVA
Linear Range (µM)	2.5 – 80	10 – 160
Sensitivity (µM <sup>-1</sup> )	0.031	0.014
$r^2$	0.978	0.993

## Oxygen Scavenger

Initially, the nitrite biosensors were prepared using single-used carbon SPEs modified with the ccNiR enzyme as biological recognition element GOx/Cat mix or AOx, as the main components of the oxygen scavenger.

Molecular oxygen is an interfering species in the electrochemical assays that masks the electrocatalytic signal, due to enzyme catalysis in the presence of nitrite. Following the previous works developed in our group (**Thesis T. Monteiro, 2020**), herein we tested different biochemical oxygen scavenger systems and compared their efficiency. First, the bienzymatic system GOx/Cat coupled to glucose was used, and then, we tested the novel single-enzyme system composed of AOx/ascorbate. While AOx catalyzes the direct reduction of oxygen into water, the GOx converts this gas into hydrogen peroxide, which is subsequently reduced into the water by the second enzyme, Catalase (**Monteiro, 2022**). Figure 3.3 shows the background CVs obtained with the two oxygen scavenger systems.

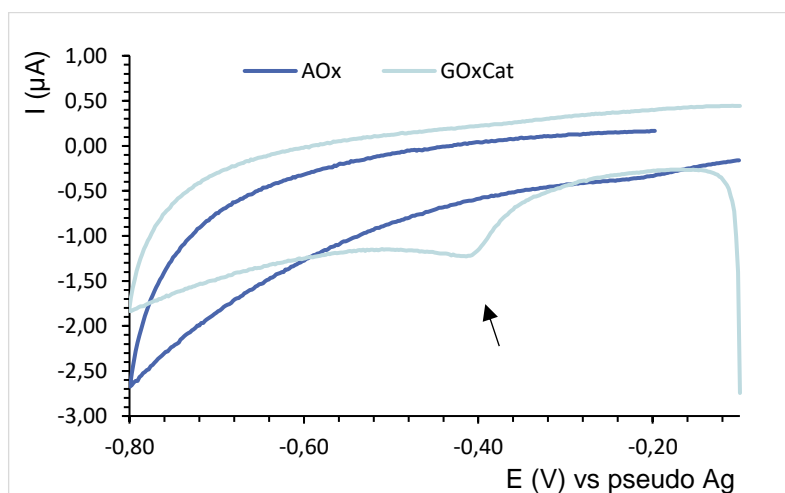


**Figure 3.3** - Cyclic voltammograms ( $20 \text{ mV s}^{-1}$  scan rate) of the supporting electrolyte 0.1 M Tris-HCl buffer, pH 7.6, with 0.1M KCl, recorded with AOx/SPE (dark blue) and GOx/Cat/SPE (light blue) modified electrodes, in the presence of their substrates, i.e., 100 mM ascorbate, and 80 mM glucose, respectively.

As shown, besides the risk of  $\text{H}_2\text{O}_2$  release, the GOx/Cat enzyme mix may present some impurities, like the FAD cofactor usually present in GOx's commercial batches, which can originate a cathodic signal at about -400 mV vs pseudoAg (see arrow in Fig. 3.3). Therefore, in this study, we opted to replace the GOx/Cat/glucose scavenging system with AOx/ascorbate.

## Electrochemical Method

For the electrochemical measurements, we used two dynamic methods, namely, cyclic voltammetry (Fig. 3.4) and amperometry (Fig. 3.5). Comparing the analytical performance of both transducing techniques, we found that for the CV assays, the linear range was 20 - 200  $\mu\text{M}$ , with a sensitivity of  $0.014 \mu\text{M}^{-1}$ , and for amperometry, the linear range was 5 - 300  $\mu\text{M}$ , with a sensitivity of  $0.015 \mu\text{M}^{-1}$ . The sensitivities are thus similar, but the linear range is wider when using the amperometric method; furthermore, this technique is quicker and the results are easier to analyze, so we chose to use it in clinical tests. Nevertheless, CV is a more useful method in the early stage of development, since it provides information about the ongoing processes, and shows the influence of interfering species, such as molecular oxygen.

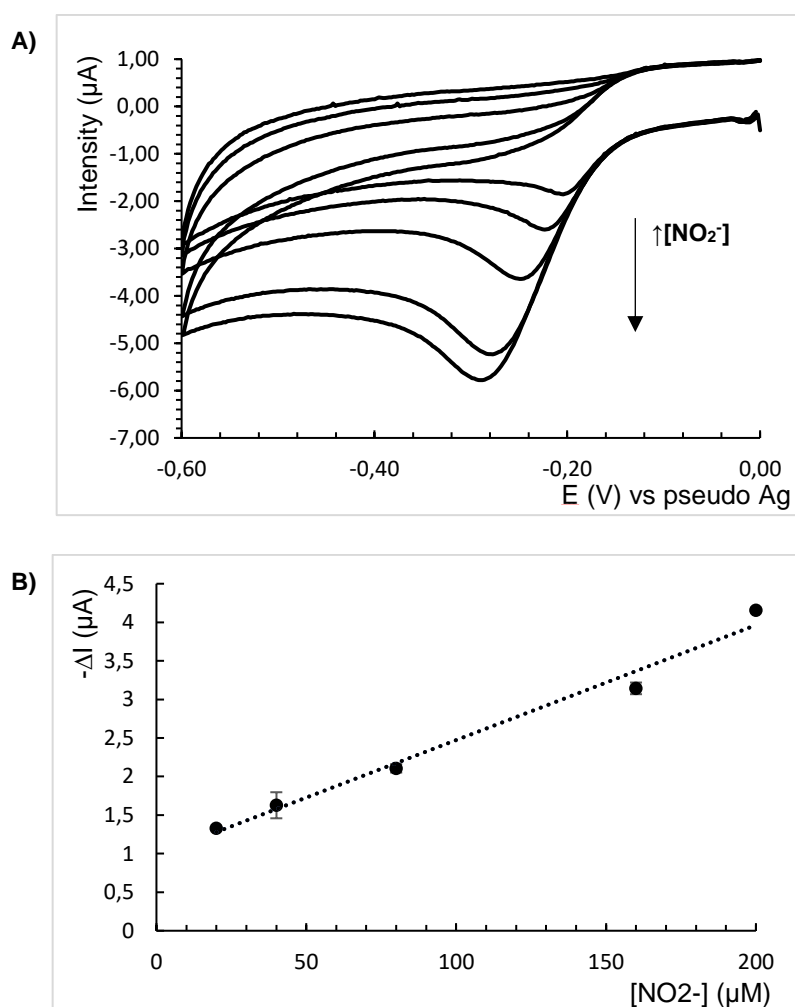


**Figure 3.4 - A)** Cyclic voltammograms ( $20 \text{ mV s}^{-1}$  scan rate) of supporting electrolyte (0.1 M Tris-HCl buffer, pH 7.6, 0.1M KCl) containing the 100 mM ascorbate and nitrite (linear range, 20-200  $\mu\text{M}$ ). Measurements were recorded with ccNiR/AOx/PVA/SPE and the  $\Delta I_{\text{cat}}$  was measured at the cathodic peak height. **B)** Nitrite calibration curve using the CV electrochemical technique. Each data point is the average of duplicates. The data were fitted to a straight line using the linear regression method, resulting in the following equation:  $\Delta I_{\text{cat}} = 0.014 [\text{NO}_2^-] + 0.981$ ,  $r^2 = 0.982$ , and a linear range of 20 to 200  $\mu\text{M}$ .

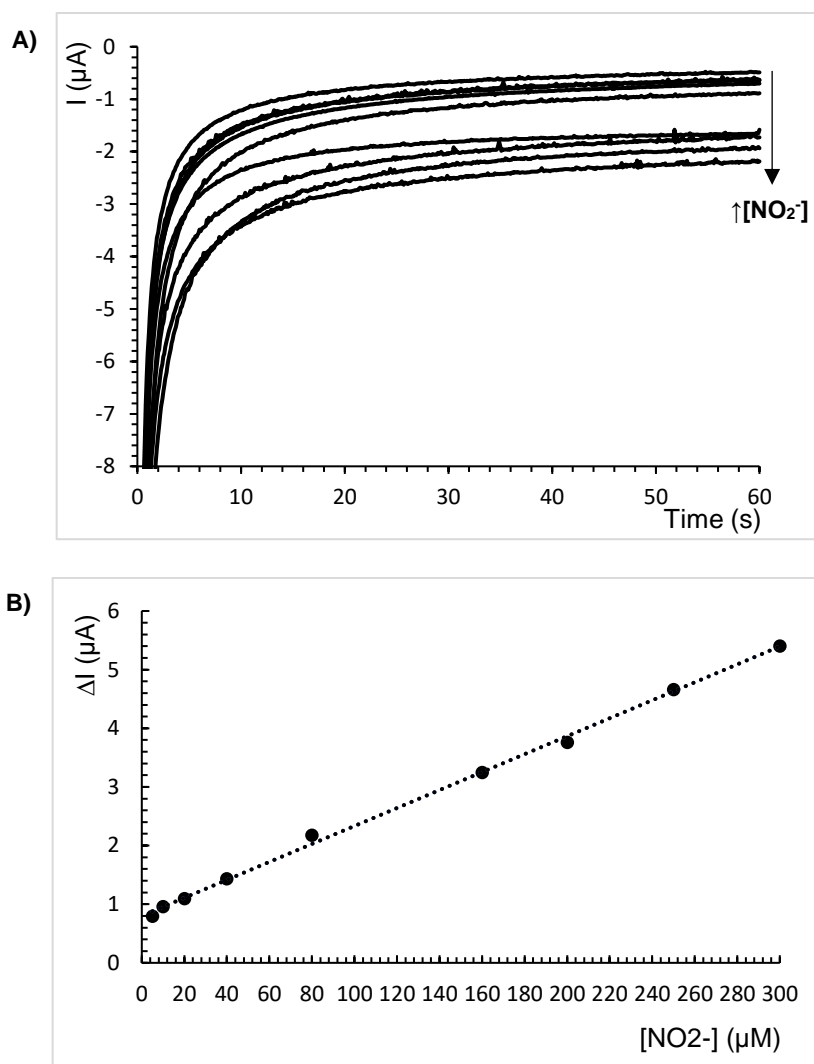


**Figure 3.5 - A)** Amperograms at  $-0.5$  V of supporting electrolyte (0.1 M Tris-HCl buffer, pH 7.6, with 0.1M KCl) containing the 100 mM ascorbate and nitrite (linear range of 2.5-300  $\mu\text{M}$ ). Measurements were recorded with ccNiR/AOx/PVA/SPE and the  $\Delta I_{\text{cat}}$  was measured at time = 60 s. **B)** Nitrite calibration curve using the CV technique. Each data point is the average of duplicates. The data were fitted to a straight line using the linear regression method, resulting in the following equation:  $\Delta I_{\text{cat}} = 0.015 [\text{NO}_2^-] + 0.802$ ,  $r^2 = 0.998$ , and a linear range of 5 to 300  $\mu\text{M}$ .

Table 3.2. compares the analytical performance of the nitrite biosensor, using both electrochemical methods for signal transduction with the one provided by the Griess reaction. Accordingly, we can conclude that the biosensor provides broader linear ranges, whereas the Griess is a more sensitive technique.

**Table 3.2** - Analytical parameters of the calibration curves obtained with the SPE/ccNiR/AOx/PVA biosensor and the Griess methods.

Parameters	Biosensor Method		Griess Method
	CV	Amperometry	
Linear Range ( $\mu\text{M}$ )	20 – 200	5 – 300	2.5 – 25
Sensitivity ( $\mu\text{M}^{-1}$ )	0.014	0.015	0.965
$r^2$	0.982	0.998	0.997

## 3.2. Sample pretreatment – a preliminary study

Sample turbidity is significant interference in optical methods. For this reason, turbid samples such as saliva, are usually first centrifuged to clean suspension particles. Since this operation is time-consuming and requires a refrigerated centrifuge, and the colorimetric nitrite determination is performed in a bench spectrophotometer, both placed in central laboratories, saliva samples are often frozen before analysis. Therefore, in the early stage of this work, we examined the influence of centrifugation and freezing of saliva specimens on nitrite quantification via the spectrophotometric method, and later with the bioelectrochemical approach. Initially, a set of four samples were analyzed before and after these two sample preparation steps (alone or combined).

### 3.2.1. Turbidity Influence

To evaluate the influence of turbidity in the nitrite quantification by the Griess method, we performed a preliminary study with four saliva samples, from two females (S1 and S2) and two males (S3 and S4), in a laboratory setting. Samples were cleaned up by centrifugation and quantified before and after this operation (Table 3.3).

**Table 3.3** - Centrifugation influence on the  $\text{NO}_2^-$  quantification in saliva specimens by the Griess method.

Sample	Griess Method [ $\text{NO}_2^-$ ] ( $\mu\text{M}$ )	
	Before centrifugation	After centrifugation
1	$30.1 \pm 0.7$	$29.4 \pm 0.3$
2	$32.7 \pm 3$	$27.8 \pm 0.7$
3	$29.0 \pm 3$	$21.5 \pm 1$
4	$74.2 \pm 8$	$40.0 \pm 2$

These results show that the nitrite concentration decreases in centrifuged samples, compared with those not centrifuged, which means that the sample turbidity enhances the nitrite levels. In other words, the absorbance of the azo compound formed during the Griess reaction increases due to the presence of suspended materials, resulting in the up deviation of nitrite levels. Therefore, saliva clearance is fundamental in this optical method.

### 3.2.2. Effect of freezing

As explained before, saliva samples are usually frozen until laboratory quantification. To evaluate the influence of the freezing effect in nitrite quantification by the Griess we performed an early study of this operation on results, with the same four saliva samples (S1-S4), used to evaluate the turbidity influence in section 3.2.1. Samples were analyzed freshly and then stored at -20 °C temperature, for 3 and 5 days. To eliminate the turbidity influence, samples were first centrifuged.

**Table 3.4** - The influence of sample freezing on nitrite quantification in saliva samples by the Griess method. All the samples were centrifuged prior to measurements.

Sample	T (°C)	Quantification moment (days)	Griess Method ([NO <sub>2</sub> <sup>-</sup> ] μM)
1	23	Immediately quantified	30.1 ± 0.7
	-20	3	7.0 ± 0.4
		5	6.6 ± 0.2
2	23	Immediately quantified	32.7 ± 3
	-20	3	*
		5	*
3	23	Immediately quantified	29.0 ± 3
	-20	3	*
		5	*
4	23	Immediately quantified	74.2 ± 8
	-20	3	32.0 ± 2
		5	26.1 ± 0.4

\* below the detection limit

As seen in Table 3.4, the nitrite concentrations were significantly lower when samples were frozen. These results showed the importance of performing nitrite analysis in real-time, without sample freezing, to eliminate the time variable. For the latter, we evaluate this parameter in Egas Moniz Dental Clinic, using both Griess and biosensor methods.

### 3.3. Pilot Clinical Study

A set of 61 participants were recruited at the Egas Moniz Dental Clinic and were asked to donate saliva samples for:

- 1) testing and validating the new point-of-care test based on the nitrite biosensor developed herein.
- 2) assessing the saliva nitrite concentrations in the saliva of two study groups (PD patients vs healthy) and evaluating possible correlations between the nitrite levels, the PD's progress, and its risk factors.

Because the preliminary study on the influence of sample pretreatment in nitrite quantification (section 3.2) showed that both centrifugation and freezing have a significant impact, some of the samples were aliquoted and analyzed either in real-time, without any treatment, or after centrifugation and storage at -20 °C. For validation purposes, all samples were also analyzed onsite through the Griess method, using a portable spectrophotometer. These data were used to understand the relevance of samples pre-treatment for each analytical technique.

According to the specific requisites of each study, several samples had to be excluded, so the total number of samples statistically analyzed was case-dependent.

#### 3.3.1. Biosensor Validation

##### 3.3.1.1. Centrifugation effect

A total of 44 participants were included in this study. All saliva samples were analyzed using both experimental techniques comparing the “biosensor vs Griess method”, in the following conditions:

- Freshly collected without centrifugation.
- Freshly collected and centrifuged.

As shown in Fig. 3.6, the results provided by the biosensor are not dependent on centrifugation (linear correlation), whereas those delivered by the Griess method, are affected by sample centrifugation, and the nitrite concentration is substantially lower. As discussed in section 3.2 this behavior is most likely due to sample turbidity. Saliva is a non-clear fluid that usually contains cells and food particles (**Gassmann, 2016**). These materials can scatter the incident light, thereby increasing the absorbance and contributing to a higher apparent nitrite concentration. Additionally, the obtained results are less reproducible. To validate this conclusion,



results were statistically analyzed by testing the following hypothesis: “The Griess method is affected by centrifugation” and “The biosensor performance is affected by centrifugation”.

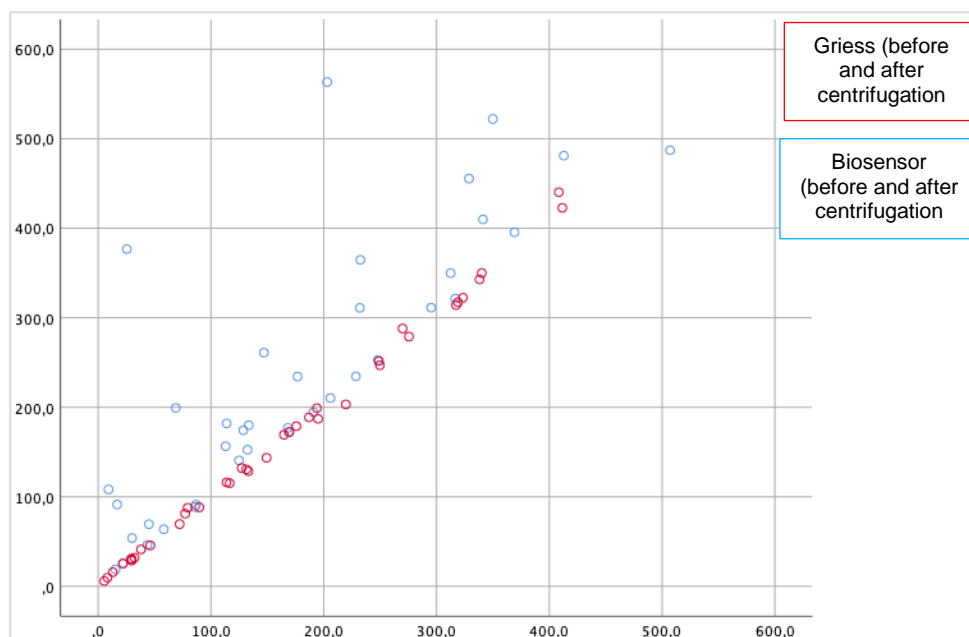


**Figure 3.6** - Influence of centrifugation on the biosensor (red circles) and Griess (blue circles) methods. Dispersion plot of nitrite concentration in saliva samples (freshly collected) before (y-axis), and after (x-axis) centrifugation.

As we can see in table 3.5, the Griess method is influenced by sample centrifugation, i.e., the hypothesis “The Griess method is affected by centrifugation” is not rejected because the  $p$ -value is lower than 0.05. As for the “the biosensor performance is affected by centrifugation” the answer is no because the  $p$ -value is higher than 0.05.

**Table 3.5** - Statistical analysis of the nitrite levels obtained with the Griess method, and with the biosensor approach, before and after centrifugation. The hypotheses tested are the following: “Griess method is affected by centrifugation” and “Biosensor performance is affected by centrifugation”.

Method	$N$	Average (SE) [NO <sub>2</sub> ] μM	$r$	$p$
Griess (before)	44	237.58 (22.4)	0.825	< 0.001
Griess (after)		182.69 (19.2)		
Biosensor (before)	38	163.99 (19.9)	0.998	0.087
Biosensor (after)		161.86 (19.4)		

To better understand the effect of saliva clearance on the method used for nitrite analysis, the turbidity of the sample was classified semi-quantitatively using the following criteria: level #0 represents clear samples, level #1 corresponds to low turbid samples, level #2 is assigned to turbid samples, and level 3 relates to the highest level of turbidity. The data were reassessed, as

shown in Figures 3.7 and 3.8, and the table. Accordingly, the biosensor response (Figure 3.7) is independent of the turbidity level (correlation coefficient ( $r$ ) close to 1), while in the Griess method (Figure 3.8) we see that the effect increases with sample turbidity ( $r$  distant from 1), being more effective above #2. Furthermore, the higher the saliva turbidity level, the lower the  $r$ .

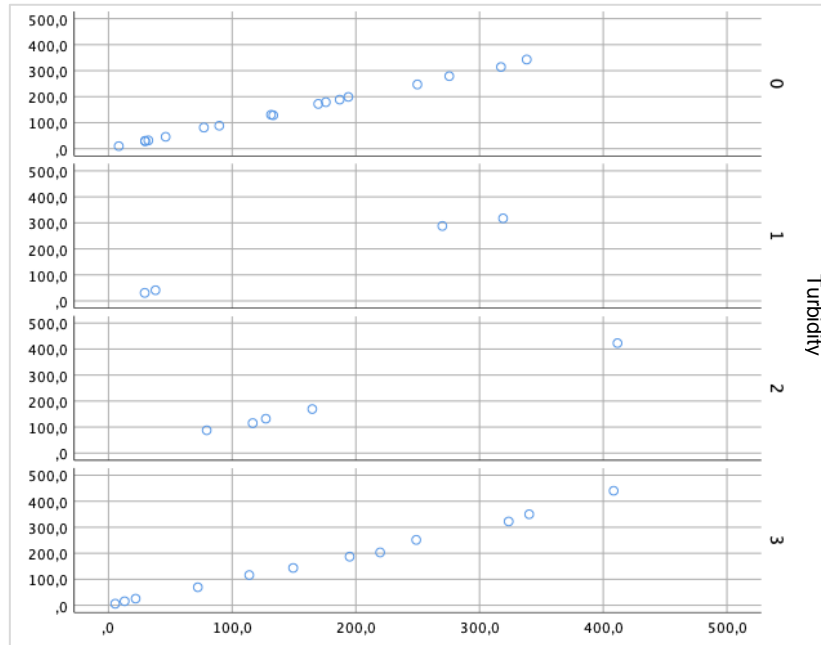


**Figure 3.7** - Dispersion plot of nitrite concentration, measured using the biosensor, according to turbidity levels: 0 – clear samples, 1 – low turbid samples, 2 – turbid samples, 3 – very turbid samples. For that analysis, 38 samples were quantified.

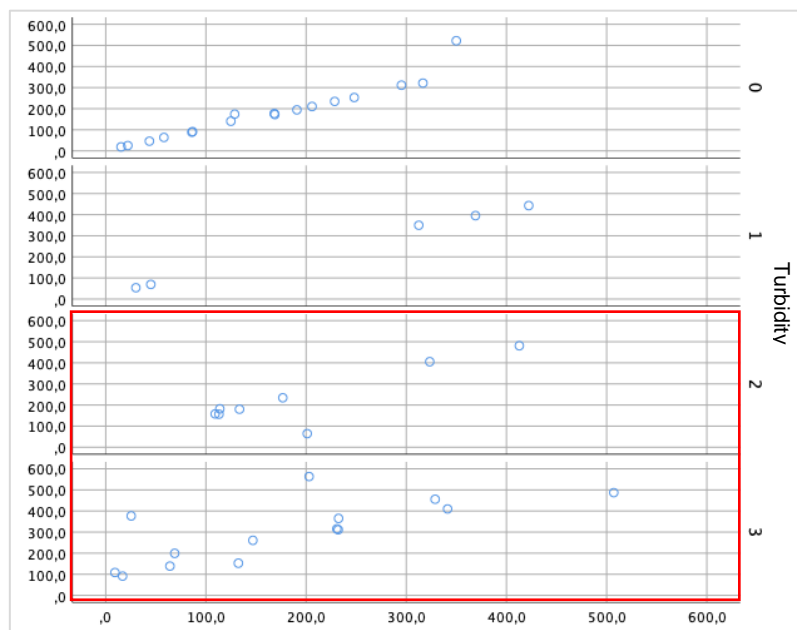


**Figure 3.8** – Dispersion plot of nitrite concentration, measured using the Griess method, according to turbidity levels: 0 – clear samples, 1 – low turbid samples, 2 – turbid samples, 3 – very turbid samples. For that analysis, 44 samples were quantified.

The statistical study shows that, for the biosensor, the correlation coefficient is similar to all turbidity levels and variations in clear samples are insignificant compared with turbid samples. For the Griess method, the higher the sample turbidity level, the lower the  $r$ .

**Table 3.6** - Influence of turbidity in both methods before and after centrifugation considering turbidity levels: 0 – clear samples, 1 – low turbid samples, 2 – turbid samples, 3 – very turbid samples.

Method	Turbidity	$N$	$r$	$p$
Griess	0	17	0.960	< 0.001
	1	5	0.999	< 0.001
	2	8	0.866	0.005
	3	14	0.732	0.003
Biosensor	0	17	1	< 0.001
	1	4	0.998	0.002
	2	5	1	< 0.001
	3	12	0.997	< 0.001

\*t-Student test

### 3.3.1.2. Effect of sample freezing

Following the preliminary results obtained in section 3.2. on the effect of sample freezing on the Griess method, we performed a more comprehensive study (14 samples) to understand the influence of sample storage at -20°C, in the biosensor response as well as on the Griess method. All samples were first evaluated as collected, within a timeframe of 10 min. Afterward, the specimens were centrifuged and re-assessed. Finally, both centrifuged and non-centrifuged samples were frozen at -20°C and re-analyzed after 10 days. This protocol originated four samples groups, as below:

- Freshly collected without centrifugation.
- Freshly collected and centrifuged.
- Frozen without centrifugation.
- Frozen and centrifuged.

As shown in Tables 3.7 and 3.8, if samples are centrifuged before freezing, the nitrite concentration decreases. On the contrary, if samples are frozen without centrifugation, the nitrite concentration increases between 10 to 50 %. These trends do not depend on the technique used.

**Table 3.7** - Freezing effect on saliva samples.

Centrifugation before freezing samples	N	Number of samples with NO <sub>2</sub> <sup>-</sup> variation above the error	
		Griess	Biosensor
Yes	14	12 ↓	12 ↓
No	14	12 ↑	12 ↑

**Table 3.8** - Nitrite concentration in salivary fluid samples of fourteen volunteers to evaluate two important parameters: the influence of centrifugation in both methods and the nitrite stability in frozen samples.

Samples			[NO <sub>2</sub> <sup>-</sup> ] μM			
#	Turbidity level	State	Griess Method		Biosensor Method	
			Fresh	Frozen	Fresh	Frozen
S1	0	Non-centrifuged	63.7±0.7	113.2±4	30.1	32.4
		Centrifuged	58.1±0.3	37.8±3	29.6	19.6
S2	3	Non-centrifuged	108.2±24	129.6±0.9	5.9	9.3
		Centrifuged	19.2±0.3	13.8±2	5.4	2.1
S3	2	Non-centrifuged	405.4±66	424.2±3	domed	domed
		Centrifuged	323.4±0.3	305.6±3	domed	306.4
S4	1	Non-centrifuged	69.4±0.6	71.5±0.9	30.8	33.8
		Centrifuged	45.0±0.7	*	29.3	19.9
S36	3	Non-centrifuged	409.9±40	393.3±0.3	349.9	domed
		Centrifuged	341.2±0.3	311.1±0.9	340.1	307.7
S38	0	Non-centrifuged	253.0±0.8	271.0±2	247.0	310.5
		Centrifuged	248.0±0.1	205.1±3	249.7	210.1
S39	3	Non-centrifuged	311.1±2	631.2±0.5	251.5	289.9
		Centrifuged	232.0±0.5	444.3±0.9	248.8	230.3
S41	3	Non-centrifuged	91.3±2	45.1±5	15.7	6.1
		Centrifuged	16.8±0.5	16.0±1	13.0	n.d.
S43	0	Non-centrifuged	311.3±0.7	332.9±0.4	278.9	284.3
		Centrifuged	295.2±0.9	274.1±0.2	275.5	260.4
S48	0	Non-centrifuged	172.5±1	199.8±1	188.7	196.6
		Centrifuged	168.8±1	140.4±0.8	186.9	138.3
S49	3	Non-centrifuged	199.3±2	222.7±3	69.5	214.5
		Centrifuged	68.8±0.5	55.6±1	72.2	56.7
S50	2	Non-centrifuged	156.5±0.5	184.4±2	115.2	189.7
		Centrifuged	113.0±1	106.0±0.5	116.6	102.9
S51	1	Non-centrifuged	53.9±5	63.4±2	41.2	58.7
		Centrifuged	30.1±2	22.2±0.4	38.0	20.3
S52	0	Non-centrifuged	140.6±1	160.4±4	128.5	164.9
		Centrifuged	124.9±0.5	111.5±0.2	133.2	112.3

\* Insufficient sample volume

The decay in nitrite concentration in cleared samples may indicate that this ion is not stable upon storage in the freezer (e.g., it might be oxidized into nitrate). Though, the increase in nitrite levels after sample storage without previous centrifugation is more difficult to explain. We propose that the nitrite reductase activity of some commensal bacteria present in the oral cavity (**Kevil et al., 2011**) might be contributing to the nitrite concentration enhancement. In future studies, it would be important to study a new hypothesis centered on nitrate reduction by the oral cavity microflora, for which the  $\text{NO}_3^-$  concentration should be evaluated.

### 3.3.1.3. Method Validation

Our previous results suggested that the biosensors' response to nitrite does not depend on saliva pre-treatment, which paves the way for the implementation of a point-of-care test that allows the real-time and less time-consuming quantification of nitrite. Nevertheless, the analytical method used to validate the biosensor approach (Griess method), requires sample centrifugation prior to the measurements.

The statistic (t-student) comparison of both techniques (Table 3.9) shows that the results provided by the two techniques are comparable, so the application of the nitrite biosensor in the saliva is validated ( $p < 0.05$ ). This is an important result, that will enable the transference of this methodology to clinical settings.

**Table 3.9** - Comparison of nitrite concentrations obtained with both techniques (Griess and biosensor).

Methods	N	R	P
Griess vs. Biosensor	38	0.967	< 0.001

t-Student test

Furthermore, we selected two previously frozen-centrifuged saliva samples and analyzed their nitrite content by HPLC-ionic chromatography, which is characterized by its high sensitivity in complex matrices (**Jiang, 2012**). The obtained results (Table 3.10) demonstrate the consistency of the nitrite biosensor performance since the nitrite values are in agreement with those delivered by both Griess and HPLC techniques.

**Table 3.10** – Nitrite content in two saliva samples, quantified by Griess, biosensor, and HPLC techniques.

Samples	NO <sub>2</sub> <sup>-</sup> concentration (µM)		
	Griess	Biosensor	HPLC
S28	81.9 ± 3	80.5 ± 3	75.7 ± 0.5
S50	55.8 ± 2	53.3 ± 2	45.8

The biosensor is thus, a new and reliable option for nitrite quantification in complex matrices. Table 3.11 highlights the pros and cons of this approach.

**Table 3.11** - Pros and cons of the new nitrite biosensor (SPE/ccNiR/AOx/PVA) and the Griess method.

Method	Griess	Biosensor
<b>Pros</b>	Cheap Easy to implement	Point-of-care testing Does not require sample centrifugation Easy to use Quick Potential for digitation
<b>Cons</b>	Laboratory method Large equipment Operated by technicians Centrifugation is required	Shelf-life stability (ongoing study)

### 3.3.2. Nitrite and Periodontal disease

Upon checking the full list of participants initially engaged in the first part of the study, where the sample preparation and the performance of the biosensor were assessed, only 35 individuals proceed to the clinical study. The trial was subdivided into three groups according to the volunteer's health condition, genre, and age. Regarding the health status, it was subdivided into individuals with periodontal disease ( $N=21$ ), periimplantitis (a localized PD condition) ( $N=3$ ), and healthy participants ( $N=11$ ) (Figure 3.9). Furthermore, PD is subdivided into four Stages (I, II, III, and IV) and three Grades (A, B, and C), parameters which we aim to understand and correlate with saliva samples' nitrite content.

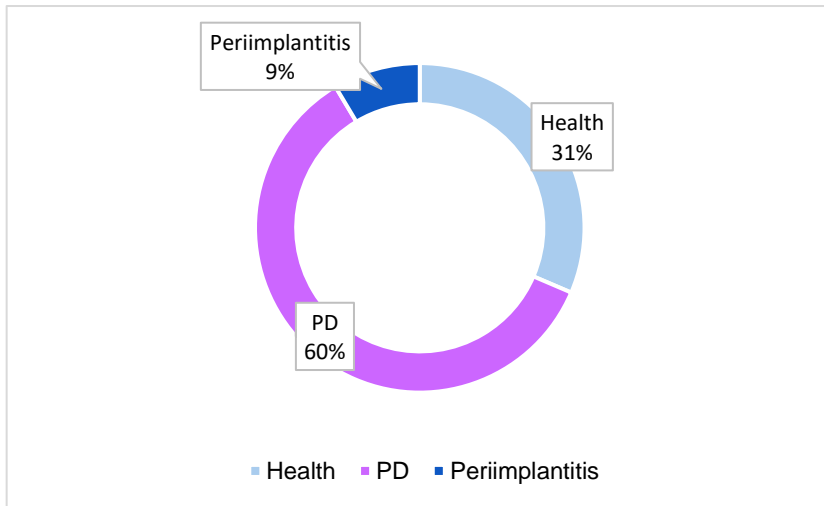


**Figure 3.9** – Characterization of the study populations accordingly to health status.

This part of the work was composed of 35 participants, which are subdivided into the female and male genres, to evaluate, furthermore, the genre influence on the PD (Table 3.12).

**Table 3.12** - Sample trial genre distribution according to female and male.

Genre	Healthy	Periodontal Disease	Periimplantitis	TOTAL
Female	10	13	2	25
Male	1	8	1	10
TOTAL	11	21	3	35

Our trial was composed of individuals from all established age groups (Table 3.13) to evaluate the influence of PD on the population in the next section.

**Table 3.13** - Sample trial age distribution according to different age groups.

Age	Healthy	Periodontal Disease	Periimplantitis	TOTAL
18-30	10	2	0	12
31-41	1	1	0	2
42-52	0	6	0	6
53-63	0	8	0	8
≥64	0	4	3	7
TOTAL	11	21	3	35

According to patients' data, the age average was  $45 \pm 18.8$  years old. The youngest participants have 22 years old and the oldest has 80 years old, at the sample collection moment. For the PD group, the average age was  $53 \pm 12.5$  years old, out of 21 participants. Considering the individuals with periimplantitis, the average age increases a little bit up to  $55 \pm 13.5$  years old, out of 24 participants.

The main objective of this second part of the work is to understand a potential relationship between nitrite concentration in saliva samples and periodontal disease using the ccNiR/AOx/PVA/SPE biosensor.

To this end, all samples were submitted to the same analytical methodology, i.e., centrifugation/non-centrifugation, and freezing/non-freezing. Fresh samples were analyzed no more than 10 minutes after collection.

The first parameter evaluated was the disease stage (**Figure 3.10**). The trial was composed of 24 participants with PD or periimplantitis.

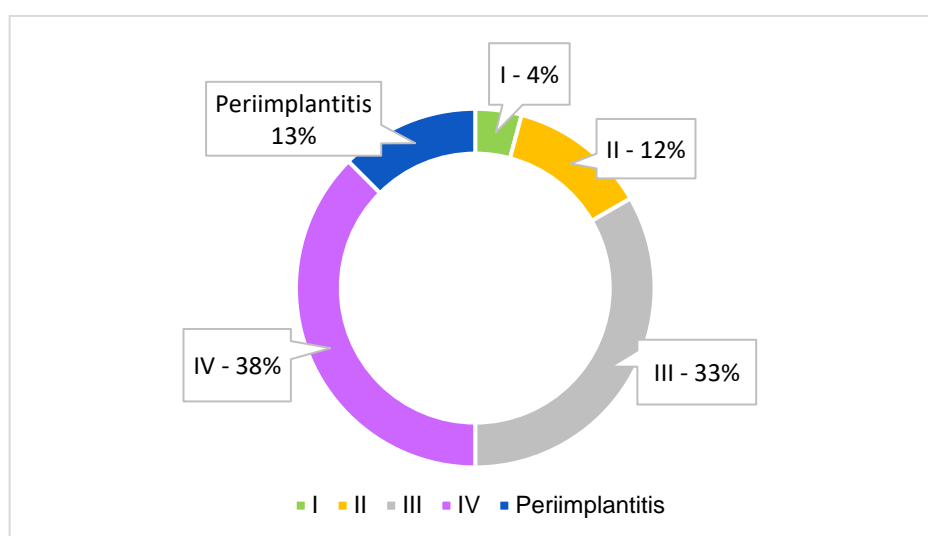


**Figure 3.10** - PD stages distribution. Of the 24 participants, 1 is on stage I, 3 in II, 8 in III, and 9 in IV. 3 of the patients have periimplantitis.

The obtained results were surprising since higher nitrite concentrations are seen in the healthy people group, which is not in agreement with most clinical studies. However, the two study groups here compared are not homogeneous since the size and the participants' age are very different and might be impacting the results. The great majority of young participants (10 with 22 years old) are included in the healthy group (control), which was compared with the larger PD group, composed of much older people. The metabolism, health conditions, and diet habits should be different and may introduce bias in data analysis. In the future, a larger control group should be considered. Nevertheless, some works have found significantly lower levels of NO-metabolites in the serum and saliva fluids of periodontitis patients (**Topcu, 2014**). Furthermore,



PD patients' assessment covers a wide range of nitrite concentrations, so it was difficult to establish concrete differences between stages (Figure 3.11). As demonstrated, herein, healthy people have higher values or no significant differences in nitrite concentrations than PD patients. However, we see no trend between the enhanced nitrite levels and the degree stage, which go up and down as shown in Fig. 3.13 (stage II:  $54.9 \pm 18.3 \mu\text{M}$ ; stage IV:  $107.0 \pm 31.4 \mu\text{M}$ ; and stage III:  $210.1 \pm 39.6 \mu\text{M}$ ). Statistically, the subgroups stage III, healthy ( $257.0 \pm 30.4 \mu\text{M}$ ), and periimplantitis condition ( $242.7 \pm 47 \mu\text{M}$ ), are not different. However, the nitrite concentrations are significantly different in stages II and IV. Stage I was not considered since there was only one participant in that condition. These results are not consistent, so no conclusions on the nitrite variations in saliva with PD can be made yet.

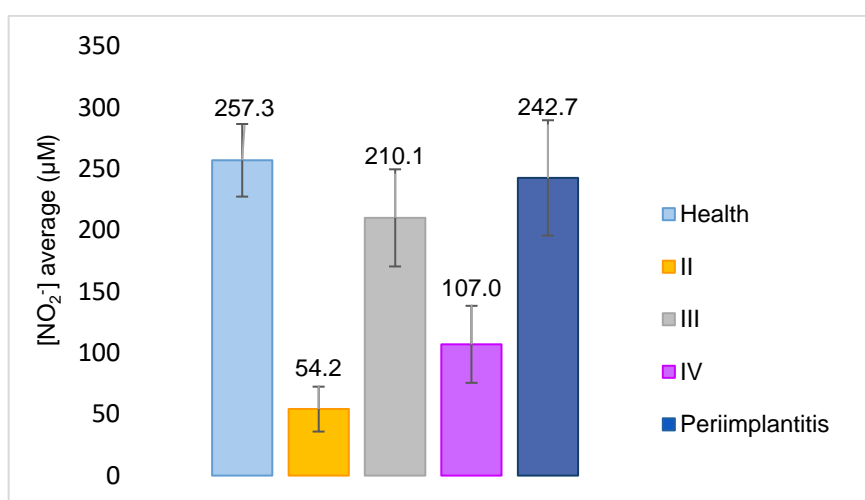


**Figure 3.11** - Mean nitrite concentration in different PD Stages. Results were obtained with the ccNiR/AOx/PVA/SPE biosensors and using amperometric transduction.

One should emphasize, that the higher nitrite values found in healthy people may be due to factors that were estimated in this project, particularly, the food habits of each participant, or commensal bacteria present in the oral cavity, factors that should be well included in future work.

As for PD grades, there was 1 patient in grade A, 12 patients in grade B, and 8 in grade C, in addition to the 3 with individual periimplantitis. According to the results (Figure 3.12), the highest grades, B and C, did not present significant differences in their means. In addition, healthy individuals still have higher nitrite concentrations than those recorded in people with PD.

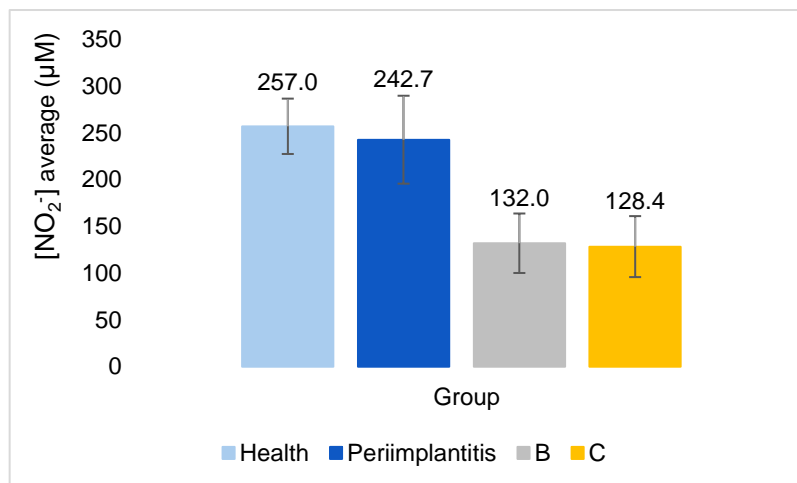


**Figure 3.12** - Mean nitrite concentration in different PD Grades. Results were obtained with the ccNiR/AOx/PVA/SPE biosensors and using amperometric transduction.

The working hypothesis in this study was that there is a relationship between saliva nitrite levels with PD stages and grades. The main conclusion of this study is that to better understand this question, other variables should be included in the study design. For example, commensal bacteria present in the oral cavity have nitrate reductases that can reduce nitrate into nitrite. The microflora depends on some medicines and/or antiseptic mouthwashes, commonly used by people who have some oral condition, which can contribute to lowering the nitrite concentration (Kevil et al., 2011). Another factor is food habits: the higher the nitrate concentration in the diet, the higher the nitrite levels in saliva (Bryan, 2016). The age of participants should be equally balanced in all study groups. Furthermore, the size of subgroups should increase to allow statistical analysis of PD risk factors (see below).

### 3.3.3. Periodontal disease risk factors

According to our results, the female genre has the predisposition to show higher nitrite levels. However, the associated errors are too big, we cannot draw reliable conclusions. Once again, this indicates that the groups need to be more homogenous to enable a consistent analysis.

**Table 3.14** - Nitrite concentrations according to periodontitis participants' genre.

Genre	N	[NO <sub>2</sub> <sup>-</sup> ] µM
Male	9 (37.5 %)	182.1 ± 65
Female	15 (62.5 %)	210.4 ± 100

In the literature, a higher oral nitrite concentration was seen in females, which is important to consider since the trial was performed with more women than men (**Kapil, 2018**). This could happen due to higher oral nitrate reduction and enhanced systemic nitrite reported for women (**Kapil, 2018**).

In the future, an equal number of participants in both groups, need to be evaluated.

Next, we evaluated the influence of PD predominance in all age groups. Different samples differ largely due to the patient's disease stages and grades. Of the 24 participants, only 3 are in the youngest age groups (18-30 and 31-41). To compare the obtained results of the oldest age groups with the youngest ones, the trial needs to be larger to statistically compare all the age groups. However, comparing the oldest groups, the results show higher concentrations in the  $\geq 64$  years group.

**Table 3.15** - Nitrite concentrations according to periodontitis participants' age group.

Age Groups	N	[NO <sub>2</sub> <sup>-</sup> ] (μM)
18-30	2	117.7 ± 77
31-41	1	169.9
42-52	6	129.4 ± 105
53-63	8	168.4 ± 80
≥64	7	207.0 ± 57

Earlier studies reveal that the periodontal condition is prevalent in the population between 50 to 69 years old (**Rheu, 2011**). According to literature, in Portugal older age groups are more affected by this disease. In future work, an equal number of participants of all age groups need to be evaluated, comparing with correspondent age groups from healthy participants.

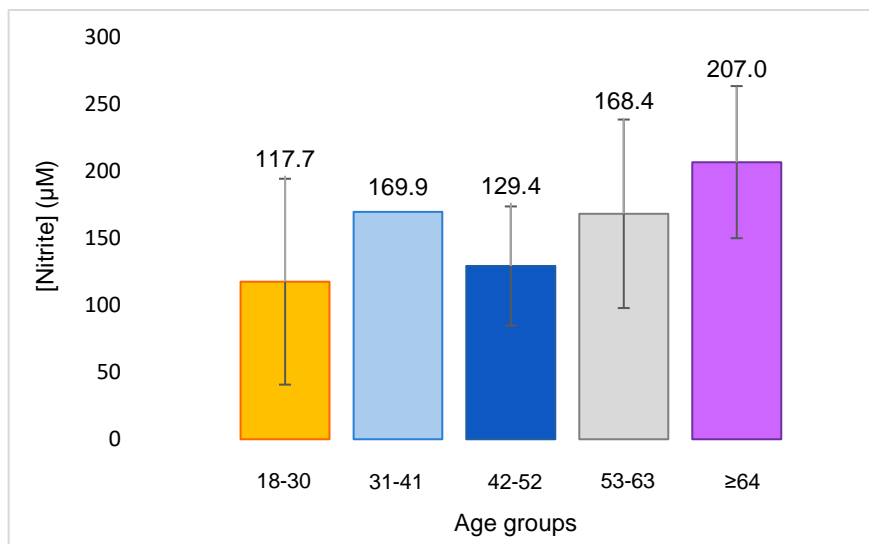


**Figure 3.13** - Nitrite content according to the age group. This trial was performed using 24 PD different saliva samples. Results were obtained with ccNiR/AOx/PVA/SPE and using amperometric transduction.

In addition to the genre, age, and food, smoking habits could also affect both PD predisposition and nitrite concentration. Another known risk factor for PD is smoking habits. Past studies have revealed that people who smoke do not present higher concentrations of nitrite than individuals who smoke. From the results obtained, ex-smokers have higher nitrite concentrations ( $227.3 \pm 1.7 \mu\text{M}$ ), followed by non-smokers ( $199.7 \pm 3.8 \mu\text{M}$ ) and smokers ( $130.2 \pm 0.9 \mu\text{M}$ ). Of these 24 individuals, 13 are smokers, 7 are non-smokers, and 4 are ex-smokers. Considering these values, it is not possible to establish a direct correlation between the concentrations of nitrite and smoking habits.

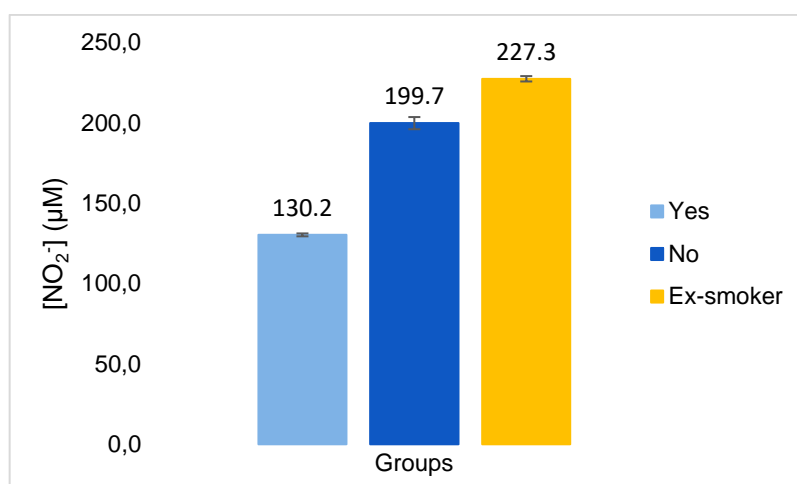


**Figure 3.14** - Nitrite content according to the smoke habits. This trial was performed using saliva samples from 24 persons with PD. Results were obtained with ccNiR/AOx/PVA/SPE and using amperometric transduction.

According to our results, individuals who smoke have lower nitrite concentrations in saliva than individuals who do not smoke or who are ex-smokers. In this sample, 54% of the participants are smokers, and 46% have never smoked or are ex-smokers, which makes the sample quite homogeneous. The information available in the literature is contradictory, since some studies report low NO<sub>2</sub><sup>-</sup> production in smokers (Wang, 2019), whereas other studies indicate that the production of NO<sub>2</sub><sup>-</sup> and its metabolites increased (Bachtiar, 2019). According to Wang (Wang, 2019), smoking habits are periodontal condition modifiers, increasing the disease level.

Nitrate-rich fruits and vegetables, water, and meats are normally consumed in the human diet contributing to a higher nitrite concentration in the human organism (Hord, 2009 and Hou, 2013). Therefore, the questionnaire included questions on the participants' dietary habits. The data is presented below (Table 3.16).

**Table 3.16** - Food habits of participants.

Parameters	Health	Periodontal Disease	Periimplantitis	Total
<b>Fruits</b> (pomegranate juice, orange, banana)				
No	1	1	0	2
Small quantities	0	2	0	2
Yes	10	18	3	31
Total	11	21	3	35
<b>Vegetables</b> (spinach, beetroot, cabbage, vegetable juice)				
No	2	3	1	6
Small quantities	0	1	0	1
Yes	9	17	2	28
Total	11	21	3	35
<b>Processed meats</b> (ham, bacon, sausage)				
No	5	9	1	15
Small quantities	3	7	1	11
Yes	3	5	1	9
Total	11	21	3	35

The correlation between the saliva's nitrite content and diet features presented in Figure 3.15. Generally, the error bars are too high to enable reliable comparisons.

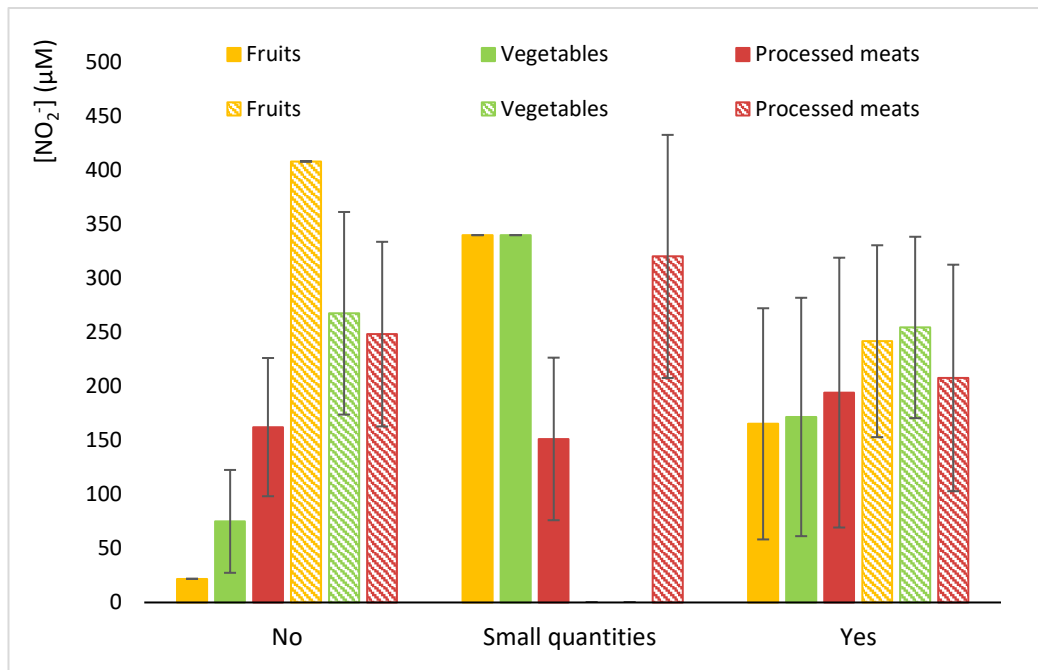


**Figure 3.15** - Nitrite quantification according to food habits. This trial was performed using 24 PD different saliva samples (full), and 11 healthy individuals (stripes). Results were obtained with ccNiR/AOx/PVA/SPE and using amperometric transducing.

The nitrite higher concentration in healthy people could be a consequence of food habits. First, exists a nitrates intake from food or endogenous  $\text{NO}\cdot$  oxidation (Rocha, 2011), a topic well developed in the introduction section  $\text{NO}_3^- - \text{NO}_2^- - \text{NO}\cdot$  pathway. The nitrate provided by the diet is reduced into nitrite by the facultative anaerobic commensal bacteria, present in the oral cavity. This oral reduction is extremely dependent on the oral microbiome.

In addition, some studies revealed a higher oral nitrite concentration in females than in males, which is important to consider since the trial was performed with more women than men. Moreover, anti-bacterial mouthwashes disable the normal nitrate into nitrite conversion (Kapil, 2018). Thus, microbiome analysis is an important step to consider in future work.



Chapter

4

# Conclusions





## 4. CONCLUSIONS

This study aimed to understand the correlation between nitrite concentration and Periodontal Disease using a POCT as a novel approach.

The first part of the study evaluated the two steps of sample pre-preparation usually performed in the saliva specimen, namely, centrifugation and freezing. For centrifugation, we conclude that the biosensor does not need this step since it was not affected by the turbidity of the samples. Sample freezing affects the nitrite content in saliva, demonstrating the need for real-time analysis, i.e., saliva samples should be always freshly analyzed. This is a very important outcome of this project since it calls the attention of the scientific community to the relevance of the sample treatment protocol. Moreover, the data published in some papers should be reviewed, for example, obtained results from Reher or Topcu (**Reher, 2007 and Topcu, 2014**).

After establishing the pre-treatment conditions, we analyzed the results of nitrite quantification in unstimulated saliva samples. According to our preliminary data, there are higher nitrite levels in healthy individuals than in PD patients. However, a careful analysis of the group composition shows that the age distribution was not uniform in the two main study groups, so we cannot draw definitive conclusions yet. In future works, the study design should include a larger and more diversified healthy control group, regarding the participants' age. Furthermore, all groups should be also diversified according to, smoking, and diet habits, two risk factors that we consider to be great influencers in the nitrite concentration in saliva. The PD group should include more individuals presenting different disease stages/grades. Despite not allowing to test of the working hypothesis on the relationship between saliva's nitrite and PD, with this work we made considerable progress in the study design that will be followed in the next studies, aiming at providing the clinicians' community with a faster, sensible, and specific biosensor for nitrite.

## 4.1. FUTURE WORK

Regarding future perspectives, aiming for the employment of the miniaturized nitrite biosensor in clinical diagnosis for periodontal disease, several aspects should be considered.

The group's composition deserves more attention. The age groups must be composed of an equal number of participants. Furthermore, the control groups must also meet certain criteria:

- Equal participants number in each PD and healthy group;
- Healthy samples collection in different appointments than the periodontology.

Aiming to understand the diet contributes to the nitrite levels in saliva samples, nitrates should be analyzed, and the diet habits should be largely evaluated.

The inclusion and exclusion criteria need to be revised. Since PD is an inflammatory disease dependent on bacterial presence, people who are taking antibiotics (at least for the last 6 months), should be excluded. As a quotidian practice or in a clinical context, the use of elixirs such as chlorohexidine solutions should be also considered.



Chapter

5

# References



## REFERENCES

- Almeida, M. G., et al. (2003). The isolation and characterization of cytochrome c nitrite reductase subunits (NrfA and NrfH) from *Desulfovibrio desulfuricans* ATCC 27774. *Eur. J. Biochem.* 270, 3904–3915. DOI: 10.1046/j.1432-1033.2003.03772.x.
- Almeida, M. G., et al. (2010) Nitrite Biosensing via Selective Enzymes – A Long but Promising Route. *Sensors*, 10, 11530-11555. doi:10.3390/s101211530
- Almeida et al. (2007). Biosensing nitrite using the system nitrite reductase/Nafion/methyl-viologen – a voltammetric study. *Biosensors and Bioelectronics*, 22, 2485-2492. doi:10.1016/j.bios.2006.09.027
- Amdahl, M. B., DeMartino, A. W., & Gladwin, M. T. (2019). Inorganic nitrite bioactivation and role in physiological signaling and therapeutics. *Biological chemistry*, 401(1), 201–211. <https://doi.org/10.1515/hsz-2019-0349>
- Azmi, A., et al. (2017) Techniques in advancing the capabilities of various nitrate detection methods: a review. *International Journal on Smart Sensing and Intelligent Systems*, 10(2), 223-261. <https://doi.org/10.21307/ijssis-2017-210>
- Bachtiar, E. W., Putri, A. C., & Bachtiar, B. M. (2019). Salivary nitric oxide, Simplified Oral Hygiene Index, and salivary flow rate in smokers and non-smokers: a cross-sectional study. *F1000Research*, 8, 1–15. <https://doi.org/10.12688/f1000research.20099.2>
- Bejeh-Mir, A. P. et al. (2014) Diagnostic Role of Salivary and GCF Nitrite, Nitrate and Nitric Oxide to Distinguish Healthy Periodontium from Gingivitis and Periodontitis. *Int J Mol Cell Med*, 3(3), 138-145. PMID: [25317400](https://pubmed.ncbi.nlm.nih.gov/25317400/)
- Björne, H., et al. (2004) Nitrite in saliva increases gastric mucosal blood flow and mucus thickness. *Clin Invest.*; 113(1):106-114. <https://doi.org/10.1172/JCI19019>
- Bryan, N., et al. (2005). Nitrite is a signaling molecule and regulator of gene expression in mammalian tissues. *Nat Chem Biol* 1, 290–297. <https://doi.org/10.1038/nchembio734>
- Bryan, N.S. (2016). Nitrite and Nitrates. *Encyclopedia of Food and Health*, 73–78. <http://dx.doi.org/10.1016/B978-0-12-384947-2.00484-0>
- Cosby, K., et al. (2003). Nitrite reduction to nitric oxide by deoxyhemoglobin vasodilates the human circulation. *Nature medicine*, 9(12), 1498–1505. <https://doi.org/10.1038/nm954>
- Costa, R. (2019). Nova classificação das doenças e condições periodontais – um algoritmo de diagnóstico. [Mestrado Integrado em Medicina Dentária, Faculdade de Medicina Dentária da Universidade do Porto].

- Monteiro, T., Almeida, M. G. (2020). Development of point-of-care tests using enzyme (NiR & PON) based electrochemical biosensors. [Biotechnology Master, NOVA University of Lisbon].
- Cross, A. J., et al. (2011). Meat consumption and risk of esophageal and gastric cancer in a large prospective study. *Am J Gastroenterol*, 106(3), 432-442. doi: 10.1038/ajg.2010.415.
- Cunha, C. A., et al. (2003). Cytochrome c Nitrite Reductase from *Desulfovibrio desulfuricans* ATCC 27774. *The Journal of Biological Chemistry*, 278(18), 17455-17465. DOI 10.1074/jbc.M211777200
- Dalsgaard, T., Simonsen, U., Fag, o A. (2007). Nitrite-dependent vasodilation is facilitated by hypoxia and is independent of known NO-generating nitrite reductase activities. *American journal of physiology Heart and circulatory physiology*. 292(6) doi:10.1152/ajpheart.01298.2006
- EFSA. (2008). Nitrate in vegetables. Scientific opinion of the panel on contaminants in the food chain. *EFSA J.*, 689, 1–79. <https://doi.org/10.2903/j.efsa.2008.689>
- Fajardo-Gutiérrez, A. (2017). Medición en epidemiología: prevalencia, incidencia, riesgo, medidas de impacto. *Revista Alergia México*, 64(1), 109–120. <https://doi.org/10.29262/ram.v64i1.252>
- Flores, M., & Toldrá, F. (2021). Chemistry, safety, and regulatory considerations in the use of nitrite and nitrate from natural origin in meat products. *Meat Science*. Elsevier Ltd. <https://doi.org/10.1016/j.meatsci.2020.108272>
- Forstermann, U., Sessa, W. C. (2012). Nitric oxide synthases: regulation and function. *European Heart Journal*, 33(7), 829–837. doi:10.1093/eurheartj/ehr304
- Gassmann, S., Schuette, H., Thoma, Ch. (2016). Colorimetric microfluidic Nitrite sensor with optical fiber coupling. *IECON*, DOI: 10.1109/IECON.2016.7793716
- Gladwin, M (2005). Nitrite as an intrinsic signaling molecule. *Nat Chem Biol* 1, 245–246. <https://doi.org/10.1038/nchembio1005-245>
- Gladwin, M. T., et al. (2005). The emerging biology of the nitrite anion. *Nature chemical biology*, 1(6), 308–314. <https://doi.org/10.1038/nchembio1105-308>
- He, W., et al. (2018). Point-of-Care Periodontitis Testing: Biomarkers, Current Technologies, and Perspectives. *Trends in Biotechnology*, S0167779918301483–. doi:10.1016/j.tibtech.2018.05.013
- Hickey, T., MacNeil, J. A., Hansmeyer, C., Pickup, M. J. (2021). Fatal methemoglobinemia: A case series highlighting a new trend in intentional sodium nitrite or sodium nitrate ingestion as a method of suicide. *Forensic science international*, 326, 110907. <https://doi.org/10.1016/j.forsciint.2021.110907>



- Highfield, J. (2009). Diagnosis and classification of periodontal disease. *Australian dental journal*, 54 Suppl 1, S11–S26. <https://doi.org/10.1111/j.1834-7819.2009.01140.x>
- Hord, N. G., Tang, Y., Bryan, N. S. (2009). Food sources of nitrates and nitrite: the physiologic context for potential health benefits. *Am J Clin Nutr*, 90(1), 1-10. <https://doi.org/10.3945/ajcn.2008.27131>
- Hou, C. J., Jaing, C. G., Long, Z. C. (2013). Nitrite level of pickled vegetables in Northeast China. *Food Control*, 29, 7-10. doi:10.1016/j.foodcont.2012.05.067
- Jain, P., et al. (2021). Periodontitis and Systemic Disorder – An Overview of Relation and Novel Treatment Modalities. *Pharmaceutics*, 13, 1175. <https://doi.org/10.3390/pharmaceutics13081175>
- Jiang, H., et al. (2012). Analytical Techniques for Assaying Nitric Oxide Bioactivity. *JoVE*, 64, e3722, DOI : 10.3791/3722 (2012).
- Kapil, V., et al. (2018). Sex differences in the nitrate-nitrite-NO• pathway: Role of oral nitrate-reducing bacteria. *Free Radical Biology and Medicine*, 126, 113–121. <https://doi.org/10.1016/j.freeradbiomed.2018.07.010>
- Karwowska, M., & Kononiuk, A. (2020). Nitrates/Nitrite in Food-Risk for Nitrosative Stress and Benefits. *Antioxidants*, 9(3), 1–17. <https://doi.org/10.3390/antiox9030241>
- Kevil, C. G., Kolluru, G. K., Pattillo, C. B., Giordano, T. (2011). Inorganic nitrite therapy: Historical perspective and future directions. *Free Radical Biology and Medicine*, 51(3), 576–593. Elsevier. <http://doi.org/10.1016/j.freeradbiomed.2011.04.042>
- Khan, F. A., et al. (2020). Headache and Methemoglobinemia. *Headache*, 60(1), 291–297. <https://doi.org/10.1111/head.13696>
- Kleinbongard, P., et al. (2006). Plasma nitrite concentrations reflect the degree of endothelial dysfunction in humans. *Free Radical Biology and Medicine*, 40(2), 295–302. <https://doi.org/10.1016/j.freeradbiomed.2005.08.025>
- Laranjinha, J. et al. (2021). The Peculiar Facets of Nitric Oxide as a Cellular Messenger: From Disease-Associated Signaling to the Regulation of Brain Bioenergetics and Neurovascular Coupling. *Neurochemical research*, 46(1), 64–76. <https://doi.org/10.1007/s11064-020-03015-0>
- Li, D., et al. (2018). Griess reaction-based paper strip for colorimetric/fluorescent/SERS triple sensing of nitrite. *Biosensors and Bioelectronics*, 99, 389–398. <https://doi.org/10.1016/j.bios.2017.08.008>
- Li, H., et al. (2014) Structures of human constitutive nitric oxide synthases. *Biological Crystallography*, D70, 2667–2674. doi:10.1107/S1399004714017064

- Lindhe, J., Karring, T., & Lang, N.P. (2003). Clinical Periodontology and Implant Dentistry (4<sup>a</sup> edição). *Blackwell Munksgaard*. <https://doi.org/10.1038/sj.bdj.4810851>
- Ling, W. C., Mustafa, M. R., & Murugan, D. D. (2020). Therapeutic Implications of Nitrite in Hypertension. *Journal of cardiovascular pharmacology*, 75(2), 123–134. <https://doi.org/10.1097/FJC.0000000000000771>
- Liu, Z., Manikandan, V. S., Chen, A. (2019). Recent advances in nanomaterial-based electrochemical sensing of nitric oxide and nitrite for biomedical and food research. *Current Opinion in Electrochemistry*. 16, 127–133 <https://doi.org/10.1016/j.coelec.2019.05.013>
- Ledezma-Zamora, et al. (2021) Residual nitrite in processed meat products in Costa Rica: Method validation, long-term survey and intake estimations. *Food Chemistry*, 361, 130082. <https://doi.org/10.1016/j.foodchem.2021.130082>
- Lozano, M. G. et al. (2019). Biosensors for Food Quality and Safety Monitoring: Fundamentals and Applications. *Enzymes in Food Biotechnology*, 40, 691-709. <https://doi.org/10.1016/B978-0-12-813280-7.00040-2>
- Lundberg, J. et al. (1994) Intra-gastric nitric oxide production in humans: measurements in expelled air. *Gut*. 35, 1543–1546
- Lundberg, J., Weitzberg, E., Gladwin, M. (2008). The nitrate–nitrite–nitric oxide pathway in physiology and therapeutics. *Nature Reviews Drug Discovery*, 156–167. <https://doi.org/10.1038/nrd2466>
- Ma, L., Hu, L., Feng, X., Wang, S. (2017). Nitrate and Nitrite in Health and Disease. *Aging and Disease*. ISSN: 2152-5250 Vol. 9 (5) 938-945. <http://dx.doi.org/10.14336/AD.2017.1207>
- Mariotti, A., Hefti, A. F. (2015). Defining periodontal health. *BMC oral health*, 15 <https://doi.org/10.1186/1472-6831-15-S1-S6>.
- Mehrotra, P. (2016). Biosensors and their applications - A review. *Journal of Oral Biology and Craniofacial Research*, 6, 153-159. <http://dx.doi.org/10.1016/j.jobcr.2015.12.002>
- Mejri, A., Mars, A., Elfil, H., & Hamzaoui, A. H. (2020). Curcumin graphite pencil electrode modified with molybdenum disulfide nanosheets decorated gold foams for simultaneous quantification of nitrite and hydrazine in water samples. *Analytica Chimica Acta*, 1137, 19–27. <https://doi.org/10.1016/j.aca.2020.08.032>
- Meschiari, C. A., et al. (2015). Salivary, blood and plasma nitrite concentrations in periodontal patients and healthy individuals before and after periodontal treatment. *Clinica Chimica Acta*, 444, 293-296. <https://doi.org/10.1016/j.cca.2015.02.045>
- Monteiro, T. (2020). Development of point-of-care tests using enzyme (NiR & PON) based electrochemical biosensors. [Biotechnology Master, NOVA University of Lisbon].

- Monteiro, T., Almeida, M .G. (2018). Electrochemical Enzyme Biosensors Revisited: Old Solutions for New Problems. *Critical Reviews in Analytical Chemistry*, 9:2622 <https://doi.org/10.1080/10408347.2018.1461552>.
- Monteiro, T., Moreira, M., **Gaspar, S. B. R.**, Almeida, M. G. (2022). Bilirubin oxidase as a single enzymatic scavenger for the application of reductase-based biosensors in the open air and its application on a nitrite biosensor. *Biosensors and Bioelectronics*. <https://doi.org/10.1016/j.bios.2022.114720>
- Monteiro, T., et al. (2019). A quasi-reagentless point-of-care test for nitrite and unaffected by oxygen and cyanide. *Scientific Reports*. <https://doi.org/10.1038/s41598-019-39209-y>
- Mudan, A., et al. (2020). Severe Methemoglobinemia and Death From Intentional Sodium Nitrite Ingestions. *Journal of Emergency Medicine*, 59(3), e85–e88. <https://doi.org/10.1016/j.jemermed.2020.06.031>
- Muhaidat, R., et al. (2019). Assessment of nitrate and nitrite levels in treated wastewater, soil, and vegetable crops at the upper reach of Zarqa River in Jordan. *Environmental Monitoring and Assessment*, 191(3), 153–160. doi:10.1007/s10661-019-7292-8
- Nazir, M. A. (2017). Prevalence of periodontal disease, its association with systemic diseases and prevention. *International journal of health sciences*, 11(2), 72–80. <https://pubmed.ncbi.nlm.nih.gov/28539867/>
- Pereira, C., et al. (2013). The redox interplay between nitrite and nitric oxide: From the gut to the brain. *Redox Biology*, 1(1), 276–284. doi:10.1016/j.redox.2013.04.004
- Pignatelli, P., et al. (2020). How Periodontal Disease and Presence of Nitric Oxide Reducing Oral Bacteria Can Affect Blood Pressure. *International journal of molecular sciences*, 21(20), 7538. <https://doi.org/10.3390/ijms21207538>
- Pletcher, D., et al. (2001). *Instrumental Methods in Electrochemistry*, 1st ed., Woodhead Publishing
- Plumère, N. (2013). Interferences from oxygen reduction reactions in bioelectroanalytical measurements: the case study of nitrate and nitrite biosensors. *Anal Bioanal Chem*, 405, 3731–3738. DOI 10.1007/s00216-013-6827-z
- Reher, V. G., et al. (2007). Nitric oxide levels in saliva increase with severity of chronic periodontitis. *Journal of oral science*, 49(4), 271-276. <https://doi.org/10.2334/josnusd.49.271>
- Rheu, G. B., et al. (2011). Risk assessment for clinical attachment loss of periodontal tissue in Korean adults. *The Journal of Advanced Prosthodontics*, 3(1), 25–32. <https://doi.org/10.4047/jap.2011.3.1.25>

- Rocha, B. S., et al. (2011). Dietary Nitrite in Nitric Oxide Biology: A Redox Interplay Implications for Pathophysiology and Therapeutics. *Current Drug Targets*, 12(5). DOI: 10.2174/138945011796150334
- Rowe, J.J., Yarbrough, J.M., Rake, J.B. et al. (1979). Nitrite inhibition of aerobic bacteria. *Current Microbiology* 2(1), 51–54. <https://doi.org/10.1007/BF02601735>
- Salter, M., Duffy, C., Garthwaite, J., Strijbos, P. J. L. M. (1996). Ex Vivo Measurement of Brain Tissue Nitrite and Nitrate Accurately Reflects Nitric Oxide Synthase Activity In Vivo. *Journal Of Neurochemistry*, 66(4), 1683–1690. doi:10.1046/j.1471-4159.1996.66041683.x
- Sánchez, G. A., et al. (2014). Total salivary nitrates and nitrite in oral health and periodontal disease. *Nitric Oxide - Biology and Chemistry*, 36, 31–35. <https://doi.org/10.1016/j.niox.2013.10.012>
- Shiva, S. (2010). Nitrite and Heme Globins. *Nitric Oxide: Biology and Pathobiology*, 19 (2), 605–626. doi:10.1016/b978-0-12-373866-0.00019-8
- Silva, R. O., Agricola, N. & Guillo, L. (2018). Salivary cortisol and nitrite concentrations in school teachers: A longitudinal pilot study. *Endocrine Regulations*, 52(3) 128-133. <https://doi.org/10.2478/enr-2018-0015>
- Steffens, J. P., & Marcantonio, R. A. C. (2018). Classificação das doenças e condições periodontais e peri-implantares 2018: guia Prático e Pontos-Chave. *Revista de Odontologia da Universidade Estadual Paulista*, 47(4), 189-197. <https://doi.org/10.1590/1807-2577.04704>
- Sundar, N. M., et al. (2013). Comparison of the salivary and the serum nitric oxide levels in chronic and aggressive periodontitis: a biochemical study. *Journal of Clinical and Diagnostic Research*, 7(6), 1223–1227. <https://doi.org/10.7860/JCDR/2013/5386.3068>
- Tang, Y., Jaing, H., Bryan, N. S. (2011) Nitrite and nitrate: cardiovascular risk-benefit and metabolic effect. *Lippincott Williams & Wilkins*. DOI:10.1097/MOL.0b013e328341942c
- Tonetti, M. S., Greenwell, H., & Kornman, K. S. (2018). Staging and grading of periodontitis: Framework and proposal of a new classification and case definition. *Journal of periodontology*, 89 Suppl 1, S159–S172. <https://doi.org/10.1002/JPER.18-0006>
- Topcu, A. O. et al. (2014). Nitrite and Nitrate Levels of Gingival Crevicular Fluid and Saliva in Subjects with Gingivitis and Chronic Periodontitis. *Journal of Oral and Maxillofacial Research*, 5(2), 1-10. doi:10.5037/jomr.2014.5205
- Van Dyke, T. E., & Dave, S. (2005). Risk factors for periodontitis. *Journal of the International Academy of Periodontology*, 7(1), 1–8. <https://pubmed.ncbi.nlm.nih.gov/15736889/>

Vishwakarma, A., et al. (2019). Current approaches to measure nitric oxide in plants. *Journal of Experimental Botany*, 70(17), 1–11. <https://doi.org/10.1093/jxb/erz242>

Wang, Y., Huang, X., & He, F. (2019). Mechanism and role of nitric oxide signaling in periodontitis. *Experimental and therapeutic medicine*, 18(5), 3929–3935. <https://doi.org/10.3892/etm.2019.8044>

Zhao, Y., Vanhoutte, P. M., Leung, S.W.S., (2015). *Vascular nitric oxide: Beyond eNOS*. *Journal of Pharmacological Sciences*, doi:10.1016/j.jphs.2015.09.002

## **WEBGRAPHY**

Bank, **R. C. S. B. P. D.** (n.d.). 1OAH: Cytochrome c nitrite reductase from desulfovibrio desulfuricans ATCC 27774: The relevance of the two calcium sites in the structure of the catalytic subunit (NRFA). RCSB PDB. Consulted on April 11, 2022, from <https://www.rcsb.org/structure/1OAH>

Bank, **R. C. S. B. P. D.** (n.d.). 1OAH: Cytochrome c nitrite reductase from desulfovibrio desulfuricans ATCC 27774: The relevance of the two calcium sites in the structure of the catalytic subunit (NRFA). RCSB PDB. Consulted on April 11, 2022, from <https://www.rcsb.org/structure/1OAH>

**Centers for Disease Control (CDC) and Prevention.** (2013, July 10). *Periodontal disease*. Centers for Disease Control and Prevention. Consulted on December 4, 2021, from <https://www.cdc.gov/oralhealth/conditions/periodontal-disease.html>

Classification of periodontal and peri-implant diseases and conditions. **American Academy of Periodontology (AAP)**. (2022, August 31). Retrieved September 24, 2022, from <https://www.perio.org/research-science/2017-classification-of-periodontal-and-peri-implant-diseases-and-conditions/>

**GBD compare.** Institute for Health Metrics and Evaluation. (n.d.). Consulted on December 12, 2021, from <https://vizhub.healthdata.org/gbd-compare/>

**Genomenet.** KEGG. (n.d.). Consulted on June 6, 2022, from <https://www.genome.jp/entry/1.14.13.39>.

**Genomenet.** KEGG. (n.d.). Consulted on June 6, 2022, from <https://www.genome.jp/entry/1.7.2.2>.

Pinheiro, D. P. et al. (2022, July 29). *Hemoglobina Glicada hba1c: Entenda OS RESULTADOS*. MD.Saúde. Consulted on August 4, 2022, from <https://www.mdsaude.com/endocrinologia/hemoglobina-glicada/>

**World Health Organization (WHO)**. (n.d.). *Oral Health*. World Health Organization. Retrieved August 23, 2022, from <https://www.who.int/news-room/fact-sheets/detail/oral-health>



Chapter

6

# Appendices





# Appendices

A1 – Patients' questionnaire:



Monte da Caparica, \_\_\_ de \_\_\_ de 2022

Nº do questionário: \_\_\_\_\_

## Questionário:

1. É fumador/a?

	Não, nunca fumei.
	Não, mas sou ex-fumador/a. Foi fumador/a durante quanto tempo? _____ Há quanto tempo deixou de fumar? _____ Quantos cigarros fumava/dia _____
	Sim: É fumador há quanto tempo _____ Quantos cigarros fuma/dia _____

2. Costuma ingerir bebidas alcoólicas ?

	Não.
	Sim. <input type="checkbox"/> Nunca <input type="checkbox"/> Ocasionalmente (2 a 3 vezes/mês) <input type="checkbox"/> Frequentemente (várias vezes por semana)

3. Qual a quantidade de água ingerida diariamente?

<input type="checkbox"/> < 1L <input type="checkbox"/> 1 L a 3L <input type="checkbox"/> > 3 L
--

4. Costuma ter uma dieta rica em vegetais e fruta?

	Não.
	<p>Sim. Inger habitualmente (3 a 4 vezes por semana), algum destes vegetais?</p> <p><input type="checkbox"/> &lt; 1 chávena de <math>\cong</math> 120 g de espinafres não cozinhados.</p> <p><input type="checkbox"/> <math>\geq</math> 1 chávena de <math>\cong</math> 120 g de espinafres não cozinhados.</p> <p><input type="checkbox"/> &lt; 1 chávena de <math>\cong</math> 120 g de beterraba</p> <p><input type="checkbox"/> <math>\geq</math> 1 chávena de 120 g de beterraba.</p> <p><input type="checkbox"/> &lt; 1/2 chávena de 120 g de couve</p> <p><input type="checkbox"/> <math>\geq</math> 1/2 chávena de 120 g de couve.</p> <p><input type="checkbox"/> &lt; 1/2 chávena de 120 g de sumo vegetal</p> <p><input type="checkbox"/> <math>\geq</math> 1/2 chávena de 120g de sumo vegetal</p> <p><input type="checkbox"/> &lt; 1/2 chávena de 120 g de sumo de romã</p> <p><input type="checkbox"/> <math>\geq</math> 1/2 chávena de 120 g sumo de romã</p> <p><input type="checkbox"/> 1 banana média</p> <p><input type="checkbox"/> &gt; do que 1 banana média</p> <p><input type="checkbox"/> 1 laranja média</p> <p><input type="checkbox"/> &gt; do que 1 laranja média</p> <p>Outros _____</p>

5. Costuma ter uma dieta rica em carnes processadas:

	Não.
	<p>Sim. Diariamente, durante a sua refeição a quantidade de carnes processadas consumidas é de:</p> <p><input type="checkbox"/> &lt; 30 g de bacon (estimativa de 3 fatias de 10 g) <input type="checkbox"/> <math>\geq</math> 30 g de bacon.</p> <p><input type="checkbox"/> &lt; 60 g de fiambre (estimativa de 3 fatias de 20 g) <input type="checkbox"/> <math>\geq</math> 60 g de fiambre.</p> <p><input type="checkbox"/> &lt; 75 g de salsichas (estimativa de 3 salsichas de 25 g) <input type="checkbox"/> <math>\geq</math> 75 g de salsichas.</p> <p>Outros _____</p>

6. Está a fazer alguma suplementação vitamínica?

- Não.  Se sim, qual? \_\_\_\_\_

7. Tem sensação de boca seca?

Não.  Sim.

8. Tem alguma lesão oral?

Não.  Se sim, qual? \_\_\_\_\_

9. Considera que tem uma elevada quantidade de stress psicológico, cansaço físico ou ansiedade na sua vida?

	Stress psicológico
	Cansaço físico
	Ansiedade